

AMERICAN UNIVERSITY OF BEIRUT

Interference Management for Device-to-Device
Communications in 5G Networks

by

SALAM ADNAN DOUMIATI

A dissertation
submitted in partial fulfillment of the requirements
for the degree of Doctor of Philosophy
to the Department of Electrical and Computer Engineering
of the Maroun Semaan Faculty of Engineering and Architecture
at the American University of Beirut

Beirut, Lebanon
November 2019

AMERICAN UNIVERSITY OF BEIRUT

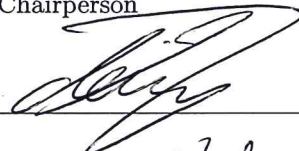
Interference Management for Device-to-Device Communications in 5G Networks

by
SALAM ADNAN DOUMIATI

Approved by:

Prof. Zaher Dawy, Professor
Electrical and Computer Engineering, AUB

Chairperson



Prof. Hassan Ali Artail, Professor
Electrical and Computer Engineering, AUB

Advisor



Prof. Joseph Costantine, Associate Professor
Electrical and Computer Engineering, AUB

Member of Committee



Prof. Oussama Bazzi, Professor
Lebanese University, Lebanon

Member of Committee



for Prof. Mohamad Assaad, Professor
CentraleSupélec, France

Member of Committee



for Prof. Didier Le Ruyet, Professor
CNAM, France

Member of Committee



Date of thesis defense: November, 2019

AMERICAN UNIVERSITY OF BEIRUT


THESIS, DISSERTATION, PROJECT RELEASE FORM

Student Name: Doumiati Salam Adnan
Last First Middle

Master's Thesis Master's Project Doctoral Dissertation

I authorize the American University of Beirut to: (a) reproduce hard or electronic copies of my thesis, dissertation, or project; (b) include such copies in the archives and digital repositories of the University; and (c) make freely available such copies to third parties for research or educational purposes.

I authorize the American University of Beirut, to: (a) reproduce hard or electronic copies of it; (b) include such copies in the archives and digital repositories of the University; and (c) make freely available such copies to third parties for research or educational purposes after: One ___ year from the date of submission of my thesis, dissertation or project.
Two ___ years from the date of submission of my thesis, dissertation or project.
Three ___ years from the date of submission of my thesis, dissertation or project.



Signature

Nov. 20, 2019

Date

Acknowledgements

First and foremost, I am grateful to Allah for the good health and well-being that were necessary to complete this dissertation. I thank Allah for the numerous blessings He has bestowed upon me throughout my dissertation journey.

At this moment of accomplishment, it gives me a great pleasure in expressing my gratitude to all those people who have supported me and had their contributions in making this thesis possible. I would like to thank my supervisor, Prof. Hassan Artail, for the patient guidance, encouragement and advice he has provided throughout my time as his student. Thank you for allowing me to grow as a research scientist. Your advice on both research as well as on my career have been invaluable. My sincere thanks also go to Prof. Mohamad Assaad, who provided me an opportunity to join his team as a visiting researcher in Centrale-Supelec. I am extremely thankful and indebted to him for sharing expertise, and sincere and valuable guidance and encouragement. Thank you for steering me in the right the direction whenever you thought I needed it.

I would also like to thank my committee members, Prof. Zaher Dawy, Prof. Joseph Costantine, Prof. Oussama Bazzi and Prof. Didier Le Ruyet for serving as my committee members even at hardship. I also want to thank you for your very valuable comments and suggestions on this thesis. Besides the committee members, I would also like to thank AUB and the Lebanese National Council for Scientific Research (CNRS-L) for their financial support granted through predoctoral fellowship.

I would like to also place on record, my sense of gratitude to the U.S Embassy of Beirut for nominating me to represent my country, Lebanon, in the “International Visitor Leadership Program” (IVLP) for advancing women in STEM, where I met wonderful ladies from all over the world and I learnt a lot from their experiences and stories. Thank you #HNM organizers, liaisons, “hidden no more” ladies for making this event a turning point in my life.

I would like also to thank my friends: Rasha El Khansa (for the special mo-

ments in France, Murex and Kerr), Asmaa Abdallah, Nadine Abbas, Nour Baalbaki, Raneen Daher, Reem Melki, Reem Brome, Lama Shaer, Nour Kouzayha, Mariam Issa, Alaa Maarouf and Sara Jaleddine for all the fun we have had in the last four years. Thank you ladies for always being there for me.

A special thanks to my parents whose undying love, unconditional support and guidance are with me in whatever I pursue. They are my ultimate role models. Words cannot express how grateful I am to my father Adnan and my mother Hana for all of the sacrifices that you have made on my behalf. Your prayer for me was what sustained me thus far. Thank you mom and dad for showing faith in me and giving me the liberty to choose what I desired. You shaped my values and made me the person that I am today.

I would like to express my special appreciation and gratitude to Yehya, my soulmate, my beloved fiancé and my best friend, for providing me with unfailing support and continuous encouragement throughout my years of study and through the process of researching and writing this thesis. He experienced all of the ups and downs of my research and so he deserves big thanks for helping me keep things in perspective. Thank you Yehya for providing me with all the love and caring I needed to stay strong and to continue till the end to achieve my goals. Thank you for your concerned, late night vigils despite the geographical distance between you (in France) and me (in Lebanon). Thank you for the sleepless nights you had when I was in the U.S. due to the time difference. Thank you for always showing how proud you are of me. Thank you so much for the valuable advice, constructive criticism and timely suggestions throughout my research work. It is such a nice feeling to have a partner with the same engineering spirit like you. Without your precious support, and persistent help, this dissertation would not have been possible.

It is my fortune to gratefully acknowledge the people who mean a lot to me. Thank you my sister Samah for providing me an unending inspiration and for supporting me spiritually throughout writing this thesis and for always cheering me up. Thank you for listening to my problems and providing perspective. I salute you for the selfless love, care, pain and sacrifice you did to shape my life, from the day I was a baby . . . till now. Namaste!

I would like also to thank my brothers Moustapha and Hassan, on whose shoulders I stand. I would never be able to pay back the love and affection showed upon by my brothers. Thank you for the unceasing encouragement, support and attention, and for always listening to my problems.

Special thanks are extended to my sisters-in-law Nisrine and Nadia for their continued support and encouragement. Thank you Nisrine for the unforgettable

moments we had together in France and for continuous help. Thank you Nadia for listening to me during our rides from AUB to our home and for always lifting me up.

Thank you to my extended family, my mother-in-law Fawzia, my father-in-law Abdel Fattah and my sister-in-law Doha for your constant love, understanding and encouraging.

I consider myself the luckiest in the world to have such a lovely and caring family, standing beside me with their love.

Last but not least, thank you to my little guardian angels, my nieces and nephews, Hana, Adnan, Julia Maria for bringing happiness and joy to my life, and a much needed form of escape from my studies.

To not forget, my thesis was defended during the Lebanese Revolution 2019...

An Abstract of the Dissertation of

SALAM ADNAN DOUMIATI for Doctor of Philosophy
Major: Electrical and Computer Engineering

Title: Interference Management for Device-to-Device Communications in 5G Networks

While offloading has great potentials to relieve increasingly congested cellular networks, its benefits come at a cost, namely uncoordinated interference resulting from other Device-to-Device (D2D) pairs, which reduces wireless network capacity. In this dissertation, we propose to align the interference occurring from nearby D2D pairs using Topological Interference Management (TIM) instead of depending on the instantaneous channel state information (CSI), which is a task that hinders the practicality of D2D technology. We recast the TIM problem as a low-rank matrix completion problem (LRMC), which is usually NP hard due to the rank's non-convex and discontinuous nature. For this, we have progressively developed three efficient and novel approximation solutions to overcome the TIM matrix special structure with hard constraints (having all ones on the diagonal entries). While dealing with large networks in practice, we proposed to divide the whole network into clusters, and apply TIM on each of the resulting sub-groups in a parallel way, so that the scalability issue gets resolved. To this end, we carefully designed a clustering framework that works in favor of the LRMC-based TIM scheme, by relying on graph theory. Moreover, to make TIM more realistic, we also considered practical scenarios through accounting for path losses and mobility. Simulations have shown that the proposed methods minimize the matrix rank better than the existing works, while maintaining a polynomial complexity. By successfully approximating the rank completion problem, the system degrees-of-freedom (DoF) of a partially connected network of D2D-enabled devices (even of large dimensions) with no CSI increases, the occurred interference is managed, and hence the network throughput increases. To improve the DoF values even further, we also have utilized the successive interference cancellation (SIC) built-in capability in the 5G handsets for decoding, while maintaining in the overall

an LRMC-based TIM approach.

Contents

Acknowledgements	v
Abstract	viii
1 Introduction	1
1.1 Dissertation Objectives	5
1.2 Organization of the Dissertation	6
1.3 Publications and Awards	8
1.3.1 Journal Papers	8
1.3.2 International Conference Papers	8
1.3.3 Awards	8
2 Background	10
2.1 Topological Interference Management	10
2.1.1 Low-rank Matrix Completion Problem Approach	12
2.1.2 Degrees-of-Freedom	13
2.1.3 Relation between TIM and Index Coding	14
2.2 Mathematical Background	16
2.2.1 Basic Notions	16
2.2.1.1 Norms	16
2.2.1.2 Trace	17
2.2.1.3 Rank	17
2.2.1.4 M-matrix	18
2.2.1.5 Singular Value Decomposition	18
2.2.1.6 Pseudo-inverse or Moore-Penrose inverse	18
2.2.2 Tikhonov Regularization	19
2.2.3 Eckart and Young Theorem	20
2.2.4 QR Decomposition	21
2.2.5 Semi-definite Programming	22
2.2.5.1 Basic Facts	22
2.2.5.2 Cholesky Decomposition	23
2.2.5.3 Schur Complements	24
2.2.5.4 Linear Matrix Inequalities	24

2.2.6	Second-order Cone Programming	25
2.2.7	Characteristic Polynomial Function	26
2.3	Maximum-k-cut	27
2.3.1	Laplacian Matrix	27
2.3.2	Laplacian Algebra	28
2.4	Successive Interference Cancellation	29
3	Literature Review	31
3.1	Topological Interference Management	32
3.2	Low-Rank Matrix Completion Methods	33
3.3	Clustering Algorithms	36
3.4	Successive Interference Cancellation Technique	37
4	Recasting TIM as a Low-rank Matrix Completion Problem	40
4.1	Modeling the LRMC-based TIM Approach	41
4.1.1	Choice of D2D Transmission Mode	41
4.1.2	Learning about the Topology Information	42
4.1.3	System Model for the LRMC-based TIM Framework	45
4.1.4	Rank Approximation Algorithm Assessment	48
4.1.5	Deducing the Optimal Rank	49
4.1.6	Parameters and Variables	51
4.2	Developing Solutions for LRMC-based TIM Approach	52
4.2.1	Fazel's Lemma	52
4.2.2	<i>RM-TIM</i> : Generic-Rank Approximation Method	53
4.2.2.1	Step 5. Solution for the Diagonal Issue	55
4.2.2.2	Simulation Setup and Parameters	57
4.2.2.3	Parameters Assumptions Justification	57
4.2.2.4	Results and Analysis	59
4.2.2.5	<i>RM-TIM</i> 's Complexity	63
4.2.2.6	Summary	65
4.2.3	<i>eRM-TIM</i> : "Tweaked" Nuclear Norm-Rank Approximation Method	65
4.2.3.1	Solution for the Diagonal Issue	66
4.2.3.2	Simulation Setup	67
4.2.3.3	Results and Analysis	68
4.2.3.4	<i>eRM-TIM</i> 's Complexity	68
4.2.3.5	Summary	69
4.2.4	Summary	69
4.3	Extending TIM using SIC	70
4.3.1	System Model for Joint TIM-SIC	71
4.3.2	Two-Stage Rank Minimization	74
4.3.2.1	Stage 1: <i>cRM-TIM</i>	75
4.3.2.2	Stage 2: <i>eRM-TIM</i>	77

4.3.3	Joint TIM-SIC Framework's Complexity	78
4.3.4	Experimental Results	79
4.3.4.1	Scenario 1: No differentiation among the interferences	79
4.3.4.2	Scenario 2: Rank minimization without feedback	80
4.3.4.3	Scenario 3: Running the rank minimization method with feedback	80
4.3.5	Summary	81
4.4	Adapting TIM to Work for Practical Scenarios with Pathloss and Mobility	82
4.4.1	System Model for Pathloss and Mobility	82
4.4.2	TIM with Path Loss	83
4.4.3	TIM with Mobility	85
4.4.4	Mathematical Model of TIM in Such Real Scenario	86
4.4.5	Complexity	87
4.4.6	Experimental Results	87
4.4.6.1	DoF Achieved	88
4.4.6.2	CPU Time	88
4.4.7	Summary	89
5	Providing Scalability through TIM-tailored Clustering Method	90
5.1	System Model for Joint TIM-Clustering	91
5.1.1	Interpreting the Interference Network as a Graph	95
5.1.2	Clustered TIM	96
5.1.3	Parameters and Variables	98
5.2	Mathematical Model	98
5.2.1	Original Problem	98
5.2.2	SDP Relaxation	99
5.3	Heuristic Clustering Algorithm	102
5.4	Bounds Analysis	103
5.4.1	Randomized Policy	103
5.4.2	Upper Bound (SDP Relaxation)	105
5.4.2.1	Eigenvalue Bound	105
5.4.2.2	Strengthened Eigenvalue Bound	107
5.4.2.3	Perturbed Bound	107
5.4.3	Performance Guarantee	108
5.5	Experimental Results	109
5.5.1	Clustering Algorithm Evaluation	110
5.5.1.1	Comparison against the Exhaustive Search Method	110
5.5.2	Clustering Bounds Evaluation	111
5.6	Clustering Combined with TIM Evaluation	112
5.6.1	DoF Achieved	113
5.6.2	Effect of the Number of Clusters on the DoF	114

5.6.3	Complexity and Computation Time	114
5.7	Summary	115
6	Conclusion	117
6.1	Open Research Directions and Future Work	118
A	Proofs for Chapter 5	120
A.1	Proof of the Nuclear Norm Providing a Diagonal Matrix	120
A.2	Proof of Getting \mathbf{K} and \mathbf{E} Matrices as Diagonal Ones	120
A.3	Proof of the Smooth Rank Function in terms of Trace	122
B	Proofs for Chapter 6	123
B.1	Proof of the Randomized Policy Bound	123
B.2	Proof of the Eigenvalue Bound	124
B.3	Proof of the Strengthened Bound	125
B.4	Tightening the Clusters' Sizes Constraint	127

List of Figures

1.1	Cisco traffic forecast [1]	1
1.2	Device-to-Device (D2D) concept	2
2.1	(a) TIM of a network of 5 D2D pairs [2], and (b) its associated incomplete matrix	11
2.2	(a) Corresponding index coding problem to the 5×5 topology of Fig. 2.1, and (b) its associated incomplete matrix	16
2.3	Successive interference cancellation technique (SIC)	30
4.1	(a) TIM for a 12×12 D2D network and its (b) TIM matrix	43
4.2	Flow of <i>RM-TIM</i> method	57
4.3	(a) Topology pattern of an example network of 30 D2D pairs, (b) interference representation matrix of the first 15 D2D pairs	67
4.4	The achieved symmetric DoF by different rank minimization methods	68
4.5	CPU time comparison between <i>RM-TIM</i> and <i>eRM-TIM</i>	69
4.6	A network of 18×18 D2D-enabled devices with SIC capabilities	71
4.7	Interference cancellation at the receiver using TIM and SIC	75
4.8	Two-stage rank minimization of \mathbf{X}	77
4.9	(a) Topology pattern of an example network of 6 D2D pairs, and its (b) interference representation matrix	82
4.10	Effect of speed on re-running TIM algorithm	86
4.11	CPU time function of the topology dimensions	89
5.1	(a) TIM pattern of a 15×15 D2D network, (b) its corresponding matrix, and c) sub-matrices (after clustering)	93
5.2	TIM clustering of the 15×15 D2D network	94
5.3	TIM conflict graph with assigned weights for the 15×15 network	96
5.4	TIM conflict graph with assigned weights for the 30×30 network	109
5.5	The effect of the number of D2D pairs on the interference intensity	110
5.6	Resulting sub-matrices for the 30×30 network	114
5.7	Effect of the number of clusters on DoF	114
5.8	The gain in CPU time, after combining LRMC-based TIM with clustering	115

List of Tables

3.1	Rank minimization methods	35
4.1	Parameters and variables used in Chapter 4	51
4.2	Continuation of Table 4.1	52
4.3	Resulting \mathbf{X}	60
4.4	Applying SVD on the resulting \mathbf{X}	61
4.5	Approximate \mathbf{S} by $\hat{\mathbf{S}}$ after zeroing the two smallest singular values	61
4.6	$\hat{\mathbf{X}}$: Approximated \mathbf{X}	61
4.7	Comparison of <i>RM-TIM</i> against dirAP	63
4.8	Applying QR decomposition on \mathbf{X} resulting from <i>RM-TIM</i>	63
4.9	Truncating \mathbf{Q} and \mathbf{R}	64
4.10	Approximated \mathbf{X} with $r=3$	64
4.11	Rank minimization performance with different values for \dagger	81
4.12	Path loss effect on the achieved DoF	88
5.1	Parameters and variables used in Chapter 5	98
5.2	Lower and upper bounds for different topologies for the 15×15 D2D pairs network	112
5.3	Improvement of the total sum of symmetric DoF due to clustering	113

Chapter 1

Introduction

Measurements in cellular networks predict a fast increase in the amount of mobile data wirelessly transferred [1]. The current Cisco Visual Networking Index (VNI) forecast projects global IP traffic to nearly triple from 2017 to 2022 and an overall IP traffic is expected to grow to 396EB per month by 2022, as shown in Fig. 1.1. Hence, solutions are needed in order to cope with this problem and offload data from the core network.



Figure 1.1: Cisco traffic forecast [1]

In this vein, Device-to-Device (D2D) communication is considered as a promising technique, where devices in proximity can communicate in a direct link and bypass the base station [3], as illustrated in Fig. 1.2. In the literature, D2D has received extensive attention and many works have shown the benefits brought by D2D communication since 1) it increases the system capacity and spectrum efficiency, thanks to the reuse and hop gains; 2) it improves the peak rate due to the proximity gain [4] [5]; 3) it reduces latency, and 4) it serves as a technology enabler for proximity-based social networking [6]. The benefit from D2D can be further improved to boost the data rate by enabling D2D multicasting for group communication using clustering to share data among users. The effectiveness of the system in properly clustering the devices, which are in proximity and share

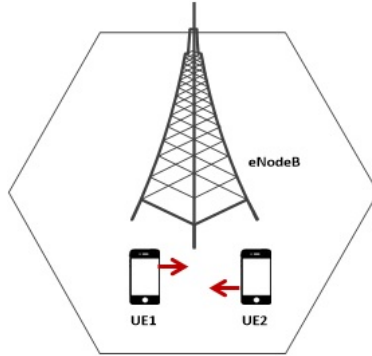


Figure 1.2: Device-to-Device (D2D) concept

similar interests, was proved in a preliminary work we accomplished in [7], where we developed a clustering algorithm for group D2D communication that selects clusterheads based on UEs' interest, neighborhood, channel condition information and battery energy. However, this algorithm works under the assumption of abundant channel state information (CSI) which is too optimistic, since it is difficult to translate it into practice, where CSI is rarely available.

Therefore, taking the interference factor into account is essential, knowing that it represents a serious limitation that faces the development of D2D technology and reduces the network throughput. To deal with this interference, several management schemes have been proposed, such as mode selection [8], resource allocation [9], power control [10], and a combination of these methods [11]. However, the 5G networks with Internet of Things (IoT) applications, are expected to become highly dense, which makes the interference more complex, and hence the applicability of the aforementioned approaches no more sufficient [12].

Recently, interference alignment (IA) technique has evolved in D2D communication, while requiring the knowledge of CSI among D2D devices in order to align and then cancel the interference [13–16]. However, exploiting CSI instantaneously is a burdensome task in a D2D network, knowing that the UE has limited capabilities in terms of battery energy and memory availability. Exchanging CSI also loads the network with signaling overhead, hindering by this CSI practicality. Because of this, the channel measurement on the sidelink between D2D enabled devices is still in the standardization process [17], and has turned the attention of network researchers to managing interference based on criteria other than the instantaneous CSI. Several alternative schemes to IA have been proposed to minimize the dependance on CSI and reduce signaling, including the well-know time-division multiple access (TDMA), frequency-division multiple access (FDMA), and code-division multiple access (CDMA) techniques. These actually can be regarded as special cases of a more general scheme, namely the topological

interference management (TIM) method [18], which works based on knowledge of the network topology, and not the instantaneous CSI [19–21]. TIM was also considered as a promising solution for peer-to-peer networks [19], like D2D communication.

In the TIM technique, the connectivity pattern is represented by an adjacency matrix known by all the nodes in the network and is based on a 1-bit interference data (weaker or stronger than the noise floor), depending on the propagation physical phenomena in the network [19]. Hence, the matrix entries illustrate the interference relation among the transmitters (columns) and receivers (rows). It has been established that the TIM problem, in terms of degrees-of-freedom (DoF), is equivalent to the index coding problem with linear schemes, where the received signals are linear combinations of transmitted ones [19, 20, 22]. As for DoF, it is considered as the pre-log factor of the information-theoretic capacity at high signal-to-noise ratio (SNR) [23]. This is using the fact that the optimal linear index code length is equal to the minimum rank of a matrix that fits the side information graph. This graph is a directed graph which is defined on the vertex set that represents the users and on the edge set where an edge (i, j) exists if and only if user i has packet j as side information. Therefore, it is possible to solve the TIM problem by equivalently solving a matrix completion problem over a finite or real field based on a few known entries of this matrix [24].

Inspired by the recent works in [24–26], in this thesis, we recast the original TIM problem as a low-rank matrix completion (LRMC) problem to find linear solutions that maximize the achievable symmetric DoF (and hence maximize the number of parallel transmissions) for any given network topology, as the SNR approaches infinity. This approach has been recently applied to linear index coding over the finite field [25], and to TIM with symmetric DoFs [26], [27]. In particular, the achievable symmetric DoF and the reciprocal of the optimal value of the rank of the resulted LRMC model are equivalent. We restrict here the class of interference management strategies to linear schemes, knowing their low-complexity and their achievable DoF optimality [27]. The aim is then to minimize the matrix rank, and hence deduce the independent columns (transmitters) that can transmit simultaneously (without interfering), increasing the system DoF which is inversely proportional to the rank. The factorization of this matrix solution leads to the appropriate precoding and decoding matrices that cancel the interference.

On a hand, we realize that a list of challenges is associated with LRMC-based TIM: 1) the sparsity of the data (0s denoting interference) and the unique data set associated with the D2D network (the matrix diagonal entries are all ones, i.e., each D2D-transmitter transmits to its intended D2D-receiver), which restricts the rank flexibility, and 2) its applicability to large scale networks.

To overcome the first challenge, i.e., the TIM matrix special structure with hard constraints, we propose three novel approximation solutions (knowing the NP-hardness of the rank function in the LRMC problem) that can handle any general matrix. These heuristics are numerically efficient and do not require a user-specified initial point. In the first method that we call *RM-TIM*, we approximate the TIM matrix rank by a continuous generic approximation function that uses Tikhonov regularization and we formulate the problem as SDP. Although the proposed method has a polynomial complexity, however, its complexity remains high. To this end, we develop (also using SDP) an improved TIM rank minimization method that we name *eRM-TIM*, which is a “tweaked” nuclear norm heuristic, with much lower complexity, while achieving similar rank minimization performance. In the third method that we call *cRM-TIM*, we rely on the coefficients of the characteristic polynomial function of a matrix and their relation with the rank matrix. Our developed rank minimization methods outperform other existing methods in terms of the minimum rank attained (while maintaining accuracy and low complexity), and thus corresponds to a lessening in signal interference (without knowing the instantaneous CSI): a key need in D2D networks. This hence leads to an increase in the system DoF.

To deal with the second challenge, i.e., the limitation of the LRMC-based TIM approach to medium networks, we propose a hierarchical approach, where the network is first clustered into groups, then the efficient LRMC optimal solution is applied within each group. Hence, we propose to combine clustering with LRMC-based TIM and we formulate the clustering scheme (using graph theory) as a relaxed SDP problem. We develop a heuristic algorithm with polynomial complexity, that can successfully group D2D devices with mutual interference in separate clusters. Simulations show that the joint clustering-TIM framework renders the LRMC-based TIM more scalable, significantly improves the system DoF as compared to only using TIM, especially in large D2D networks, and also reduces the computation time.

On the other hand, other challenges arise while applying TIM to D2D, specifically: conventional TIM 1) cannot manage the very strong interference that can be even stronger than the desired signal and cancel it: this scenario may frequently occur in D2D communications which usually happen in close proximity (e.g., in crowded D2D networks, such as malls, concerts or stadiums), and 2) ignores the differences of differences of signal strengths due to propagation path loss, which represents an important physical phenomenon in D2D scenario.

To handle the first point, we propose to combine TIM with a technique usually used in non-orthogonal multiple access (NOMA), i.e., the successive interference cancellation (SIC). In this framework, a finer classification of interference takes

place, where a strong interference can be managed by TIM and the very strong one by SIC. We also model this problem using LRMC approach and we apply the third rank approximation method to solve it. Results show that the employment of this smooth and successful combination of TIM with SIC can offer promising improvement in terms of network performance.

To manage the second point, we reflect from the information theoretic perspective (DoF metric) towards practical wireless interference networks, while taking the physical phenomena, like path loss and mobility, into consideration. Numerical results show the implication of these scenarios in constraining the DoF achieved.

1.1 Dissertation Objectives

Our work gives rise to some essential questions, which can be translated into objectives:

1. To offer advantages over recent interference alignment works that depend on the availability of channel state information (CSI), since the topological interference management (TIM) problem is expected to cancel the interference by only making use of the network topology information. Indeed, having to acquire CSI in a Device-to-Device (D2D) network poses a burden on a device having limited capabilities, and increases its power consumption.

This objective was attained in all our journal [28–30] and conference papers [31, 32].

2. To develop a novel formulation of the TIM problem in a network where D2D-enabled devices are not aware of the surrounding user equipment’s CSI but only of the network topology. To recast the problem as a low-rank matrix completion (LRMC) problem, and to consider the degrees-of-freedom (DoF), as our main figure of merit. To formulate the mathematical models for three novel approaches using the semi-definite programming (SDP) by addressing the NP-hardness of the non-convex rank objective functions, while respecting the special structure of the underlying TIM matrix that limits the applicability of well-known rank minimization methods.

These objectives were realized in our two published journal papers [28, 29] and our submitted journal paper [30].

3. To incorporate D2D in 5G networks with regards to the interference management by using built-in device capabilities, like successive interference cancellation (SIC) technique.

This objective was achieved in the submitted journal paper [30].

4. To propose a clustering algorithm in a multiuser D2D interference network, without exploiting the CSI statistics, but only relying on the connectivity pattern, i.e., on the TIM adjacency matrix. TIM clusters should be formed such that strong interference are cut and captured among inter-cluster interference. To this end, we base our method on the maximum-k-cut algorithm, but with a "tweak", in order to count for the maximum number of devices allowed inside a cluster. The "tweaked" maximum-k-cut problem is also formulated as a semi-definite problem (SDP).

This objective was accomplished in the published journal paper [29] and conference paper [32].

5. To analyze how the DoF results can be translated into practical signal-to-noise ratios (SNR), turning the scenarios into much more realistic ones, while integrating path loss and mobility effect.

This objective was fulfilled in the accepted conference paper [31].

1.2 Organization of the Dissertation

In Chapter 1 of this thesis, we list the several benefits of device-to-device (D2D) technology that are limited by interference. Then, we discuss the motivation behind using the topological interference management (TIM) technique in managing the interference in a D2D network, without relying on the instantaneous CSI.

In Chapter 2, we present some background information that are related to TIM and its relation with the index coding problem, as well as the low-rank matrix completion (LRMC) approach that we adopt to solve TIM. In this chapter, we also detail some mathematical background information that help the reader in understanding the mathematical notions used throughout the thesis, along with some explanations about some problems in graph theory, like maximum-k-cut problem, over which we rely in our clustering approach. We also describe the successive interference cancellation (SIC) technique and its different steps.

In Chapter 3, we cover the existing works that are related to TIM and to the different rank minimization methods that are typically used to solve the low-rank matrix completion (LRMC) problems. We also discuss the different clustering algorithms and physical layer interference management techniques that exist in the literature and are applied in the context of D2D.

In Chapter 4, we apply TIM in a partially connected network, where D2D-enabled devices are not aware of the surrounding devices' CSI, but only of the network connectivity which helps in canceling the interference occurred.

In the first part of this chapter, we model TIM as an LRMC problem and solve it using three novel schemes based on semi-definite programming (SDP) while overcoming TIM matrix special structure with hard constraints: 1) having all ones of the diagonal entries, 2) having some predefined zeros in predefined positions, 3) being a square matrix knowing that the rows and the columns of this matrix correspond to the transmitters and receivers pairs, and 4) being a general matrix, not necessarily symmetric nor positive semi-definite (PSD). We also compare the performance of these schemes, the so-called *RM-TIM*, *eRM-TIM* and *cRM-TIM*, against the existing works in the literature, in terms of the minimum rank achieved as well as the problem complexity. At the end of this part, we also combine the TIM framework with the successive interference cancellation (SIC) technique and apply it in D2D networks. While the TIM problem was originally studied in a partially connected network, the novelty appears here in classifying the occurred interference into two categories: strong and very strong interference (that may overwhelm the desired signal). Moreover, we propose to manage the first type of interference using TIM, while the second one we hand over to SIC.

In the second part of Chapter 4, we also explore the performance of TIM in practical scenarios, where path losses exist, especially that the TIM problem was originally studied in a partially connected network. In addition to this, we define the conditions under which TIM should re-run in order to save processing time when mobility is taken into account.

In Chapter 5, we build a joint clustering and TIM framework for a D2D network. We develop a clustering algorithm that is suited for the LRMC approach to solve TIM, while building on the SDP relaxation of the maximum-k-cut algorithm, and extending it to account for each cluster's capacity. This clustering problem turns out to be a capacitated maximum-k-cut problem, for which we derive relatively tight upper bound, that helps in determining the performance guarantee of many clustering algorithms.

In Chapter 6, we conclude the thesis and we open new research directions for future works. In Appendices A and B, we include some proofs that are related to Chapter 4 and Chapter 5. Note that we defer these proofs till the end to maintain the thesis flow.

1.3 Publications and Awards

The following publications were produced during the Ph.D. journey.

1.3.1 Journal Papers

1. **S. Doumiati**, H. A. Artail, and M. Assaad, “Toward optimal DoF maximization with interference categorization using TIM and SIC,” in *IEEE Transactions on Communications*, submitted
2. **S. Doumiati**, M. Assaad, and H. A. Artail, “A framework of topological interference management and clustering for D2D networks,” in *IEEE Transactions on Communications*, July 2019 DOI:10.1109/TCOMM.2019.2931319
3. **S. Doumiati**, M. Assaad, and H. A. Artail, “Topological interference management framework for device-to-device communication”, in *IEEE Wireless Communication Letters*, vol. PP, no. 99, pp. 1-4, 2018 (invited paper at *IEEE International Conference on Communications, ICC 2018*).

1.3.2 International Conference Papers

1. **S. Doumiati**, H. A. Artail, and M. Assaad, “Application of the Topological Interference Management Method in Practical Scenarios,” in *2019 IEEE 15th International Conference on Wireless and Mobile Computing, Networking and Communications (WiMob 2019)*, accepted, Barcelona, Spain, Oct. 2019
2. **S. Doumiati**, H. A. Artail and M. Assaad, “Managing interference in D2D networks via clustering and topological awareness”, in *23rd IEEE International Workshop on Computer-Aided Modeling Analysis and Design of Communication Links and Networks (CAMAD)*, Barcelona, Spain, Sept. 2018.
3. **S. Doumiati**, H. Artail and K. Kabalan, “A framework for clustering LTE devices for implementing group D2D communication and multicast capability”, in *8th International Conference on Information and Communication System (ICICS)*, Irbid, April 2017.

1.3.3 Awards

In recognition of my reseearch efforts during my Ph.D. journey, I received many prestigious awards:

- Nominated by the U.S. Embassy to represent Lebanon in the ‘Advancing Women in STEAM Fields’ International Visitor Leadership Program

(IVLP) that took place over 4 different states of the U.S. (Washington DC, Huntsville Alabama, Chicago, and Los Angeles), Oct. 29 - Nov.16, 2018.

- Received the CNRS-L/AUB doctoral scholarship award from the Lebanese National Council for Scientific Research (CNRS), Sept. 2018
- Endorsed as the only Lebanese recipient of the Grace Hopper Celebration of Women in Computing (GHC) Student Scholarship, Orlando, U.S., Oct. 2017

Chapter 2

Background

The objective of this chapter is to give a general overview of some important concepts related to the thesis work.

2.1 Topological Interference Management

Several methods have been proposed in the literature to manage interference in wireless methods. One of the well-known methods is interference alignment (IA). The main concept of this technique is to minimize the interference every transmitter causes to unintended receivers instead of maximizing each receiver's own signal-to-interference-plus-noise ratio (SINR) independently. Hence, this leads to a better network performance, in terms of sum-capacity. With this, multiple interference signals are consolidated into a small subspace at each receiver, allowing the desired signal to be transmitted in the interference-free subspace [15]. In this case, every user in the network is able to achieve nearly one half of the capacity that s/he could achieve in the absence of all interference. However, the main problem of IA is that the closed form expression for interference alignment requires the global channel knowledge, which adds an overhead on the network [33]. This problem becomes even more critical when it is applied on D2D networks, especially that it will drain the device's battery, which is limited.

All of this motivated the researchers to explore another interference management technique that manages interference in D2D networks, without relying on the instantaneous exchange of channel state information (CSI). A promising solution in this context is the Topological Interference Management (TIM) method. In this technique, the interference can be suppressed among the devices in proximity, without being aware of the surrounding devices' CSI, but only based on the network topology. This topology is also known by all the nodes in the network, facilitating by this the decoding of the intended signal with less consumed energy. The connectivity pattern among these D2D devices is represented by an

adjacency matrix and is based on one-bit knowledge of the interference strength. This value is deduced after comparing the received nominal power from other devices than the intended one (weaker or stronger) against a prechosen threshold value. This threshold is usually considered as the acceptable noise floor: if the power value is less than this threshold, then the link between this transmitter and the receiver is considered as a weak one, and hence can be neglected (and so ignored in the connectivity pattern at little cost). However, if it is greater than the acceptable noise floor, then this link is a significant one and should be taken into account [19]. Therefore, an interesting issue here is the optimal choice of the effective noise floor threshold by the receiver. This is because if the threshold is too low, then the number of interferes increases and hence most of the links will be considered as significant ones. By this, the matrix becomes so sparse and thus applying TIM turns to be useless. On the other hand, if this threshold is chosen to be high, then the topology pattern will be highly disconnected, and hence the matrix will be full of missing entries. Although this may help the TIM performance, but it negatively affects the SNR itself. In all, the threshold choice is out of the scope of this thesis, but it can be considered as an interesting direction for future work.

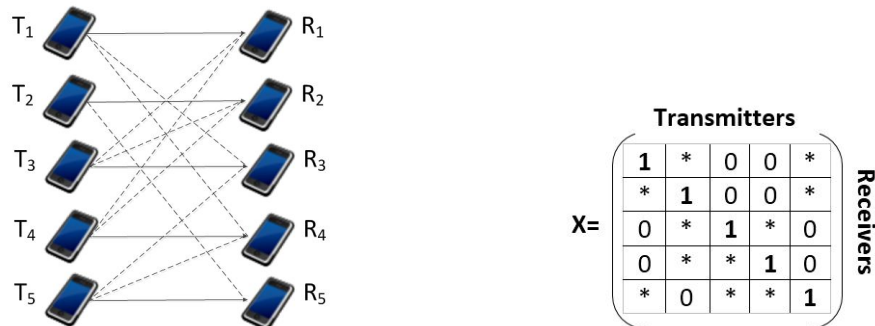


Figure 2.1: (a) TIM of a network of 5 D2D pairs [2], and (b) its associated incomplete matrix

As an illustration for the TIM method, we present in Fig. 2.1 an instance of a 5×5 network, where TIM is applied. We consider here an interference network consisting of the same number p of single-antenna wireless transmitters T and receivers R working in pairs in a D2D scenario with a multiple unicast setting, i.e., the number of users p is equal to the number of s messages sent by T , $p = s$. This example of 5×5 network is chosen not because it is particularly challenging (indeed we will deal with more challenging instances, and with larger dimensions, of TIM problems later in this thesis) but rather for its historical significance: this is the first known interference alignment example, originally considered by Birk and Kol in [2]. In Fig. 2.1(a), the solid and dotted lines represent here the desired channel links and interfering links, respectively. For instance, transmitter

T_1 is communicating with its intended receiver R_1 . While this link is active, T_1 is interfering to R_3 and R_4 but does not represent a source of interference for R_2 and R_5 . Hence, there are no lines (not solid nor dotted) between T_1 and these devices. On the right of this figure, we show the associated incomplete matrix that corresponds to the 5×5 D2D network of (a), with “*” representing arbitrary values. The columns and rows of this matrix \mathbf{X} (called as TIM adjacency matrix) refer to the transmitters’ and receivers’ indices, respectively. As for the entries of \mathbf{X} , they illustrate the interference relation among these devices. This matrix has all ones in its diagonal entries to indicate that each receiver desires a message from its intended transmitter. Now for the same example of $(T_1 - R_1)$ link and considering the 1st column which corresponds to T_1 , the 0 values in the third and fourth rows designate the occurring interference at R_3 and R_4 . As for the don’t care values (“*”), they indicate that $T_1 - R_1$ link does not affect on R_2 and R_5 . The indication of the TIM adjacency matrix entries can be summarized as follows:

$$\mathbf{X} = [X_{i,j}] = \begin{cases} 1 & \text{each } R_i \text{ wants a message from } T_i \\ 0 & \text{interference should be aligned} \\ * & \text{no interference occurred} \end{cases} \quad (2.1)$$

More details about the meaning of these entries and how they are obtained can be found in Chapter 4. It is good to mention here that the missing entries in the adjacency matrix remind us of the low-rank matrix completion (LRMC) problem that will be detailed in the following sub-section.

2.1.1 Low-rank Matrix Completion Problem Approach

Real-world datasets are usually incomplete and hence represented in a matrix with missing entries. The most well-know example is the Netflix problem [34], where each column represents a movie and each row corresponds to a user. Based on some ratings of the movies, the users’ preferences on other movies can be predicted while applying the low-rank matrix completion (LRMC) problem. The assumption here that the rating matrix should be low rank goes back to the fact that a subgroup of users are likely to share similar preferences and their ratings will be highly correlated. The direct approach to recovering a low-rank matrix is then to minimize the rank of the matrix with certain constraints that make the estimated matrix consistent with the original data [35]. Mathematically speaking, one would recover the data matrix by solving the following optimization problem:

$$\begin{aligned} \min_{\mathbf{X} \in \mathbb{R}^{n \times n}} \quad & \text{rank}(\mathbf{X}) \\ \text{s.t.} \quad & X_{i,j} = M_{i,j}, (i,j) \in \Omega \end{aligned} \quad (2.2)$$

where \mathbf{X} is the decision variable, Ω represents the set of locations corresponding to the observed entries ($(i,j) \in \Omega$ if $M_{i,j}$ is observed), and $\mathbf{M} = [M_{i,j}]$ is a matrix

of same dimensions of \mathbf{X} , with some unknown entries.

Comparing this problem definition to the TIM problem of Section 2.1, one can observe that TIM can also be formulated as an LRMC problem. The reason is that the TIM adjacency matrix includes also some missing entries. As for the set Ω , it contains the indices that correspond to the positions of the predefined 0s and ones (all ones on the diagonal entries). The objective of TIM is then to minimize the rank of the TIM adjacency matrix knowing the relation between the rank of this matrix and the degrees-of-freedom (DoF) of the system (as will be shown in Section 2.1.2). The aim is then to fill the missing entries in such a way to minimize the matrix rank. In other words, minimizing the rank leads to an increase in the system DoF, and hence to know the transmitters that can send simultaneously.

Unfortunately, the rank minimization problem is NP-hard [24]. However, many relaxation methods have been proposed in the literature (as will be shown in Chapter 3). Although these methods proved their efficiency in minimizing the rank in different LRMC problems, but they cannot be directly applied here. The reason for this is the presence of all ones on the diagonal entries. To this end, we develop, in Chapter 4, three rank minimization methods that overcome the TIM matrix special structure.

2.1.2 Degrees-of-Freedom

The main metric considered in this thesis is the symmetric degrees-of-freedom (DoF), in line with existing works on TIM [26]. The reason behind using this metric (which is widely used in different contexts and not only TIM) in specific is that it considerably simplifies the analysis and gives useful insights on the network performance [26]. In the following, we state the definition for DoF as it appears in the literature.

DoF is defined as the pre-log factor of the information-theoretic capacity at high signal-to-noise ratio (SNR) [23]: it actually represents the capacity of the underlying linear communication network, where the received signals are simply linear combinations of transmitted signals, and weak channels are set to zero, making the DoF a first-order capacity approximation. DoF evaluates the achievable rates normalized by $\log(SNR)$, and hence, it indicates the system throughput in the high SNR regime, where every source's transmit power is increased proportionately, while the noise floor is fixed. If there exists a sequence of achievable rate allocations $R(W)$, such that the limit $R(W)/\log(SNR)$ exists for all $W \in \mathcal{W}$ as $SNR \rightarrow \infty$, then these limiting values are said to be an achievable

DoF allocation [19]:

$$\text{DoF}(W) = \lim_{SNR \rightarrow \infty} \frac{R(W)}{\log(SNR)}, \forall W \in \mathcal{W} \quad (2.3)$$

The closure of the set of achievable DoF allocations is called the DoF region and denoted as \mathcal{DOF} . The symmetric DoF value, DoF_{sym} of the network is the largest value DoF_o , such that the DoF allocation $\text{DoF}(W) = \text{DoF}_o, \forall W \in \mathcal{W}$, is inside the DoF region. It also represents the DoF value that can be achieved by all users simultaneously:

$$\text{DoF}_{\text{sym}} = \lim_{P \rightarrow \infty} \sup \sup_{(R_{\text{sym}}, \dots, R_{\text{sym}}) \in \mathcal{C}} \frac{R_{\text{sym}}}{\log P} \quad (2.4)$$

where P denotes the average transmit power, \mathcal{C} stands for the set of all achievable rate tuples, and \sup is the supremum, the maximum value.

In TIM, where the network is partially connected, there exists a relation between the rank r of the adjacency matrix and the symmetric DoF achieved. If we use M_1, \dots, M_n to denote the number of streams in a network of n D2D pairs, the achievable DoFs will be given by $\frac{M_1}{\text{rank}(\mathbf{X}^*)}, \dots, \frac{M_n}{\text{rank}(\mathbf{X}^*)}$ where \mathbf{X}^* is the matrix with the lowest rank. In this work, we assume for convenience a single data stream transmission per D2D pair (i.e., $M_i = 1, \forall i$). This implies that the DoF for each user is $\text{DoF} = \frac{1}{\text{rank}(\mathbf{X}^*)} = \frac{1}{r}$. By this, changing r affects the number of non-interfering Gaussian channels that the network can support simultaneously [19], i.e., minimizing r increases the system degrees-of-freedom (DoF). Therefore, the DoF of an interference channel can be interpreted as the multiplexing gain, i.e., the number of interference free signaling dimensions, including time, frequency, or space.

One of the main objectives of this thesis is thus to propose rank minimization methods that allow to minimize the rank of the adjacency matrix, while respecting the special structure of the TIM matrix (having all ones on its main diagonal).

2.1.3 Relation between TIM and Index Coding

It has been established in the literature that the topological interference management (TIM) problem, in terms of degrees-of-freedom (DoF), is equivalent to the index coding problem with linear schemes [19, 22]. More specifically, the optimal solution to the latter is the outer bound of the former, and the linear solution to the former is automatically transferrable to the latter. As for the considered matrices in both problems, the index coding matrix \mathbf{N} is the complement of the TIM adjacency matrix \mathbf{X} : the rows of the TIM adjacency matrix are equal to the column of the index coding problem. However, both matrices will be reduced

to the same rank since the row rank is equal to the column rank.

The importance of the aforementioned relation between the TIM problem and the index coding problem appears in Chapter 4, where we adopt the low-rank matrix completion (LRMC) approach to solve TIM. In Chapter 4, we compare the performance of our proposed rank minimization algorithms against other methods that are usually used for the index coding problem, such as directional alternating projection (dirAP), alternating projection via singular value decomposition (SVDAP) and directional alternating projection via SVD (dirSVDAP). The adjacency matrix \mathbf{X} and its complement \mathbf{N} will be used as inputs to our algorithm and to the different index coding methods, respectively. Then, the rank of the output matrices are compared.

Recall that an index coding problem arises when a single source intends to communicate to a number of receivers over a rate-limited noiseless broadcast channel. The sender has a number of messages and each receiver desires a specific subset of messages, while having another subset as side information. A single encoding of these messages can be transmitted in each channel use [36]. The incomplete matrix $\mathbf{N} = [N_{i,j}]$ of the index coding problem has as dimensions the number of rows equal to number of messages and the number of columns equal to number of receivers, as for its elements $N_{i,j}$:

$$N_{i,j} = \begin{cases} 1 & \text{if the receiver } j \text{ desires the message } i \\ 0 & \text{if receiver } j \text{ neither desires message } i \text{ nor has it as side information} \\ * & \text{if the receiver } j \text{ has the message } i \text{ as side information (caches it)} \end{cases} \quad (2.5)$$

Note here that if $N_{i,j} = "*"$, the message may be removed from the received signal if it arrives. Identifying unknown elements of the incomplete matrix in a way that the completed matrix has the minimum possible rank is equivalent to designing a binary scalar linear index code with minimum number of channel uses. The objective is to design an encoding scheme at the transmitter, called index code, with minimum number of channel uses that satisfies all clients [2]. The index code has as a goal to reduce the number of bits broadcasted by a transmitter with different demands and side infos. This can be seen as finding L_{min} , the minimum number of broadcasted messages achieved by scalar linear index codes, which is equivalent to minimizing the rank of the matrix \mathbf{N} . In the i^{th} transmission, a combination of messages specified by the i^{th} independent column is transmitted. Each receiver decodes its desired message knowing how its corresponding column is constructed based on the independent columns. As a result, the number of independent columns is the length of the index code, and the minimum rank matrix completion is an approach to design a code with minimum possible length over a finite field. Each user can decode its requested packet by using the broadcast packets and its side information. An index coding scheme is said to be achievable if each destination is able to decode its intended

message successfully [21].

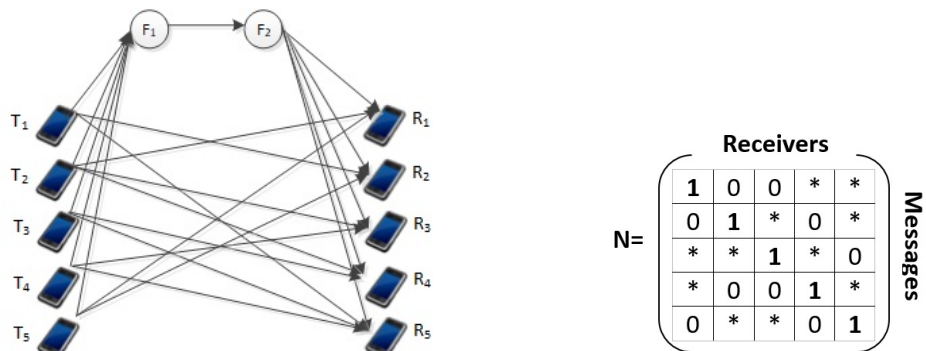


Figure 2.2: (a) Corresponding index coding problem to the 5×5 topology of Fig. 2.1, and (b) its associated incomplete matrix

As an illustration, we show in Fig. 2.2(a) a directed graph having exactly one link with finite capacity (also known as the bottleneck link) and multiple unicast wireline communication networks, and in (b) its associated incomplete matrix. For instance, in the TIM context, receiver R_1 (1st row in the TIM adjacency matrix \mathbf{X} in Fig. 2.1(b)) does not suffer from interference coming from transmitters T_2 and T_5 (second and fifth column of \mathbf{X}). From index coding perspective, this can be explained as R_1 (first column of \mathbf{N}) possesses the messages of T_2 and T_5 as side information, so that it can cancel them out.

2.2 Mathematical Background

In this section, we give a brief review of some basic concepts from linear algebra. The treatment is by no means complete, and is meant mostly to set out our notation throughout the thesis.

2.2.1 Basic Notions

Dealing with matrices in our optimization problems, several norms and functions are borrowed from linear algebra such as nuclear norm, frobenius norm, ℓ_2 norm and trace function that can be defined as follows:

2.2.1.1 Norms

For an $n \times n$ matrix \mathbf{A} , the matrix norms can be defined as follows:

- Nuclear norm: $\|\mathbf{A}\|_* := \sum_i^n \sigma_i$, where σ_i is the i^{th} singular value of \mathbf{A}

- Frobenius norm: $\|\mathbf{A}\|_F := \sqrt{(\sum_i^n \sum_j^n |A_{i,j}|^2)} = \sqrt{\sum_i^n \sigma_i^2}$
- ℓ_2 norm: $\|\mathbf{A}\|_2 := \sqrt{\sum_{k=1}^n |A_k|^2}$

2.2.1.2 Trace

Definition 1. (*Trace*) The trace of an $n \times n$ matrix \mathbf{A} is defined as $\text{Trace}(\mathbf{A}) = \sum_{i=1}^n A_{i,i}$. It is a linear form on $\mathbb{R}^{n \times n}$ and fulfills the following properties [37]:

- $\text{Trace}(\mathbf{A}) = \text{Trace}(\mathbf{A}^T)$
- $\text{Trace}(\mathbf{A}\mathbf{B}) = \text{Trace}(\mathbf{B}\mathbf{A})$
- If \mathbf{A} is symmetric, then the trace of \mathbf{A} is equal to the sum of the eigenvalues of \mathbf{A} .

2.2.1.3 Rank

One of the main objectives of this thesis is to develop rank minimization methods, as presented in Chapter 4. The reason is that when the low-rank matrix completion approach (LRMC) is adopted to solve TIM, the system degrees-of-freedom (DoF) metric (which we consider as our main figure of merit) is inversely proportional to the rank (as discussed in Section 2.1.2). To this end, we provide here multiple equivalent definitions for the rank.

Definition 2. (*Rank*) The rank of a matrix $\mathbf{A} \in \mathbb{R}^{m \times n}$ (where $m \geq n$) is equal to:

- the number of non-zero and independent columns or rows of this matrix: these columns or rows are linearly independent if and only if $\det(\mathbf{A}) \neq 0$ (the column rank and the row rank are always equal).
- the number of non-zero rows in a row-reduced echelon form.
- the number of pivots in a row-reduced echelon form.
- the number of non-zero singular values.
- the upper bound of the number of the non-zero eigenvalues, i.e., the number of non-zero eigenvalues of a matrix \mathbf{A} is at most $\text{rank}(\mathbf{A})$.

The rank of a matrix is equal to 0 only if the matrix has no elements. If a matrix has even one element, its minimum rank is equal to 1. A matrix is said to be a full rank matrix, when its rank is equal to n . The nuclear norm of a matrix is related to its rank because while the rank measures the number of non-zero singular values, the nuclear norm is their sum.

2.2.1.4 M-matrix

In Chapter 5, we use the concept of M-matrices [38] while applying the diagonal perturbation method in order to improve the eigenvalue-based bound that corresponds to the clustering problem.

Definition 3. (*M-matrix*) A matrix \mathbf{A} is an M-matrix if $\mathbf{A} = \alpha\mathbf{I} - \mathbf{B}$ with $\mathbf{B} \geq 0$ and $\alpha \geq \rho(\mathbf{B})$, where \mathbf{I} is the all ones matrix and $\rho(\mathbf{B})$ stands for the spectral radius of \mathbf{B} , and so ρ represents the largest absolute value of \mathbf{B} 's eigenvalues.

2.2.1.5 Singular Value Decomposition

The singular value decomposition (SVD) problem is used in Eckart and Young theorem (explained in Section 2.2.3) that helps in assessing the rank of the output matrices of Chapter 4.

Definition 4. (*Singular Value Decomposition, SVD*) The singular value decomposition (SVD) is a decomposition of a general $m \times n$ matrix \mathbf{A} with $m \geq n$ of the form [39]

$$\mathbf{A} = \sum_{i=1}^n \mathbf{u}_i \sigma_i \mathbf{v}_i^T \quad (2.6)$$

where \mathbf{u}_i and \mathbf{v}_i are orthonormal, i.e., $\mathbf{u}_i^T \mathbf{u}_j = \mathbf{v}_i^T \mathbf{v}_j = \delta_{i,j}$, and the singular values σ_i are nonnegative quantities which appear in non-decreasing order,

$$\sigma_1 \geq \sigma_2 \geq \dots \geq \sigma_n \geq 0 \quad (2.7)$$

2.2.1.6 Pseudo-inverse or Moore-Penrose inverse

The use of the pseudo-inverse appears in the Tikhonov regularization (detailed in Section 2.2.2), as well as in the conditions of the Schur complement for the positive semi-definiteness (detailed in Section 2.2.5).

Definition 5. (*Pseudo-inverse*) Let $\mathbf{A} = \mathbf{U}\mathbf{\Sigma}\mathbf{V}^T$ be the SVD of $\mathbf{A} \in \mathbb{R}^{m \times n}$ with $\text{rank}(\mathbf{A}) = r$. The pseudo-inverse or Moore-Penrose inverse of \mathbf{A} is defined as:

$$\mathbf{A}^\dagger = \mathbf{V}\mathbf{\Sigma}^{-1}\mathbf{U}^T \in \mathbb{R}^{n \times m} \quad (2.8)$$

Alternative expressions for the pseudo-inverse are also:

$$\mathbf{A}^\dagger = \lim_{\epsilon \rightarrow 0} (\mathbf{A}^T \mathbf{A} + \epsilon \mathbf{I})^{-1} \mathbf{A}^T = \lim_{\epsilon \rightarrow 0} \mathbf{A}^T (\mathbf{A} \mathbf{A}^T + \epsilon \mathbf{I})^{-1} \quad (2.9)$$

where the limits are taken with $\epsilon > 0$, which ensures that the inverses in the expressions exist. If $\text{rank}(\mathbf{A}) = n$, then $\mathbf{A}^\dagger = (\mathbf{A}^T \mathbf{A})^{-1} \mathbf{A}^T$. If $\text{rank}(\mathbf{A}) = m$, then $\mathbf{A}^\dagger = \mathbf{A}^T (\mathbf{A} \mathbf{A}^T)^{-1}$. If \mathbf{A} is square and nonsingular, then $\mathbf{A}^\dagger = \mathbf{A}^{-1}$ [40].

2.2.2 Tikhonov Regularization

Several semi-definite rank minimization algorithms have been studied in the literature. One of which is the pseudo-inverse reformulation [41], based on which we develop our first rank minimization method in Chapter 4, named as *RM-TIM*. In this method, the rank function is equivalently formulated as: $\text{rank}(\mathbf{A}) = \text{Trace}(\mathbf{A}^\dagger \mathbf{A})$. However, the pseudo-inverse function is not continuous (similar to the rank function), and one can use a Tikhonov regularization technique to approximate the pseudo-inverse as follows:

$$\mathbf{A}^\dagger = \lim_{\epsilon \rightarrow 0} (\mathbf{A}^T \mathbf{A} + \epsilon \mathbf{I})^{-1} \mathbf{A}^T = \lim_{\epsilon \rightarrow 0} \mathbf{A}^T (\mathbf{A} \mathbf{A}^T + \epsilon \mathbf{I})^{-1} \quad (2.10)$$

By this, the rank minimization method can be approximated to any level of accuracy via a continuous optimization. In the following, we define Tikhonov regularization, as a method that permits to inverse a matrix not well-conditioned. Recall that the matrix is well conditioned when its inverse can be computed with good accuracy. If the condition number is very large, then the matrix is said to be ill-conditioned.

Definition 6. (Tikhonov Regularization) *Suppose that for a known matrix \mathbf{A} and vector \mathbf{y} , we wish to find a vector \mathbf{x} such that [42]:*

$$\mathbf{A} \mathbf{x} = \mathbf{b} \quad (2.11)$$

The standard approach is ordinary least squares linear regression. However, if no solutions exist or multiple solutions exist, the problem is said to be ill-posed. Therefore, in order to give preference to a particular solution with desirable properties, a regularization term can be included in this minimization:

$$\mathbf{x}_\Gamma = \arg \min \|\mathbf{A} \mathbf{x} - \mathbf{b}\|_2^2 + \|\Gamma \mathbf{x}\|_2^2 \quad (2.12)$$

or some suitably chosen Tikhonov matrix Γ . In many cases, this matrix is chosen as a multiple of the identity matrix ($\Gamma = \epsilon \mathbf{I}$), giving preference to solutions with smaller norms, and penalizing solutions of large norms; this is known as L_2 regularization. The problem in (2.12) then becomes:

$$\mathbf{x}_\epsilon = \underbrace{(\mathbf{A}^T \mathbf{A} + \epsilon \mathbf{I}) \mathbf{A}^T}_{R_\epsilon} \mathbf{y} \quad (2.13)$$

Definition 7. (Tikhonov Filtering) *In case of Tikhonov regularization, using the SVD of an $n \times n$ matrix \mathbf{A} , as $\mathbf{A} = \mathbf{U} \mathbf{S} \mathbf{V}^T$ (with $\sigma_i > 0$), then R_ϵ in (2.13)*

can be written as:

$$\begin{aligned}
R_\epsilon &= (\mathbf{A}^T \mathbf{A} + \epsilon \mathbf{I}) \mathbf{A}^T \\
&= (\mathbf{V} \mathbf{S}^T \mathbf{U}^T \mathbf{U} \mathbf{S} \mathbf{V}^T + \epsilon \mathbf{V} \mathbf{I} \mathbf{V}^T)^{-1} \mathbf{V} \mathbf{S}^T \mathbf{U}^T \\
&= \mathbf{V} (\mathbf{S}^T \mathbf{S} + \epsilon \mathbf{I})^{-1} \mathbf{S}^T \mathbf{U}^T \\
&= \mathbf{V} \text{diag} \left(\underbrace{\frac{\sigma_i^2}{\sigma_i^2 + \epsilon}}_{w_\epsilon(\sigma_i^2)} \quad \frac{1}{\sigma_i} \right) \mathbf{U}^T
\end{aligned} \tag{2.14}$$

if $\epsilon \rightarrow 0$, then $w_\epsilon(\sigma_i^2) \rightarrow 1$, so $R_\epsilon \rightarrow \mathbf{V} \text{diag}(\frac{1}{\sigma_i}) \mathbf{U}^T \stackrel{\text{def}}{=} \mathbf{A}^\dagger$, as $\epsilon \rightarrow 0$. The plot of the Tikhonov filter function $w_\epsilon^{\text{Tikh}}(\sigma_i^2) = \frac{\sigma_i^2}{\sigma_i^2 + \epsilon}$ shows that Tikhonov regularization operates like a smooth filter: it filters out the singular components that are small (relative to ϵ), while retaining the large components [43]. This approach is adjusted thanks to a regularization parameter ϵ . The optimal value of this parameter ϵ is specific to each problem and is usually unknown. In practical problems, it is determined by an ad hoc method [44].

In the first proposed rank minimization method in Chapter 4, we take benefit from Tikhonov filtering to filter out the small singular values. This hence leads to decreasing the rank up to a certain precision.

2.2.3 Eckart and Young Theorem

According to the rank definition in Section 2.2.1, the rank of a matrix is equal to number of non-zero singular values. In this thesis, we rely on Eckart and Young theorem to determine which singular values can be neglected, and hence to induce the rank of the matrix resulting from the approximation method that we developed.

Eckart and Young theorem states that approximating a matrix \mathbf{A} with another matrix $\hat{\mathbf{A}}_k$ (said as truncated) of a specific rank k , is based on minimizing the Frobenius norm of the difference between \mathbf{A} and $\hat{\mathbf{A}}_k$ under the constraint that $\text{rank}(\hat{\mathbf{A}}_k) = k$, such that $\hat{\mathbf{A}}_k = \mathbf{U}_k \mathbf{\Sigma}_k \mathbf{V}_k^T$. This is achieved by taking the sum of the biggest k elements of the Singular Value Decomposition (SVD) of $\mathbf{A} = \mathbf{U} \mathbf{\Sigma} \mathbf{V}^T$, i.e., $\mathbf{\Sigma}_k$ is the same matrix as $\mathbf{\Sigma}$ but it contains only the k largest singular values (the remaining σ_i values are replaced by zero) [45].

Definition 8. (Eckart and Young Theorem) Let $\mathbf{A} = \mathbf{U} \mathbf{\Sigma} \mathbf{V}^T \in \mathbb{R}^{m \times n}$, $m \geq n$ be the singular value decomposition (SVD) of \mathbf{A} . Then, for any rank- k matrix $\hat{\mathbf{A}}_k$:

$$\|\mathbf{A} - \hat{\mathbf{A}}_k\|_F \geq \|\mathbf{A} - \mathbf{U}_k \mathbf{\Sigma}_k \mathbf{V}_k^T\|_F = \sqrt{\sum_{i=k+1}^n \sigma_i^2} \tag{2.15}$$

The proof for this theorem can be found in [45].

2.2.4 QR Decomposition

In this thesis, we rely on the QR decomposition in order to get the precoding and decoding matrices, \mathbf{V} and \mathbf{U} , respectively. The reason for this is that the adjacency matrix \mathbf{X} is equal to $\mathbf{X} = \mathbf{UV}$.

Definition 9. (QR decomposition) Given an $m \times n$ matrix \mathbf{A} , its QR decomposition is a matrix decomposition of the form

$$\mathbf{A} = \mathbf{QR} \quad (2.16)$$

where \mathbf{R} is an upper triangular matrix and \mathbf{Q} is an orthogonal matrix, i.e., one satisfying

$$\mathbf{Q}^T \mathbf{Q} = \mathbf{I} \quad (2.17)$$

where \mathbf{Q}^T is the transpose of \mathbf{Q} and \mathbf{I} is the identity matrix [46].

If \mathbf{A} has z linearly independent columns, then the first z columns of \mathbf{Q} form an orthonormal basis for the column space of \mathbf{A} [47]. More generally, the first k columns of \mathbf{Q} form an orthonormal basis for the span of the first k columns of \mathbf{A} for any $1 \leq k \leq z$. The fact that any column k of \mathbf{A} only depends on the first k columns of \mathbf{Q} is responsible for the triangular form of \mathbf{R} .

There are several methods for actually computing the QR decomposition, such as by means of the Gram–Schmidt process, Householder transformations, or Givens rotations. Each has a number of advantages and disadvantages. As an example, we present here the Matlab code of the Gram–Schmidt process [48]:

```
[m,n] = size(A);
Q = zeros(m,n);
R = zeros(n,n);
for j = 1 : n
    v = A(:,j);
    for i = 1 : j - 1
        R(i,j) = Q(:,i)' * A(:,j);
        v = v - R(i,j) * Q(:,i);
    end
    R(j,j) = norm(v);
    Q(:,j) = v/R(j,j);
end
```

2.2.5 Semi-definite Programming

Our main analysis tool throughout the thesis is the semi-definite programming (SDP), based on which we formulate our different proposed rank minimization methods in Chapter 4, and we develop our clustering problem in Chapter 5.

2.2.5.1 Basic Facts

SDP is an example of a special kind of convex program, that is efficiently solvable in both theoretical and practical senses. It is the broadest class of convex optimization problems. In particular, SDP is the optimization problem of a linear function of a symmetric matrix subject to linear equality constraints and the constraint that the matrix be positive semi-definite [49]. More importantly, SDP can compute an optimal solution, within given additive error ϵ , in time polynomial in the input size n and $\log \epsilon^{-1}$ [49]. For this reason, we choose to use SDP as a backbone for solving our optimization problems all over this thesis. This PSD cone has properties that aid us in finding a low-rank matrix which will always lie on the boundary of the cone.

As defined in [50], the objective of an SDP problem is to minimize a linear objective over linear equalities and linear matrix inequalities (LMI) on variables $\mathbf{x} \in \mathbb{R}^n$ (more details about LMI can be found in the following subsection):

$$\begin{aligned} \min \quad & \mathbf{c}^T \mathbf{x} \\ \text{s.t.} \quad & x_1 \mathbf{F}_1 + \dots + x_n \mathbf{F}_n + \mathbf{F}_0 \succeq 0 \\ & \mathbf{A}\mathbf{x} = \mathbf{b} \end{aligned} \tag{2.18}$$

where the problem data are the scalars x_1, \dots, x_n and the $(n+1)$ symmetric matrices $\mathbf{F}_0, \dots, \mathbf{F}_n$.

In the standard form, the SDP aim corresponds to minimizing a matrix inner product over equality constraints on inner products on variables $\mathbf{X} \in \mathbb{S}^n$ as:

$$\begin{aligned} \min_{\mathbf{X} \in \mathbb{S}^n} \quad & \text{Trace}(\mathbf{C}\mathbf{X}) \\ \text{s.t.} \quad & \text{Trace}(\mathbf{A}_i \mathbf{X}) = b_i, i = 1, \dots, m \\ & \mathbf{X} \succeq 0 \end{aligned} \tag{2.19}$$

where the input data is $\mathbf{C} \in \mathbb{S}^n$, $\mathbf{A}_i \in \mathbb{S}^n$, $i = 1, \dots, m$, $b_i \in \mathbb{R}$, $i = 1, \dots, m$. As for $\succeq 0$, it denotes that the matrix is positive semi-definite (PSD) (more details about what a PSD matrix means can be found in this section)

In the following, we discuss the most important characteristics and theorems that are related to SDP and used in this work.

Definition 10. (Positive Semi-definite Matrix) A matrix $\mathbf{X} \in \mathbb{S}^n$ is said to be positive semi-definite (PSD) if for every vector $\mathbf{a} \in \mathbb{R}^n$, $\mathbf{a}^T \mathbf{X} \mathbf{a} \geq 0$. The following statements are equivalent for a symmetric matrix \mathbf{X} [37]:

1. \mathbf{X} is positive semi-definite, written as $\mathbf{X} \succeq 0$, and defined as $\mathbf{a}^T \mathbf{X} \mathbf{a} \geq 0$ for all $x \in \mathbb{R}^n$.
2. all eigenvalues of \mathbf{X} are non-negative, i.e., the spectral decomposition of \mathbf{X} is of the form $\mathbf{X} = \sum_{i=1}^n \lambda_i \mathbf{u}_i \mathbf{u}_i^T$ with all $\lambda_i \geq 0$
3. there exists a matrix \mathbf{B} such that $\mathbf{X} = \mathbf{B}^T \mathbf{B}$ where \mathbf{B} can either be a (possibly singular) $n \times n$ matrix, or an $m \times n$ matrix for some $m \leq n$. This matrix \mathbf{B} can be obtained in polynomial time using Cholesky decomposition, as will be explained later.
4. there exist vectors $\mathbf{v}_1, \dots, \mathbf{v}_n \in \mathbb{R}^k$ (for some $k \geq 1$) such that $X_{i,j} = \mathbf{v}_i^T \mathbf{v}_j$ for all $i, j \in [n]$; the vectors \mathbf{v}_i 's are called a Gram representation of \mathbf{X} .
5. all principal minors of \mathbf{X} are non-negative, where the k^{th} principal minor of \mathbf{X} is the determinant of its upper-left $k \times k$ sub-matrix.

Definition 11. (Spectral Decomposition Theorem) Any real symmetric matrix $\mathbf{X} \in \mathbb{S}^n$ can be decomposed as [37]:

$$\mathbf{X} = \sum_{i=1}^n \lambda_i \mathbf{u}_i \mathbf{u}_i^T \quad (2.20)$$

where $\lambda_1, \dots, \lambda_n \in \mathbb{R}$ are the eigenvalues of \mathbf{X} and $\mathbf{u}_1, \dots, \mathbf{u}_n \in \mathbb{R}^n$ denote the corresponding eigenvectors which form an orthonormal basis of \mathbb{R}^n . From matrix perspective, $\mathbf{X} = \mathbf{P} \mathbf{D} \mathbf{P}^T$, where \mathbf{D} is the diagonal matrix with the eigenvalues λ_i 's on the diagonal entries and \mathbf{P} is the orthogonal matrix with the \mathbf{u}_i 's as its columns.

2.2.5.2 Cholesky Decomposition

In Chapter 5, we use Cholesky Decomposition to decompose the PSD matrix \mathbf{Y}_{FJ} present in the clustering optimization problem into another matrix \mathbf{B} , where the former matrix represents the Gram matrix of the vectors of \mathbf{B} . More specifically, the columns and rows of \mathbf{Y}_{FJ} correspond to the nodes' indices present in the network. As for its entries, they give an approximate indication of which devices belong to the same cluster, but not an exact one, since the solved SDP problem is relaxed. Here appears the importance of extracting \mathbf{B} in order to give better insights about the partitions: each column of \mathbf{B} corresponds to a node, and these columns are then compared against k independent vectors. The nodes with vectors that are similar to the same independent vector are then grouped together.

Definition 12. (Cholesky Decomposition) Given a symmetric positive semi-definite matrix \mathbf{X} , the Cholesky decomposition is an upper triangular matrix \mathbf{B} with strictly positive diagonal entries such that:

$$\mathbf{X} = \mathbf{B}^T \mathbf{B} \quad (2.21)$$

where the diagonal entries $B_{j,j}$ and the off-diagonal values $B_{i,j}$ of \mathbf{B} are as follows:

$$\begin{aligned} B_{j,j} &= \sqrt{X_{j,j} - \sum_{k=1}^{j-1} B_{j,k}^2} \\ B_{i,j} &= \frac{1}{B_{j,j}} \left(X_{i,j} - \sum_{k=1}^{j-1} B_{i,k} B_{j,k} \right) \text{ for } i > j \end{aligned} \quad (2.22)$$

2.2.5.3 Schur Complements

The notion of Schur complement is very useful for showing positive semi-definiteness [51] in our work throughout the proposed rank minimization methods.

Definition 13. (Schur complement) Consider a symmetric matrix \mathbf{X} in block form as:

$$\mathbf{X} = \begin{pmatrix} \mathbf{A} & \mathbf{B} \\ \mathbf{B}^T & \mathbf{C} \end{pmatrix} \succeq 0 \quad (2.23)$$

with $\mathbf{A} \in \mathbb{R}^{n \times n}$, $\mathbf{B} \in \mathbb{R}^{n \times l}$ and $\mathbf{C} \in \mathbb{R}^{l \times l}$. Assume that \mathbf{A} is non-singular. Then the matrix $\mathbf{C} - \mathbf{B}^T \mathbf{A}^{-1} \mathbf{B}$ is called the Schur complement of \mathbf{A} in \mathbf{X} [51–53].

Lemma 1. Let $\mathbf{X} \in \mathbb{S}^n$ be in the block form of (2.23), where \mathbf{A} is non-singular [51–53]. Then,

$$\mathbf{X} \succeq 0 \iff \mathbf{A} \succeq 0 \text{ and } \mathbf{C} - \mathbf{B}^T \mathbf{A}^{-1} \mathbf{B} \succeq 0 \quad (2.24)$$

2.2.5.4 Linear Matrix Inequalities

Many optimization problems present in this thesis are formulated using linear matrix inequalities (LMI).

Definition 14. (Linear Matrix Inequality, LMI) In convex optimization, a linear matrix inequality (LMI) is an affine (linear) matrix-valued function, such as:

$$\mathbf{F}(x) = \mathbf{F}_0 + \sum_{i=1}^n x_i \mathbf{F}_i \succeq 0 \quad (2.25)$$

where $\mathbf{x} \in \mathbb{R}^n$ are called the decision variables and $\mathbf{F}_i = \mathbf{F}_i^T \in \mathbb{R}^{n \times n}$ are symmetric matrices. The LMI in (2.25) is equivalent to a set of n polynomial inequalities in x . It is a convex constraint on x , i.e., the set $\{x | \mathbf{F}(x) \succeq 0\}$ is convex [54].

When the matrices \mathbf{F}_i are diagonal, the LMI $\mathbf{F}(x) \succeq 0$ is just a set of linear inequalities.

Nonlinear (convex) inequalities can also be converted to LMI form using Schur complements. For instance, the LMI

$$\begin{pmatrix} \mathbf{A} & \mathbf{B} \\ \mathbf{B}^T & \mathbf{C} \end{pmatrix} \succeq 0 \quad (2.26)$$

where $\mathbf{A} = \mathbf{A}^T$, $\mathbf{C} = \mathbf{C}^T$, and \mathbf{B} depend affinely on x , is equivalent to

$$\mathbf{C} \succeq 0, \mathbf{A} - \mathbf{B}\mathbf{C}^{-1}\mathbf{B}^T \succeq 0 \quad (2.27)$$

In other words, the set of nonlinear inequalities (2.27) can be represented as the LMI of (2.25). These LMIs are usually solved using interior-point algorithms. For more details, the reader can refer to [54].

2.2.6 Second-order Cone Programming

One of the constraints of the optimization problem that appears in Section 4.4 of Chapter 4 is quadratic, which makes the problem a second-order cone program (SOCP) convex optimization one. To this end, we give in this section some details about SOCP, based on [53, 55].

Definition 15. (Second-order cone programming, SOCP) *SOCPs are nonlinear convex problems that include linear and (convex) quadratic programs as special cases, but are less general than semi-definite programs (SDPs) [55]. In an SOCP program, a linear function is minimized over the intersection of an affine set and the product of second-order (quadratic) cones.*

The standard form for SOCP can be written as:

$$\begin{aligned} \min_{\mathbf{x}} \quad & \mathbf{f}^T \mathbf{x} \\ \text{s.t.} \quad & \|\mathbf{A}_i \mathbf{x} + \mathbf{b}_i\|_2 \leq \mathbf{c}_i^T \mathbf{x} + \mathbf{d}_i, \quad i = 1, \dots, m \\ & \mathbf{F} \mathbf{x} = \mathbf{g} \end{aligned} \quad (2.28)$$

where the problem parameters are $\mathbf{f} \in \mathbb{R}^n$, $\mathbf{x} \in \mathbb{R}^n$ is the optimization variable, $\mathbf{A}_i \in \mathbb{R}^{k_i \times n}$, $\mathbf{b}_i \in \mathbb{R}^{k_i}$, $\mathbf{c}_i \in \mathbb{R}^n$, $\mathbf{d}_i \in \mathbb{R}$, $\mathbf{F} \in \mathbb{R}^{p \times n}$ and $\mathbf{g} \in \mathbb{R}^p$.

Therefore, a constraint of the form $\|\mathbf{A}\mathbf{x} + \mathbf{b}\|_2 \leq \mathbf{c}^T \mathbf{x} + \mathbf{d}$ is called a second-order constraint. The terminology of "SOCP" comes from its connection to the second order cone (also called the Lorentz cone or the ice-cream cone). This cone is represented as:

$$\mathcal{Q}_n := \left\{ \mathbf{x} = \begin{pmatrix} x_0 \\ \bar{x} \end{pmatrix} \succeq 0 \in \mathbb{R}^n : x_0 \geq \|\bar{x}\| \right\} \quad (2.29)$$

Or it can be written in Schur complement as:

$$\mathbf{x} = \begin{pmatrix} x_0 \\ \bar{x} \end{pmatrix} \in \mathcal{Q}_n \text{ if and only if } \begin{pmatrix} x_0 & \bar{x}^T \\ \bar{x} & x_0 \mathbf{I} \end{pmatrix} \succeq 0 \quad (2.30)$$

based on the proof present in [53]. Accordingly, the constraint $\|\mathbf{A}_i \mathbf{x} + \mathbf{b}_i\|_2 \leq \mathbf{c}_i^T \mathbf{x} + \mathbf{d}_i$ can be written as $\begin{pmatrix} \mathbf{c}_i^T \mathbf{x} + \mathbf{d}_i & (\mathbf{A}_i \mathbf{x} + \mathbf{b}_i)^T \\ \mathbf{A}_i \mathbf{x} + \mathbf{b}_i & (\mathbf{c}_i^T \mathbf{x} + \mathbf{d}_i) \mathbf{I} \end{pmatrix} \succeq 0$

2.2.7 Characteristic Polynomial Function

In Section 4.1.5 of Chapter 4, we rely on the coefficients of the characteristic polynomial function in order to deduce the optimal rank that a matrix can achieve. In Section 4.3 of the same chapter, we also make use of this polynomial function to reduce the rank of a matrix. The reason for this is that there exists a relation between the coefficients of this polynomial function and the eigenvalues of the corresponding matrix (as will be shown below). On the other hand, as previously defined in Section 2.2.1, the number of non-zero eigenvalues of a matrix is at most equal to the rank of this matrix. By this, reducing the value of the characteristic polynomial coefficients decreases the eigenvalues, and hence the matrix rank.

Definition 16. (Characteristic Polynomial Function) The characteristic polynomial function of a square $n \times n$ matrix \mathbf{X} is given by [56]:

$$\begin{aligned} p(\lambda) &= \det(\mathbf{X} - \lambda \mathbf{I}) = (-1)^n (\lambda - \lambda_1)(\lambda - \lambda_2) \dots (\lambda - \lambda_n) \\ &= (-1)^n [\lambda^n + c_1 \lambda^{n-1} + c_2 \lambda^{n-2} + \dots + c_{n-1} \lambda + c_n] \\ &= (-1)^n [\lambda^n - \lambda^{n-1} \text{Trace}(\mathbf{X}) + c_2 \lambda^{n-2} \\ &\quad + \dots + (-1)^{n-1} c_{n-1} \lambda + (-1)^n \det(\mathbf{X})] \end{aligned} \quad (2.31)$$

where the eigenvalues λ_i represent the roots of this polynomial, and \mathbf{I} stands for the identity matrix. As for the coefficients c_2, \dots, c_{n-1} , they can be expressed in terms of traces of powers of \mathbf{X} as:

$$\begin{aligned} c_m &= -\frac{t_m}{m} + \frac{1}{2!} \underbrace{\sum_{i=1}^{m-1} \sum_{j=1}^{m-1} \frac{t_i t_j}{ij}}_{i+j=m} - \frac{1}{3!} \underbrace{\sum_{i=1}^{m-2} \sum_{j=1}^{m-2} \sum_{k=1}^{m-2} \frac{t_i t_j t_k}{ijk}}_{i+j+k=m} + \dots + \frac{(-1)^m t_1^m}{m!}, \\ &\text{where } m = 1, 2, \dots, n, \text{ and } t_k = \text{Trace}(\mathbf{X}^k) \end{aligned} \quad (2.32)$$

or in terms of its eigenvalues as:

$$c_k = (-1)^k \sum_{i_1 < i_2 < \dots < i_k}^n \sum_{i_1=1}^n \sum_{i_2=1}^n \dots \sum_{i_k=1}^n \underbrace{\lambda_{i_1} \lambda_{i_2} \dots \lambda_{i_k}}_{k \text{ factors}}, \text{ for } k = 1, 2, \dots, n \quad (2.33)$$

2.3 Maximum-k-cut

In Chapter 5, we formulate a clustering scheme, that is specific for the low-rank matrix completion (LRMC) approach for solving TIM, using graph theory. This is achieved by building on the maximum-k-cut formulation, but with adding a new constraint on the cluster's size. In this section, we give a brief overview about max-k-cut, before detailing our proposed formulation in Chapter 5.

The maximum-k-cut problem is a combinatorial optimization problem which requires finding a set of edges whose removal would partition a graph into k connected components. These edges are referred to as k -cut and the goal is to find the cut with maximum weight [57]. This approach started with Goemans and Williamson [58], who considered the problem when $k = 2$, named as max-cut, and solved it using semi-definite programming (SDP) relaxation. Later, many papers in the literature based their work on [58] in order to extend the range of k to be any value. Other authors named this problem as minimum-k-partition problem, since minimizing the total weight of the edges between vertices in the same part of the partition (the induced subgraphs) is equivalent to maximizing the k-cut [59]. Eisenblatter in [59] proposed a SDP relaxation for the minimum k-partition problem using the approach similar to the one used in [57]. Existing works prove that the most attractive solution problem remains in the SDP formulation, since it leads to tighter relaxations than the classical linear programming relaxations. With this in mind, we formulate our clustering problem building on the SDP formulation of the max-k-cut problem, specifically (as will be shown in Chapter 5), while using Laplacian matrices.

2.3.1 Laplacian Matrix

To help the reader understand the formulation of the SDP formulation of the max-k-cut problem in Chapter 5, we provide here a brief overview of Laplacian matrices.

Definition 17. (Laplacian Matrix) We consider a weighted undirected graph $\mathcal{G} = (\mathcal{V}, \mathcal{E}, w)$, where $\mathcal{V} = \{1, \dots, n\}$ represents the vertex set, \mathcal{E} denotes the set of edges and $w_{i,j} = w_{j,i}$ indicates the weight for each pair of vertices i and j , $1 \leq i, j \leq n$ and $w_{i,i} = 0$. We define the adjacency matrix of this graph \mathcal{G} as $\mathbf{A}_{\mathcal{G}}$, where $\mathbf{A}_{\mathcal{G}}$ is a symmetric matrix of $n \times n$ dimensions, and its entries are such as:

$$\mathbf{A}_{\mathcal{G}} = \begin{cases} w_{i,j} & \text{if } (i, j) \in \mathcal{E} \text{ and} \\ 0 & \text{otherwise} \end{cases} \quad (2.34)$$

Additionally, we characterize the degree matrix of the weighted undirected graph

\mathcal{G} as $\mathbf{D}_{\mathcal{G}}$, where $\mathbf{D}_{\mathcal{G}}$ is a diagonal matrix such that:

$$\mathbf{D}_{\mathcal{G}}(i, i) = \sum_j \mathbf{A}_{\mathcal{G}}(i, j) \quad (2.35)$$

Consequently, we can write the Laplacian matrix of the weighted undirected graph \mathcal{G} , as $\mathbf{L}_{\mathcal{G}}$, and define it as:

$$\mathbf{L}_{\mathcal{G}} = \mathbf{D}_{\mathcal{G}} - \mathbf{A}_{\mathcal{G}} \quad (2.36)$$

Note that, for simplicity, we will omit the subscript \mathcal{G} from $\mathbf{L}_{\mathcal{G}}$, and we will write it as \mathbf{L} in the rest of the thesis. Therefore, if the Laplacian matrix $\mathbf{L} = [L_{i,j}]$, then $L_{i,j} = -w_{i,j}$ for $i \neq j$ and $L_{i,i} = \sum_{k=1}^n w_{i,k}$. This definition of \mathbf{L} implies also that $\mathbf{L}\mathbf{u}_n = 0$, where \mathbf{u}_n is the all ones n vector and that the symmetric matrix \mathbf{L} belongs to the set of positive semi-definite matrices, i.e., $\mathbf{L} \succeq 0$ in case that $\mathbf{A}_{\mathcal{G}} \geq 0$ elementwise. This is because $\mathbf{a}^T \mathbf{L} \mathbf{a} \geq 0 \forall \mathbf{a} \in \mathbb{R}^n$ leads to $\mathbf{L} \succeq 0$.

2.3.2 Laplacian Algebra

In Chapter 5, we determine some interesting bounds that serve in the computation of the performance guarantee of our proposed clustering algorithm and other algorithms as well (relatively to the optimal method). More specifically, we firstly develop an eigenvalue bound, while relying on the Laplacian algebra \mathcal{L} . To allow an easy understanding of these derivations, we provide in this section some foundations of this kind of algebra.

The Laplacian algebra \mathcal{L} is a set of matrices that is closed under addition, scalar and matrix multiplication, and conjugate transposes [60], [61]. It has a basis of matrices that are obtained from an orthonormal basis of eigenvectors corresponding to the eigenvalues of the Laplacian matrix \mathbf{L} . In particular, we let $0 = \lambda_0 \leq \lambda_1 < \dots < \lambda_d =: \lambda_{\max}(\mathbf{L})$ be the distinct eigenvalues of \mathbf{L} (note here that $d < n$ since some eigenvalues may be repeated and the objective is to search only for the span of \mathcal{L}), and \mathbf{A}_i be a matrix whose columns form an orthonormal basis of the eigenspace corresponding to the i^{th} eigenvalue λ_i , constituting $\mathbf{F}_i = \mathbf{A}_i \mathbf{A}_i^T$ for $i = 0, \dots, d$. We define $f_i = \text{rank}(\mathbf{F}_i)$ as the corresponding multiplicities. Thus, \mathcal{L} is now defined as the span of $\{\mathbf{F}_0, \dots, \mathbf{F}_d\}$, which is called the basis of idempotents of \mathcal{L} , and satisfy the following properties [60], [61]:

- $\mathbf{F}_i = \mathbf{A}_i \mathbf{A}_i^T$
- $f_i = \text{rank}(\mathbf{F}_i)$
- $\mathcal{L} = \text{span} \{ \mathbf{F}_0, \dots, \mathbf{F}_d \}$
- $\mathbf{I} = \sum_{i=0}^d \mathbf{F}_i$
- $\mathbf{L} = \sum_{i=0}^d \lambda_i \mathbf{F}_i$

- $\mathbf{F}_i \mathbf{F}_j = \delta_{i,j} \mathbf{F}_i$
- $\mathbf{F}_i = \mathbf{F}_i^*$
- $\text{Trace}(\mathbf{F}_i) = f_i = \text{rank}(\mathbf{F}_i)$
- $\mathbf{F}_0 = \frac{1}{n} \mathbf{J}_n$

2.4 Successive Interference Cancellation

In Section 4.3 of Chapter 4, we adopt the successive interference cancellation technique (SIC) to cancel the interference coming from devices in very close proximity. The effect of these devices can be really harmful, especially that their transmitted signals can be stronger than the desired one, and hence can overwhelm it.

SIC is a very well-know physical layer technique that applies nonlinear detection algorithms to cancel the interference [62]. Briefly, it is a key method for multi-user interference cancellation, that allows a user equipment (UE) to retrieve its signal and decode its own data [63]. As a matter of fact, the transmitted signals are superposed in the medium channel. Hence, the receiver receives a single waveform of superimposed information signals that are ordered by their signal strengths [64]. The receiver decodes the signals one by one until it finds the desired signal [65]. The first signal that SIC decodes is the strongest one while others are considered as interference [66]. The process continues until all the signals are detected.

In Fig. 2.3, we illustrate the multi-user signal separation procedure applied by SIC, while decoding the received signals in different stages. For instance, if the receiver receives three signals as in Fig. 2.3 (blue, green and pink waveforms), then the first stage is to decode the strongest signal (the green one) and the other two signals are considered as noise (or interference). In the second stage, the decoded signal (the green waveform) is subtracted from the combined received signal, and then the second strongest signal (the pink waveform) can be detected. This signal (the pink one) will also be subtracted in its turn from the composite signal (pink and blue waveforms) and the blue waveform (the weakest signal) is then detected. In this way, all the signals are revealed.

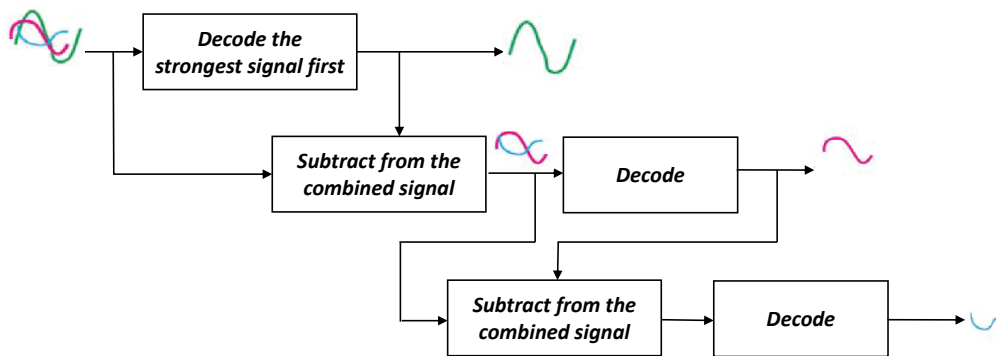


Figure 2.3: Successive interference cancellation technique (SIC)

Chapter 3

Literature Review

The aim of this chapter is to review the state-of-the-art which covers the interference management techniques that can be applied in Device-to-Device (D2D) enabled cellular networks. Then, we highlight the limitations of the existing methods for rank minimization of the TIM adjacency matrix, when modeled as a low-rank matrix completion problem (LRMC). After that, we discuss the clustering algorithms usually used in the interference alignment context and their cons. Finally, we present some existing applications for the successive interference cancellation technique (SIC).

Due to the detrimental effects of interference in D2D networks, extensive research has been conducted on the topic of interference management to offer reliable communications. Most proposed schemes can be classified into three categories: interference avoidance, interference cancellation and interference coordination [67]. First, the interference avoidance builds on orthogonal time-frequency resource allocation schemes, such as time-division multiple access (TDMA), frequency division multiple access (FDMA), and code division multiple access techniques (CDMA). These techniques are regarded as special cases of a more general scheme, namely the topological interference management (TIM) method [18]. Under the first category also fall the spectrum splitting [68], the power control [69], [70], the mode selection [71], [72], the radio resource allocation (using fractional frequency reuse [73], time-frequency hopping [74], graph theory [75], cognitive radio networks [76], clustering [77] or game theory [78]), the joint mode selection power control and the radio resource allocation [79]. The second scheme is interference cancellation which applies advanced signal processing techniques on the D2D links, including spatial diversity techniques, such as multiple-input multiple output (MIMO) (using precoding [80] and relay [81]), interference cancellation and regeneration [67], beamforming [82], coding (superposition coding [83] and rate splitting [84]), cooperative multipoint [85] and interference alignment [86], [87]. For example, a receive mode selection strategy for middle interference is proposed in [88] to mitigate the interference among the

users, and hence to improve the reliability of the users. Thirdly, the interference coordination method that employs intelligent power control and link scheduling schemes. For instance, a distributed dynamic spectrum protocol is proposed in [89] for multi-hop D2D users' opportunistic access in which the interference caused by the D2D users is reduced and kept within the allowed threshold. This requires significant intelligence to coordinate simultaneously active user and deal with harmful interference between them. In [90], a spectrum sharing protocol is designed for a scenario of D2D communications overlaying a cellular network. In this protocol, the D2D users can communicate in bidirectional communication mode, while assisting the two-way communications between the cellular base station and the cellular user. This hence optimises the resource allocation for an overlay cellular system and maximise sum rate of D2D system.

However, all these methods require either a *feedback* from the device or an exchange of channel state information (CSI). This rises the flag to find new schemes that do not depend on this heavy signaling, like the topological interference management (TIM) solution. In this thesis, we start by focusing on the interference avoidance technique, namely TIM. Then, we propose to combine it with an interference cancellation technique, like SIC. To the best of our knowledge, this is the first work that considers TIM as an interference management technique for D2D application, along with SIC.

3.1 Topological Interference Management

Interference avoidance, and TIM in specific, attracted a lot of follow-up research with various assumptions, such as transmit cooperation [21] and message passing [91], that have proved their efficiency in enhancing the achieved degrees-of-freedom (DoF). TIM has also been extended in various directions, e.g., with multiple and reconfigurable antennas [92, 93], and has been studied in cellular networks [94], where multiple layers of interference are included and its effect on DoF is analyzed. Additionally, TIM has been explored for multilevel connectivity scenarios [18], where the network is decomposed into two components, one that includes the interfering links and another that consists of the weak links which could be handled via power control. Besides, TIM has been studied in partial connectivity situations, e.g., with alternating connectivity [95], and fast fading scenarios [20], where a matrix rank-loss approach is proposed to find the network topology conditions, leading to a certain DoF. As for slow fading conditions, a direct relation between TIM and index coding has been established [19] to help solve TIM (as discussed in Section 2.1.3 of Chapter 2). However, index coding, by itself, remains an open problem, and only some special cases have been resolved [19] [22]. In this respect, the work in [26] proposes a low-rank matrix completion-based (LRMC) scheme to solve TIM in single-input single-output

(SISO) networks, with only some known matrix entries [24], and the missing values are filled so that the rank is minimized.

Comparing our work against TIM existing works, we also adopt the LRMC-based TIM approach, and we apply it in a D2D network. However, we formulate the problem differently, i.e., using semi-definite programming (SDP). The results were encouraging in that they led to an increase in the system DoF and allowed to manage the interference in D2D networks. Moreover, all the aforementioned works ignore the most critical aspect of interference management in practice, namely the variations in the signal strengths due to path loss. Most importantly, it is good to note that the wireless networks are typically not partially connected as considered in TIM. In Section 4.4 of Chapter 4, we study how TIM can behave in practical regimes of interest, where path loss exists. To the best of our knowledge, this is the first work that studies TIM in practical scenarios.

3.2 Low-Rank Matrix Completion Methods

In this thesis, we mathematically model the topological interference management problem (TIM) as a low-rank matrix completion problem (LRMC). The objective is to minimize the rank of the TIM adjacency matrix, knowing that the rank is inversely proportional to system DoF.

The rank minimization problem, in general, has been extensively studied in system theory. Recently, there has been a considerable body of work devoted to address the NP-hardness of the non-convex rank objective function by finding relaxation methods to replace the rank function, like the nuclear norm [24], the alternating projections [96], the directional alternating projections [97], the alternating minimization [98], and the least greedy algorithm [99]. These different rank minimization methods were initially used for constructing linear index codes. However, they can also be applied for TIM knowing the equivalence between the index coding problem and TIM in the linear case, as previously discussed in Section 2.1.3 of Chapter 2. This equivalence holds over any field, in particular the field of real numbers \mathbb{R} , on which we focus in this thesis.

More specifically, authors in [24] approximate the rank function using the nuclear norm method. This method represents the sum of singular values, and assumes the location of the fixed entries in the matrix is chosen uniformly at random. To benefit from algebraic approaches that need less computations, other authors view the rank minimization as a trace minimization [100], [101]. However, the adjacency matrix considered in the TIM problem is characterized by a special structure (having all ones on the diagonal) that prohibits the application of the aforementioned methods. For example, the nuclear [24] and the trace [100] norms

(which behaves same as the nuclear norm) fill the missing entries of the TIM matrix with 0 values, and thus always return the full rank diagonal matrix as the optimal solution. Other authors define the rank function using log-determinant function [102]. However, for a matrix which has ones in its diagonal, this function will always give a 0 value since the determinant of an identity matrix is equal to 1 and hence its log will be equal to 1.

As for the alternating projection (AP) method [96], it seeks a completion for a fixed rank r , instead of searching for the optimal r , by projecting the matrix in inquiry onto two sets (S1) and (S2) individually, where (S1) is the set of rank r matrices and (S2) is the set of matrices with the entry pattern having the diagonal matrix all ones. However, the convergence of this method is not always guaranteed, but it can assure that the completed matrix achieves a certain rank r , which is not always the optimal rank, constructing by that a near-optimal scalar linear index code.

As an improvement, a method called as directional alternating projection (dirAP), proposed in [97], can converge faster than AP and can give a low rank close to that of AP. dirAP represents directional Alternating Projections via eigenvalue decomposition which is used to construct near-optimal scalar linear index codes. Given two convex regions C' and D , a sequence of alternating projections between these two regions converges to a point in their intersection. The projection on C' (the set of positive semi-definite (PSD) matrices of rank less or equal to a given rank r which is equal to the coloring number returned by the greedy algorithm) is obtained by eigenvalue decomposition and taking the eigenvectors corresponding to the r largest eigenvalues. The projection on region D is obtained by setting the diagonal entries of the matrix to 1 and the ab^{th} entry to 0 if edge $(a; b)$ does not exist in the input connectivity graph. While the rank of the matrix is below r , this may take many iterations until the two regions converges to a point in their intersection. This is computed by the ℓ_2 norm (the largest singular value of the matrix) between the two obtained matrices in the two sets which should be less than a stopping criteria.

As for the alternating minimization algorithm [98], it factorizes an unknown rank- r matrix \mathbf{X} as $\mathbf{X} = \mathbf{U}\mathbf{V}^T$, where \mathbf{U} and \mathbf{V} have r columns, and then alternately optimizes over \mathbf{U} and \mathbf{V} holding the other fixed. But this fixed-rank based method needs to know the rank as a prior information, which is not always available. Moreover, it does not perform as good as the alternating projection method and its directional variant (which always outperform graph coloring algorithms) and converge much slower than AP and dirAP.

As for the least greedy algorithm, the idea is to minimize the rank of the index coding matrix \mathbf{N} by greedily searching for rows that could be made equal and

“merging” them. However, this method suffers from a slow convergence rate. It is good to mention here that the methods listed above need the optimal rank of the matrix as input, in contrast to our work, which does not require it, boosting by this its practicality. These methods also suffer from convergence issues, that were solved by using the Riemannian optimization [27].

To address these convergence issues in the aforementioned fixed rank optimization methods, other authors exploit the manifold structures and more specifically the Riemannian optimization algorithm [27], [103], [104], [105], [106]. A Riemannian manifold is equipped with an inner product defined on the tangent spaces, called the Riemannian metric, which allows one to measure distances and angles on manifolds. In particular, it is possible to use calculus on a Riemannian manifold with the Riemannian metric [104]. The main idea is to encode the constraints on the manifold into the search space and then perform descent on this manifold rather than in the ambient Euclidean space. This descent could be using the first order algorithm (steepest descent and conjugate gradients (CGs) [106] or the second order method (trust regions) [27]. The Riemannian pursuit (RP) framework detects also the rank of the matrix to be recovered by iteratively increasing the rank (a rank one update algorithm) without requiring the rank as a prior information. However, there is a tradeoff between the achievable rank and the computational complexity of these methods due to the computation expensive calculation of the Hessian [27]. Note here that this technique has a very high computational complexity, opposite to the polynomial one of our proposed algorithms.

Table 3.1: Rank minimization methods

Method	Cons
Nuclear Norm / Trace norm	Always returns the diagonal matrix as the optimal solution
Alternating Projection / Directional Alternating Projection	<ul style="list-style-type: none"> • Seeks a completion for a fixed rank, instead of searching for the optimal one • Its convergence is not always guaranteed
Alternating Minimization	<ul style="list-style-type: none"> • Needs to know the rank as a prior information • Slow convergence
Least Greedy Algorithm	Slow convergence
Riemmanian Algorithm	High computational complexity

As a conclusion, the adjacency matrix considered in the LRMC-based TIM problem has a special structure that limits the utilization of all the aforemen-

tioned methods (summarized in Table 3.1). For this, we improve the existing solutions, while respecting the matrix structure (all ones on the diagonal), by developing three approximation methods to solve TIM in D2D environments. This is in contrast to the previously detailed rank minimization algorithms that were not directly applied on D2D networks. Our proposed methods are characterized by 1) using generic rank approximations with some twists to overcome all the hard constraints, 2) developing a "tweaked" nuclear norm approach, and 3) exploiting the characteristic polynomial function of the adjacency matrix. The importance of the third method resides is that it does not suffer from the relatively high complexity of the semi-definite programming applied in the first two methods. Nevertheless, all our proposed approximation methods show a matrix rank reduction with a polynomial complexity and without requiring the optimal rank as an input, increasing by this its practicality.

3.3 Clustering Algorithms

Our results in Chapter 4 have proved that the LRMC approach to solve TIM is very useful. However, its main limitation is that its application appears better on mid-size D2D networks. Hence, this drives the need to make it more scalable by combining it with other techniques, i.e., clustering.

In the literature, the used clustering schemes in D2D scenarios are based on social interactions characteristics [107], and do not consider the interference among devices sharing similar interests in the same group, so that the D2D links remain maintained. For this, works like [108] apply the interference alignment (IA) technique inside each group to cancel the intra-cluster interference and use orthogonal resources to cancel the inter-cluster interference. One can argue that the same algorithms can be applied in the TIM context. However, the clustering formulation is different between IA and TIM, since in the former, the interference weights depend on the channel knowledge, which is not available in TIM. For instance, the grouping scheme in [109] depends on the value of the received signal-to-interference plus noise ratio (SINR). Moreover, the three low-complexity partitioning algorithms proposed in [110] also require full channel state information, to maximize the sum network throughput: the first algorithm is a balanced time allocation algorithm that creates an imbalance in the sum rate of each group, the second one is an equal rate grouping scheme that allocates different amount of time for transmission, which may lead to the probability that the group with the highest sum rate transmits for the entire frame (note that the rate here also is based on the SNR among the same user pairs), and the third one is a geographic partitioning method.

Another reason for not being able to use the clustering algorithm designed

in [108] for TIM is that this algorithm keeps the strong interfering edges within the clusters, and links them with weak interfering edges. This is the complete opposite to our objective, which is about designing a clustering algorithm that 1) maximizes the aggregated inter-cluster interference and uses frequency orthogonality among the clusters to eliminate these interference links, and 2) minimizes the intra-cluster interference by virtue of TIM. As for the clustering algorithm in [111], it cannot be also applied here since the constraint on the cluster size is soft, i.e., the algorithm could induce grouping more strong interferers within a cluster, which could lead to larger ranks for such clusters after applying TIM than what they would have been if strong interferers are distributed across different clusters. Other clustering schemes like [87, 111, 112] that are based on fuzzy C-Means clustering algorithm and ratio clustering, respectively, form clusters that are relatively balanced in size, and this is not a required constraint in our framework since it does not necessarily impact the goal of maximizing the network's DoF. Moreover, the pipage-rounding technique used in [113] to solve the capacitated clustering problem cannot be also applied here since in our problem, *all* the cluster sizes are bounded by the *same* value, while in [113] the clusters are of equal sizes.

Therefore, there is a need to develop a clustering algorithm that is *more tuned* to TIM to satisfy the need of separating the D2D pairs with mutual interference into different clusters. This is because this mutuality is translated into an abundant presence of 0s in the TIM matrix, which prohibits the rank minimization. By following this grouping technique, the resulting sub-matrices will hence include less 0s and more "*" values, which will increase the rank flexibility. Once the partitions are obtained, different frequencies are allocated to the clusters to eliminate inter-cluster interference and TIM is applied to each cluster to minimize the intra-cluster interference.

3.4 Successive Interference Cancellation Technique

Despite of the promising benefits offered by TIM, the attainable performance gains (in terms of DoF) in a D2D network may still be eroded by the presence of very strong interferences at the D2D receivers, caused by geographically close D2D transmitters. This severe interference, which may even overpower the desired signal, cannot be managed by conventional TIM, which does not differentiate among the different levels of interference. We therefore propose to use TIM along with successive interference cancellation (SIC) .

SIC is one of several interference cancellation techniques that include par-

allel interference cancellation and iterative interference cancellation. However, SIC remains the mostly used technique, since its architecture (in terms of hardware complexity and cost) is similar to the traditional non-SIC receivers, and its decoder is the same for the different decoding stages of the composite signal, without the need for complicated decoders or multiple antennas [67]. Recently, there have been increasing interests in SIC’s physical layer communications aspect [114], and in its application to cellular networks, particularly the full duplex technology and the non-orthogonal multiple access (NOMA) scheme [115]. In this regard, NOMA has gained attention due to the network level performance gains that SIC brought. It helps also to note that NOMA is applied in networks that schedule the same frequency resources to multiple users.

Several approaches also investigate the coexistence of NOMA and D2D communications with SIC-enabled receivers [62,67,116]. The authors in [116] mainly addressed the optimization issues associated with power control and data rate. As for [67], the authors use stochastic geometry tools to analyze the interference management and resource allocation problems in D2D-enabled multi-cell cellular networks, and to study the effect of the SIC technique. These tools allow for deriving the successful transmission probabilities for both the cellular uplinks and D2D links with SIC, which reveals the gain of SIC in large-scale wireless networks. In [62], the authors introduce the concept of group D2D communications, where D2D transmitter can simultaneously communicate with multiple D2D receivers with the aid of the NOMA protocol. They model the optimal resource allocation strategy of the NOMA-based D2D groups as a many-to-one matching problem, which leads to managing the interference from the underlying uplink cellular communication, and hence yield a better D2D sum-rate performance. Results have shown that the proposed NOMA-based D2D scheme is capable of delivering higher throughput than conventional D2D communication. In [117], the authors propose a new mechanism that jointly coordinates beamforming based multiuser multiple-input multiple-output, NOMA, and D2D communications in a downlink cellular network, to maximize the total system throughput. In [118], the authors specify two types of D2D-NOMA integrations: forward-D2D NOMA in which one D2D transmitter sends signals to a group of D2D receivers, and reverse-D2D NOMA, where a cluster of D2D transmitters transmits to a single D2D receivers.

While both SIC and D2D continue to mature in terms of their theoretical and practical aspects, TIM is also maturing. However, the TIM framework for NOMA users (with SIC capabilities) has not been well investigated in D2D network. Recently, few papers have appeared on the subject of combining TIM with NOMA. So far, Kalokidou et al. propose to combine TIM principles with power-domain NOMA in SISO [119] and MIMO [120] systems. They introduce a two-stage process. In the first stage, users with different channel gains are clustered into groups, and TIM manages the “inter-cluster” interference among the clusters. As

for the second stage, i.e., within each cluster, the SIC technique is applied to cancel the “intra-cluster” interference. The employment of this scheme significantly improves the sum-rate performance of the system. However, the combination of these two techniques is hierarchical and is not seen as one entity, in contrast to our work presented in Section 4.3 of Chapter 4, where SIC and TIM, are both represented by the same LRMC model. In this chapter, we got inspired by the potential benefits of the aforementioned interference management techniques: it became desirable to invoke intelligent joint interference management approaches that amalgamate TIM with the existing SIC technique, and to apply it in a D2D environment.

Chapter 4

Recasting TIM as a Low-rank Matrix Completion Problem

In the first part of this chapter, we develop two efficient and novel approximation solutions for the low-rank matrix completion (LRMC)-based topological interference management (TIM) problem, while relying on semi-definite programming (SDP). As an application for this, we consider the Device-to-Device (D2D) environment, where the D2D-enabled devices are partially connected in the network, and hence TIM can manage interference without exchanging the instantaneous channel information (which represents a serious problem in such scenario) but by only relying on the network connectivity. To the best of our knowledge, this is the first work that develops SDP solutions for this kind of problem, while overcoming also the matrix special structure with hard constraints: having all ones in the main diagonal, with some predefined 0 entries. Consequently, by successfully minimizing the rank of the TIM adjacency matrix, the system degrees-of-freedom (DoF) increases.

In the second part of this chapter, we explore the use of a physical layer technique, i.e., successive interference cancellation (SIC) technique, along with TIM to boost the system D2D network's DoF. From a different angle, it couples two interference management techniques. The first technique is interference avoidance through TIM to design the appropriate precoding and decoding matrices, \mathbf{U} and \mathbf{V} for the transmitters and receivers, respectively, in a way that their product avoids the interference. The second technique is interference cancellation which uses SIC to cancel the interfering signals at the receiver side only. To the best of our knowledge, there is no existing work that investigates the joint TIM-SIC approach and applies it in D2D communications scenarios.

In the third part of this chapter, we study how TIM can behave in practical regimes of interest, where path losses exist. To the best of our knowledge, this is the first work that studies TIM in practical scenarios.

Starting with the first part of this chapter, the main contributions can be summarized as follows:

- Proposing two topology information exchange frameworks among communicating D2D devices; one among the D2D devices themselves, and the other one involving the base station.
- Deriving a formulation of the optimal rank in the LRMC-based TIM systems.
- Recasting the TIM problem as an LRMC problem which is usually NP hard (due to its non-convex and discontinuous nature), and developing two efficient and novel approximation solutions (*RM-TIM*, *eRM-TIM*) based on SDP to overcome the TIM matrix special structure. In addition to their efficiency in rank minimization, these methods are also characterized by their polynomial complexity.
- Approximating the TIM matrix rank in *RM-TIM* by a continuous and smooth generic approximation function, while converting the problem into an SDP form, by introducing slack variables and using several transformations. The key step of our method lies in the development of a novel mathematical result that forces the SDP approximation to return a non-diagonal matrix, and hence allowing to decrease the TIM matrix rank despite the matrix special structure.
- Developing an improved TIM rank minimization, *eRM-TIM*, after modifying the nuclear norm heuristic, in order to overcome the hard constraint of all ones on the main diagonal of the adjacency matrix. This method is simpler than *RM-TIM*, with much less matrix inequalities in the constraints, while achieving similar rank minimization performance.

4.1 Modeling the LRMC-based TIM Approach

In this chapter, we start by describing the system model that is used as a foundation for all the remaining chapters in this thesis. We consider here a multi-user interference D2D network with n transmitters and intended receivers, working in pairs and operating in a single-hop transmission mode.

4.1.1 Choice of D2D Transmission Mode

There are different transmission modes in D2D: 1) direct communication (single hop) between two D2D users, and b) multihop communication through one or more relays. Although some D2D-related papers consider the multihop scenario, many existing works in the literature [9, 74, 78, 79, 121–130, 130–132] rely on the single-hop mode due to its practicality and simplicity. This motivated us then to adopt in our work this type of transmission, i.e., the single-hop mode, specially

that it is also compliant with the 3GPP standards [133].

Although the multihop scheme is out of the scope of this work, it seems to be an interesting topic that is worth tackling. To get an initial feel of what is involved, we take the two-hop (single relay) case as a scenario. In this case, a two-time-slot physical layer will be required, where the D2D device changes roles: in the first timeslot, the intermediate D2D device plays the role of a receiver, and, in the second timeslot, it acts as a transmitter (the relay's role). By this, the connectivity pattern, as well as its associated matrix, will change from time to time, depending on the role played by the D2D device (transmitter/receiver), and on the sources of interference that are present at that timeslot. For instance, while D2D transmitter T_1 is sending a message to its corresponding receiver R_1 at time t_1 , T_1 interferes with a D2D device D_2 playing the role of a receiver, i.e., R_2 . In this case, the entry $X_{2,1}$ of the adjacency matrix (where the row index refers to the receiver, and the column index denotes the transmitter) becomes equal to 0. At time t_2 , D_2 changes its role to be a transmitter, i.e., T_2 and it can happen that the communication between T_1 and R_1 is finished at that time, and hence the entry $X_{2,1}$ that was equal to 0 at t_1 is no more valid at $t_2 = t_1 + \epsilon$. This example illustrates how the matrix entries change between two instances. Consequently, TIM should be applied at each instance separately, and thus on its corresponding matrix.

4.1.2 Learning about the Topology Information

As an illustration, we show in Fig. 4.1 an example of 12 D2D-enabled devices. On the left of this figure, we represent the connectivity pattern of these devices, where solid lines denote intended signals, whereas dashed lines represent interference links. For instance, receiver R_2 is suffering from interference resulting from two transmitters T_4 and T_5 , while receiving its desired signal from T_2 . The attenuation interference network is considered here an asymmetric one in order to keep the problem more general, and hence the received signals could have differences in strengths, due to the network topology (i.e., presence/absence of obstacles). For example, T_2 is interfering to R_3 , however T_3 does not hurt R_2 while transmitting its signal. On the right of Fig. 4.1, we show the adjacency matrix that corresponds to the 12×12 D2D network, where we later describe the meaning of its content and structure.

In the TIM context, the interference is managed based on the topology (without the need of the instantaneous CSI) which may be learned in different ways. We describe here two possible schemes for learning about the global D2D network connectivity: one that only involves the D2D devices themselves, whereas the other is based on the network-assisted mode, where the base station (BS) collects information about the topology and builds the adjacency matrix.

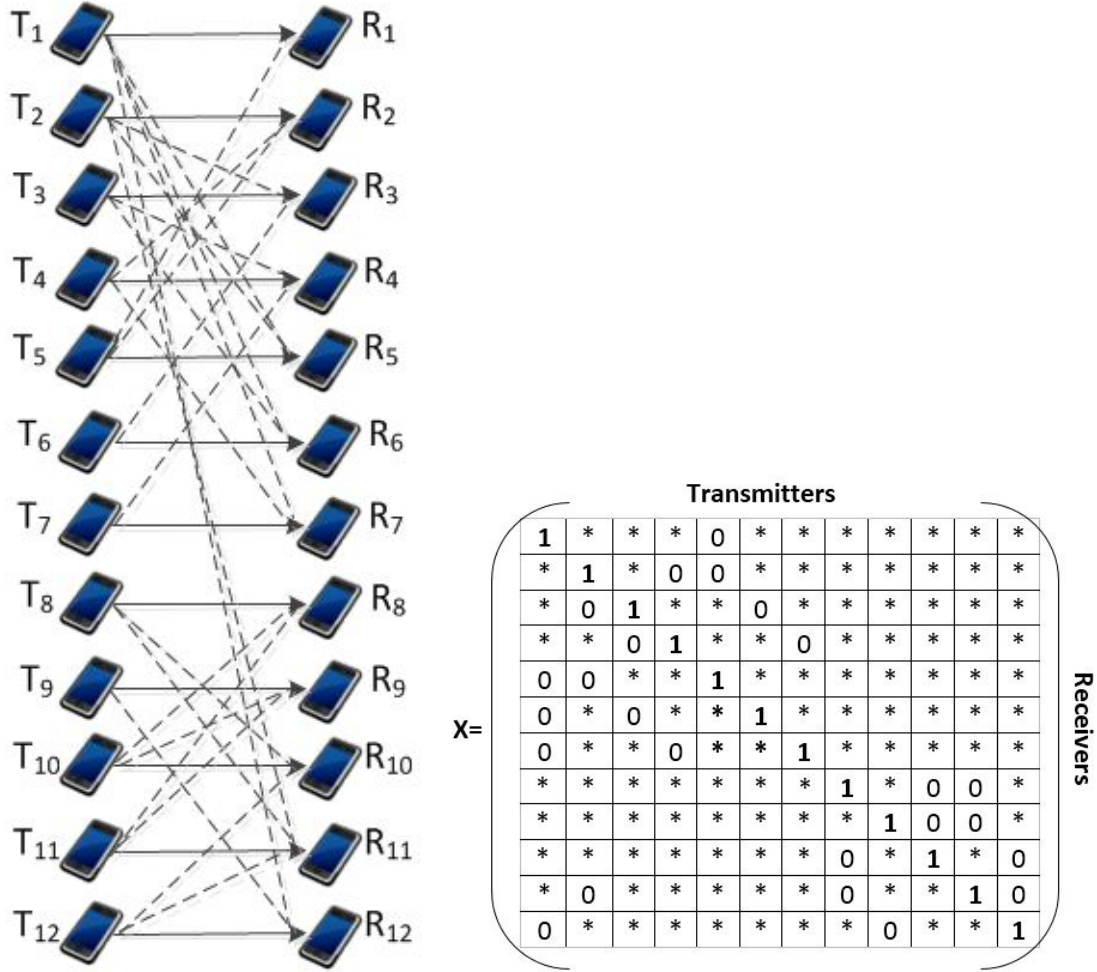


Figure 4.1: (a) TIM for a 12×12 D2D network and its (b) TIM matrix

Scenario 1 - Stand-alone Mode: The first scheme builds on the works in [134–137], according to which devices can learn about the topology information of neighboring devices through the device discovery process. This discovery is made possible by each UE broadcasting its own proximity beacon signals at given times, thus enabling nearby UEs to capture such beacons [138] that can contain the identity of each potential D2D user and also serve as reference signals for measuring the interference level. Moreover, we propose for each device to propagate the list of interfering and communicating neighbors that it learns about in its beacons, which is doable, as inferred from [139] and [140]. This information that each device sends is a list of tuples, where each one includes the id of the device and one of two associated values: interference (v_0) or an ongoing or pending D2D session (v_1). For example, when device R_2 transmits a

beacon that contains $(T_4, v0)$ and $(T_2, v1)$, it says that the strength of the beacon it heard from T_4 constitutes interference ($v0$), while $v1$ indicates that it (i.e., R_2) has an ongoing or pending D2D communication session with T_2 . In this respect, we note that a $v1$ value is only sent by D2D receivers, not transmitters. Hence, a device T_5 which hears the beacon from R_2 , adds a row in its neighborhood list that associates the values $v0$ and $v1$ with T_1 and T_2 , respectively. With this, if T_3 now wishes to establish a D2D session with another device using our scheme, it has to first construct the adjacency matrix, which it can do from the information it has collected in its neighborhood list, in particular by only considering devices that have sent $v1$ values (i.e., D2D receivers).

The above proposed scheme ensures that all neighboring (i.e., connected directly, or indirectly) transmitters (and receivers) have identical neighborhood lists, and thus can construct the same adjacency matrix (\mathbf{X}). Any of those transmitters, e.g., transmitter j (T_j) can then perform rank minimization on the adjacency matrix it has built, and extract the relevant precoding and decoding vectors \mathbf{v}_j and \mathbf{u}_j to cancel the interference (i.e., using TIM). Related to \mathbf{v}_j and \mathbf{u}_j , two options are available: T_j can produce both vectors, and send \mathbf{u}_j to R_j (i.e., its corresponding receiver), or rely on R_j to extract \mathbf{u}_j itself (since it has the same \mathbf{X}).

Since broadcasting beacons, if uncontrolled, can lead to flooding the wireless network, we propose the following four measures to make the process of sending beacons more energy efficient and less loading on the network:

- The values $v0$ and $v1$ can be specified using one bit in the beacons (0 for $v0$, and 1 for $v1$).
- The discovery process of transmitting beacons between the devices, using Orthogonal Frequency Division Multiple Access (OFDMA) as in [141] and [142], allows for the possibility of the devices to transmit beacon signals in parallel slots. As for the beacon structure, it can use the one proposed in [141] (which is built on the existing beacon design of the 3GPP Long Term Evolution (LTE)), to fit the list of neighbors in their "future use" field.
- The problem of synchronization when beacons are multiplexed together in the same OFDMA symbols can be resolved by dividing the devices into groups that use different patterns to transmit in different beaconing opportunities, as was also proposed in [141].
- The frequency of transmitting beacons can be tied to mobility: a device sends the next beacon only when its location significantly changes (using its GPS sensor), or when it receives beacons from devices it did not hear from recently.

We note that according to [139], the minimum unit of beacon is a Resource Block (RB) which carries 72 OFDM symbols [143], whereas the maximum can be two

RBs [144]. This limits the amount of information carried in a beacon, but with the application of the measures above, we enable a device to send more tuples in each beacon. Nevertheless, in case a device was not able to include all the information in one beacon, it can distribute them among consecutive ones.

Scenario 2 - Network-assisted Mode: The second scheme for learning about the D2D network topology, and consequently building the adjacency matrix is based on the D2D network-assisted mode. Here, each receiver can send a sequence of bits to a base station (BS), where every bit corresponds to a transmitter (that is heard by this receiver) based on the pilot signals. This 1-bit feedback, which is in line with [19], refers to the average interference channel strength after comparing the average power of the received links against a pre-chosen threshold value (i.e., the acceptable noise floor): it is equal to "0" for weak interference links, and "1" for significant ones. Having this information, the BS can then deduce the interfering pairs and build the connectivity pattern (i.e., construct the adjacency matrix), apply the rank minimization method on it, and then build the precoding and decoding vectors (by applying QR factorization). These vectors will be sent to the transmitters and receivers, respectively.

It is good to note here that although the first scenario is less efficient than the second one in terms of computations, but it is useful in some cases when the network is not equipped with a central entity.

4.1.3 System Model for the LRMC-based TIM Framework

In the TIM framework, each transmitter T_i is assumed not to be aware of CSI, but only of the network topology. T_i sends a signal $\mathbf{v}_i s_i$ to its intended receiver R_i (s_i is the information symbol, and \mathbf{v}_i is the i^{th} column of a precoding matrix \mathbf{V} that combines all the precoding vectors) via the sidelink channel of the PC5 interface (as defined in the 3GPP standards [145]), and R_i multiplies the received signal \mathbf{y}_i (corrupted by interference) by \mathbf{u}_i (i^{th} row of the decoding matrix \mathbf{U} that also combines all the decoding vectors). Over r channel uses, the input-output relationship becomes:

$$\mathbf{u}_i \mathbf{y}_i = \mathbf{u}_i \mathbf{v}_i h_{i,i} s_i + \mathbf{u}_i \sum_{(i,j) \in \mathcal{S}, i \neq j} \mathbf{v}_j h_{i,j} s_j + \mathbf{u}_i z_i, \quad \forall i \quad (4.1)$$

where $h_{i,i}$ and $h_{i,j}$ are the channel coefficients between $T_i - R_i$ and $T_j - R_i$ respectively, $z_i \sim \mathcal{N}(0, 1)$ is the noise, and \mathcal{S} is the index set of connected transceiver pairs such that the channel coefficient from transmitter j to receiver i with $(i, j) \in \mathcal{S}$ is non-zero, and zero when $(i, j) \notin \mathcal{S}$, and hence T_j can be

either the intended transmitter or the interfering one. For instance, \mathcal{S} includes (2,2), (2,4), and (2,5) since R_2 desires a signal from T_2 , but it is suffering from the interference resulting from T_4 and T_5 . At high SNR, to decode the intended signal s_i and to guarantee parallel interference-free channels [19], we impose the constraints that all the interference terms ($\mathbf{u}_i \sum_{(i,j) \in \mathcal{S}, i \neq j} \mathbf{v}_j h_{i,j}$) are aligned and then cancelled, while the desired signals ($\mathbf{u}_i \mathbf{v}_i h_{i,i}$) are preserved over r channels. The TIM strategies should be thus designed such that the following conditions on $\mathbf{U} = [\mathbf{u}_i]$ and $\mathbf{V} = [\mathbf{v}_j]$ are simultaneously satisfied [26]:

$$\begin{aligned} \mathbf{u}_i \mathbf{v}_j &= 0, \quad \text{for } \forall i \neq j, (i,j) \in \mathcal{S}, \text{ and} \\ \mathbf{u}_i \mathbf{v}_i &= 1, \quad \text{otherwise} \end{aligned} \quad (4.2)$$

By this, the first condition enforces all interference subspaces to have zero dimensions and the second one enforces the useful signal to span all dimensions. More details about the derivation of these equations can be found in [26]. The input-output relationship can be then written as:

$$\begin{aligned} \mathbf{u}_i \mathbf{y}_i &= \mathbf{u}_i \left(\mathbf{v}_i h_{i,i} s_i + \sum_{j, (i,j) \in \mathcal{S}} \mathbf{v}_j h_{i,j} s_j + z_i \right) \\ &= \mathbf{u}_i \mathbf{v}_i h_{i,i} s_i + \sum_{j, (i,j) \in \mathcal{S}} \underbrace{\mathbf{u}_i \mathbf{v}_j}_0 h_{i,j} s_j + \mathbf{u}_i z_i \\ &= \mathbf{u}_i \mathbf{v}_i h_{i,i} s_i + \mathbf{u}_i z_i \end{aligned} \quad (4.3)$$

In the same vein of the example previously mentioned about the content of \mathcal{S} for receiver R_2 , the conditions in (4.2) make the product between the precoding vector \mathbf{v}_1 and the decoding vector \mathbf{u}_2 equal to 0 (same for \mathbf{v}_5 and \mathbf{u}_2) so that the interference gets cancelled and the desired signal is preserved. Thus, the recovery succeeds without knowing the exact values of the channel coefficients, making the TIM problem a channel independent one. By applying TIM strategies on \mathbf{u} and \mathbf{v} , R_2 will be able then to only decode its desired signal s_2 and get rid of the interfering signals as follows:

$$\begin{aligned} \mathbf{u}_2 \mathbf{y}_2 &= \mathbf{u}_2 h_{2,2} \mathbf{v}_2 s_2 + \mathbf{u}_2 h_{2,4} \mathbf{v}_4 s_4 + \mathbf{u}_2 h_{2,5} \mathbf{v}_5 s_5 + \mathbf{u}_2 z_2 \\ &= \mathbf{u}_2 \mathbf{v}_2 h_{2,2} s_2 + \mathbf{u}_2 z_2 \end{aligned} \quad (4.4)$$

In what follows, we present our approach for a unified low-rank matrix completion (LRMC) approach. We start by observing that the above conditions can be rewritten in a matrix form such as $\mathbf{X} = [X_{i,j}]$ is an $n \times n$ real matrix, and only a subset of its entries $X_{i,j}, \forall (i,j) \in \mathcal{S}$ are known:

$$\mathbf{X} = [X_{i,j}] = \mathbf{u}_i \mathbf{v}_j = \begin{cases} 1 & \text{if } (i,j) \in \mathcal{S} \text{ \& } i = j \\ 0 & \text{if } (i,j) \in \mathcal{S} \text{ \& } i \neq j \end{cases} \quad (4.5)$$

The rank of this TIM adjacency matrix \mathbf{X} is related to the degrees-of-freedom (DoF) of the system, knowing the equivalence between TIM and index coding with linear schemes, as previously mentioned in Section 2.1.3 of Chapter 2. Recall that DoF represents the pre-log factor in the sum capacity term linked to the total number of spatial streams that the network can support simultaneously without interference [19]. In this work, we consider the symmetric DoF (DoF_{sym}) of the network (the largest DoF that can be achieved by all users simultaneously) as our main figure of merit. This is in line with existing works on TIM, knowing that this metric considerably simplifies the analysis and gives useful insights on the network performance [26].

If we use M_1, \dots, M_n to denote the number of streams for the n D2D pairs, the achievable DoFs will be given by $\frac{M_1}{\text{rank}(\mathbf{X}^*)}, \dots, \frac{M_n}{\text{rank}(\mathbf{X}^*)}$ where \mathbf{X}^* is the matrix with the lowest rank (optima of problem (4.6)). In this work, we assume for convenience a single data stream transmission per D2D pair (i.e., $M_i = 1, \forall i$), then the symmetric DoF that is attainable at high signal-to-noise ratio (SNR) (when the interference dominates the noise) will be $\text{DoF}_{\text{sym}} = \frac{1}{\text{rank}(\mathbf{X}^*)} = \frac{1}{r}$ per user. The objective is thus to fill the missing values "*" of \mathbf{X} from \mathbb{R} in a way that minimizes the rank of \mathbf{X} that corresponds to the D2D network, so that the achievable symmetric DoF gets maximized.

Then, we mainly treat TIM as a low-rank matrix completion problem (LRMC):

$$\begin{aligned} \min_{\mathbf{X} \in \mathbb{R}^{n \times n}} \quad & \text{rank}(\mathbf{X}) \\ \text{s.t.} \quad & X_{i,j} = M_{i,j}, \quad (i,j) \in \mathcal{S} \end{aligned} \quad (4.6)$$

where the missing entries of $\mathbf{X} \in \mathbb{R}^{n \times n}$ constitute the optimization variables, and the inverse of the optimal rank of \mathbf{X}^* of LRMC equals the maximum achievable DoF. We let $\mathbf{M} = [M_{i,j}]$ be an $n \times n$ matrix in \mathbb{R} , but only a subset \mathcal{S} of its entries are known, such that $(i,j) \in \mathcal{S}$ denotes that the i^{th} receiver is connected to the j^{th} transmitter: $M_{i,i} = 1$ for $i = j$, and $M_{i,j} = 0$ for $i \neq j, (i,j) \in \mathcal{S}$, (i.e., when R_i is receiving interference from T_j as defined in (4.5)). The LRMC problem is thus turned into finding \mathbf{X} having lowest rank that agrees with \mathbf{M} on \mathcal{S} . However, the special structure of \mathbf{X} (detailed below) makes the problem more challenging to be solved:

1. \mathbf{X} has all ones in its main diagonal.
2. \mathbf{X} has some predefined entries as 0s.
3. \mathbf{X} is a square matrix due to pairwise links in D2D.
4. \mathbf{X} is not necessarily symmetric, i.e., links may have different path loss, in contrast to previous works adopting a symmetric interference alignment (IA) network.
5. \mathbf{X} is not essentially a positive semi-definite matrix (PSD).

Once the optimal \mathbf{X}^* is known, the decoding and precoding matrices \mathbf{U} and \mathbf{V} respectively, can be derived using QR decomposition (described in Section 2.2.4 of Chapter 2), since $\mathbf{X}^* = \mathbf{UV}$. In the network-assisted mode, the linear TIM strategies corresponding to \mathbf{u}_i and \mathbf{v}_i vectors ($\mathbf{U} = [\mathbf{u}_i]$ and $\mathbf{V} = [\mathbf{v}_i]$) can be then determined and sent by the BS to the transmitters and receivers, respectively. As for the stand-alone mode, these strategies can be deduced by the devices themselves.

However, solving the LRMC problem in (4.6) is NP hard in general [41] [26], which implies that the exact complexity is not polynomial (at least exponential). More generally, the optimization problems, containing the non-convex matrix rank function either in the objective function or in the constraints, are usually hard to solve, and this explains why many rank approximation techniques have been developed in the literature (e.g., [41] and the references therein). Therefore, obtaining the optimal solution for \mathbf{X} by exhaustive search is not possible in this case, as the variable entries of the matrix that should be found (i.e., the "*" entries) belong to \mathbb{R} , making the exhaustive search method not easy to implement. For this, we develop, in the following subsections, several sub-optimal solutions.

4.1.4 Rank Approximation Algorithm Assessment

Before introducing our proposed rank minimization methods, we detail in this section the procedure that one should undertake to compute the rank of the adjacency matrix \mathbf{X} resulting from solving the LRMC problem.

We build here on the fact that the matrix rank is equal to the number of non-zero singular values (as explained in Section 2.2.1 of Chapter 2). To decide which singular values can be neglected while doing the rank approximation of the matrix \mathbf{X} by another matrix $\hat{\mathbf{X}}_k$, we rely on Eckart and Young Theorem [45]. This theorem states that the Frobenius norm $\|\cdot\|_F$ of the matrix that derives from the difference between the two matrices \mathbf{X} and $\hat{\mathbf{X}}_k$, i.e., $\|\mathbf{X} - \hat{\mathbf{X}}_k\|_F$, is equal to $\sqrt{\sigma_{k+1}^2 + \dots + \sigma_n^2}$, where σ_n stands for the n^{th} singular value that arises from the singular value decomposition (SVD) of \mathbf{X} (more details can be found in Sections 2.2.1.5 and 2.2.3 of Chapter 2). Hence, the smaller the value of this difference, the better the approximation.

To quantify the error resulting from this approximation in a percentage format, we define the following metric:

$$error(\%) = \frac{\|\mathbf{X} - \hat{\mathbf{X}}_k\|_F}{\|\mathbf{X}\|_F} \times 100 = \frac{\sqrt{\sigma_{k+1}^2 + \dots + \sigma_n^2}}{\|\mathbf{X}\|_F} \times 100 \quad (4.7)$$

Therefore, once the output \mathbf{X} of problem (4.6) is obtained, we approximate it

by another matrix $\hat{\mathbf{X}}_k$ after zeroing the smallest singular value, iteratively (one singular value at a time). At each iteration, we compute the error in (4.7). We repeat this as long as the error remains less than 10%. The steps of this algorithm are summarized in Algorithm 1.

Algorithm 1: Rank approximation decision

```

Input :  $\mathbf{X}$ 
Output:  $\hat{\mathbf{X}}_k, rank(\mathbf{X}), \mathbf{U}, \mathbf{V}$ 
1 Solve the problem (4.6) to get  $\mathbf{X}$  ;
2 Calculate  $\|\mathbf{X}\|_F$ ;
3 Find the SVD decomposition  $\mathbf{X} = \mathbf{Y}\mathbf{S}\mathbf{Z}^T$  with  $\mathbf{S} = \text{diag}(\sigma_1, \dots, \sigma_n)$ ,
    $\sigma_1 \geq \dots \geq \sigma_n$ ;
4 Define  $error = \frac{\|\mathbf{X} - \hat{\mathbf{X}}_k\|_F}{\|\mathbf{X}\|_F} \times 100$ ;
5 while  $error \leq 10\%$  do
6   Initialize  $i = n + 1$ ;
7   repeat
8     /* zeroing the smallest singular values */
9      $i = i - 1$ ;
10    Set  $[\sigma_i, \dots, \sigma_n] = 0$  in  $\text{diag}(\mathbf{S})$  ;
11    Get new  $\hat{\mathbf{S}}$  ;
12    Compute  $\hat{\mathbf{X}} = \mathbf{Y}\hat{\mathbf{S}}\mathbf{Z}^T$ ;
13    Calculate  $error$ ;
14  until  $error > 10\%$ ;
15  return  $i + 1, \hat{\mathbf{X}}_{i+1}$  ;
16 end
17  $rank(\mathbf{X}) = n - (i + 1)$  ;
18  $\hat{\mathbf{X}}_k = \hat{\mathbf{X}}$ ;
   /* Get the decoding and precoding matrices,  $\mathbf{U}$  and  $\mathbf{V}$ 
   respectively */
19 Apply QR factorization on  $\hat{\mathbf{X}}_k$  to get  $\mathbf{U}$  and  $\mathbf{V}$ , since  $\hat{\mathbf{X}}_k = \mathbf{U}\mathbf{V}$ 

```

4.1.5 Deducing the Optimal Rank

Now to decide whether the developed rank minimization method was successful in reducing the rank, the value of the achieved rank should be compared against an optimal value. In the TIM problem, this optimal value (i.e., the minimum rank that can be achieved) cannot be equal to 1. This can be explained by the fact that a rank-one matrix is a non-zero matrix, where all rows are multiples of each other; however, the underlying matrix in a TIM problem has a special structure by having all 1s in its diagonal entries (due to D2D application), and so, the remaining elements of the matrix should be multiple of 1s if it is to be made a rank-one matrix, i.e., all the elements should be equal to 1. Nevertheless,

the matrix has predefined values as 0s, indicating which transmitter is the source of interference for a specific receiver. By this, the optimal value of the rank can be at least 2 (knowing that the rank should be an integer value).

We also observed that this optimal value of 2 can be deduced from the characteristic polynomial function $p(\lambda)$ of the TIM adjacency matrix, represented in (2.31). Knowing that the TIM matrix includes variables in its entries (corresponding to the missing "*" values), then the coefficients of this polynomial in (2.31) will also consist of variables. The reason for this is that these coefficients can be expressed in terms of trace powers of \mathbf{X} as in Eq. (4.32) or in function of its eigenvalues, as in Eq. (4.33). The minimum rank can thus be achieved when the coefficients that are variables (and hence flexible in their values) are imposed to be equal to 0. In other words, the optimal rank value can be computed as:

$$\text{Optimal rank} = (n + 1) - (\text{number of coefficients that include variables}) \quad (4.8)$$

where n is the matrix dimensions. However, not all the n coefficients of $p(\lambda)$ are variables in the TIM case to be able to force them to be equal to 0 and hence to turn the optimal rank value to 1. This is because the c_1 factor of this polynomial is equal to $\text{Tr}(\mathbf{X})$, and in TIM, \mathbf{X} has all ones on its diagonal, which makes c_1 to always be equal to n (constant value). Therefore, the number of coefficients that can include variables can be $(n - 1)$ at maximum. Plugging this value in (4.8) gives the optimal rank value of 2.

Consequently, to assess the performance of any rank minimization method, the resulting matrix rank can be compared to the optimal rank value of 2.

4.1.6 Parameters and Variables

The list of parameters and variables used in this chapter are captured in the following tables:

Table 4.1: Parameters and variables used in Chapter 4

Parameter	Description	Values
n	Matrix dimensions	
T_i	i^{th} Transmitter	
R_i	i^{th} Receiver	
\mathbf{U}	Decoding matrix	
\mathbf{V}	Precoding matrix	
\mathbf{u}_i	Decoding vector for T_i	
\mathbf{v}_i	Precoding vector for R_i	
s_i	Information symbol sent by T_i	
\mathbf{y}_i	Signal received by R_i	
$h_{i,i}$	Channel coefficient between $T_i - R_i$	
$h_{i,j}$	Channel coefficient between $T_j - R_i$	
$T_i - R_i$	i^{th} D2D pair	
z_i	Additive isotropic white gaussian noise	
r	Rank(\mathbf{X})	
M_n	Number of streams for the n D2D pairs	
\mathbf{X}	TIM adjacency matrix	
$X_{i,j}$	Entry in matrix \mathbf{X} at i^{th} row and j^{th} column	
\mathbf{X}^*	Solution of \mathbf{X}	
$\hat{\mathbf{X}}_k$	Approximated \mathbf{X}	
\mathbf{M}	Matrix with some known entries	
\mathcal{S}	Set of known entries with indices (i, j)	
\mathbf{Y}	Unitary matrix	
\mathbf{Z}	Unitary matrix	
\mathbf{S}	Diagonal matrix with singular values of \mathbf{X} on the diagonal	
$\hat{\mathbf{S}}$	Approximated \mathbf{S}	
Φ_ϵ	Smooth version of the rank function	
$\sigma_i(\mathbf{X})$	i^{th} Singular value of matrix \mathbf{X}	
$p(\lambda)$	Characteritic polynomial function of a matrix	
ϵ	Controlling parameter	10^{-4}
γ	Penalty term	[4,20]
\mathcal{S}'	Set of known entries with indices (i, k)	
$\gamma_{i,i}$	Path loss component between T_i and R_i	
$\gamma_{i,j}$	Path loss component between T_i and R_j	
A	Path loss coefficient	28.03 dB
α	Path loss exponent	4

Table 4.2: Continuation of Table 4.1

Parameter	Description	Values
$d_{i,i}$	Distance between T_i and R_i	
$d_{i,j}$	Distance between T_j and R_i	
θ_i	Threshold for the summation of missing entries at each i^{th} receiver	
$SIR_{\text{threshold}}$	Threshold for Signal-to-Interference Ratio	2 dB
c_j	Speed of the j^{th} transmitter	
β	Direction of the movement relative to the old distance vector	
t	Elapsed time	
η	Solution precision	

4.2 Developing Solutions for LRMC-based TIM Approach

Throughout this chapter, we develop three progressively effective rank minimization methods: *RM-TIM*, *eRM-TIM* and *cRM-TIM*. Our approaches are based on several modifications of the original TIM matrix to be able to solve it using convex optimization, specifically, semi-definite programming, with a polynomial complexity. The first two methods build on Fazel’s Lemma in [101], while the third one (treated in Section 4.3) uses the characteristic polynomial function properties.

4.2.1 Fazel’s Lemma

This lemma states that a *general* matrix \mathbf{X} can be associated with a positive semi-definite (PSD) matrix ($\succeq 0$) whose rank is twice the rank of \mathbf{X} : given \mathbf{X} , $\text{rank}(\mathbf{X}) \leq r$ if and only if there exist symmetric and PSD matrices \mathbf{K} and \mathbf{E} ($\mathbf{K} = \mathbf{K}^T$, $\mathbf{E} = \mathbf{E}^T$) such that:

$$\text{rank}(\mathbf{K}) + \text{rank}(\mathbf{E}) \leq 2r$$

$$\mathbf{W} = \begin{pmatrix} \mathbf{E} & \mathbf{X} \\ \mathbf{X}^T & \mathbf{K} \end{pmatrix} \succeq 0, \quad \text{where} \quad \begin{pmatrix} \mathbf{E} & \mathbf{X} \\ \mathbf{X}^T & \mathbf{K} \end{pmatrix} \succeq 0 \Leftrightarrow \begin{cases} (i) \mathbf{E} \succeq 0, \\ (ii) \mathbf{X}^T(\mathbf{I} - \mathbf{E}\mathbf{E}^\dagger) = \mathbf{0}, \\ (iii) \mathbf{K} - \mathbf{X}^T\mathbf{E}^\dagger\mathbf{X} \succeq 0 \end{cases} \quad (4.9)$$

where \mathbf{E}^\dagger denotes the Moore-Penrose pseudoinverse of \mathbf{E} (the corresponding definition can be found in Chapter 2), and \mathbf{I} is the identity matrix of dimension n . By this Lemma, minimizing the rank of \mathbf{X} in (4.6) is equivalent to minimizing the rank of the semidefinite, block diagonal matrix $\mathbf{Diag}(\mathbf{E}, \mathbf{K})$ (i.e., the objective function in (4.9) can be replaced by $(\frac{1}{2}\text{rank } \mathbf{Diag}(\mathbf{E}, \mathbf{K}))$ with the same constraints) [101]. Having \mathbf{E} and \mathbf{K} as PSD matrices, then the direct application

is to relax the rank function by the trace heuristic, yielding to:

$$\begin{aligned} & \min \frac{1}{2}(\text{Trace}(\mathbf{K}) + \text{Trace}(\mathbf{E})) \\ \mathbf{W} = \begin{pmatrix} \mathbf{E} & \mathbf{X} \\ \mathbf{X}^T & \mathbf{K} \end{pmatrix} \succeq 0, X_{i,j} = M_{i,j}, (i, j \in \mathcal{S}) \end{aligned} \quad (4.10)$$

which remains a convex optimization problem (in variables $\mathbf{X}, \mathbf{K}, \mathbf{E}$) that can be solved to give a sub-optimal solution. It has been also shown in [101] that (4.10) is equivalent to:

$$\begin{aligned} & \min_{\mathbf{X} \in \mathbb{R}^{n \times n}} \|\mathbf{X}\|_* \\ & \text{s.t.} \quad X_{i,j} = M_{i,j} \end{aligned} \quad (4.11)$$

where $\|\mathbf{X}\|_*$ is the nuclear norm such that $\|\mathbf{X}\|_* = \sum_{i=1}^n \sigma_i(\mathbf{X})$ ($\sigma_i(\mathbf{X})$ denotes its singular value). Note that the constraint $X_{i,j} = M_{i,j}, (i, j \in \mathcal{S})$ in the TIM problem has special characteristics, i.e., 1s in the main diagonal, that makes the problem a challenging one. Under this constraint, the trivial solution of the nuclear minimization problem of (4.11) is $\mathbf{X} = \mathbf{I}$, where \mathbf{I} is the identity matrix (a full rank diagonal matrix) [26]. On the other hand, knowing the following relations $\text{rank}(\mathbf{K}) \geq \text{rank}(\mathbf{X})$ and $\text{rank}(\mathbf{E}) \geq \text{rank}(\mathbf{X})$ (for more details about the proof, the reader can refer to [101] or to Appendices A.1 and A.2), and the equivalence between (4.11) and (4.10), then solving (4.10), under the same constraint of $X_{i,j} = M_{i,j}$, will also lead to the trivial solution $\mathbf{K} = \mathbf{I}$ and $\mathbf{E} = \mathbf{I}$ (full rank diagonal matrices), which simultaneously satisfies the Schur complement conditions for positive semi-definiteness of \mathbf{W} in (4.9). The method in (4.10) is thus not applicable here, and it is more likely that by avoiding \mathbf{K} and \mathbf{E} to be diagonal (we also observed this fact numerically), the rank of \mathbf{X} gets reduced further.

Hence, other approximation methods are required to conserve the 1s in the \mathbf{X} 's diagonal and still minimize \mathbf{X} 's rank. This objective is achieved in Sections 4.2.2 and 4.2.3 of this Chapter.

4.2.2 *RM-TIM*: Generic-Rank Approximation Method

To coincide with the original problem definition, we replace the rank function in (4.9) for each of the symmetric matrices \mathbf{K} and \mathbf{E} by a continuous generic approximation function controlled by a parameter ϵ based on [41]. We explain the approximation below for \mathbf{K} only and the same procedure should be performed for \mathbf{E} as well. The approximation follows in several steps.

Step 1. To approximate $\text{rank}(\mathbf{K})$, we rely on the approach in [41] for a smooth version Φ_ϵ of the rank function, which can be written in terms of the

singular values $\sigma_i(\mathbf{K})$ of \mathbf{K} , as follows:

$$\Phi_\epsilon(\mathbf{K}) = \sum_{i=1}^{\text{rank}(\mathbf{K})} \frac{\sigma_i^2(\mathbf{K})}{\sigma_i^2(\mathbf{K}) + \epsilon}, \quad \epsilon > 0 \quad (4.12)$$

or as a trace formulation (proof in Appendix A.3), validated in [41] to be uniform and continuous w.r.t (\mathbf{K}, ϵ) over $\mathbb{R}^{n \times n} \times [0, \infty[$ for $\epsilon > 0$:

$$\Phi_\epsilon(\mathbf{K}) = \text{Tr}(\mathbf{K}(\mathbf{K}^T \mathbf{K} + \epsilon \mathbf{I})^{-1} \mathbf{K}^T) \quad (4.13)$$

This expression resembles to the Tikhonov regularization technique (validated in [43] and explained in Section 2.2.2 of Chapter 2) which can approximate the discontinuous pseudo-inverse reformulation of the rank function. This technique filters out the small singular components of \mathbf{K} and \mathbf{E} , while preserving their large components in order to make the matrix approximation more precise. As for the error difference between the rank and its approximation, it is validated in [41] to be upper bounded by:

$$\text{rank}(\mathbf{K}) - \Phi_\epsilon(\mathbf{K}) = \sum_{i=1}^{\text{rank}(\mathbf{K})} \frac{\epsilon}{\sigma_i^2(\mathbf{K}) + \epsilon} \leq \epsilon \sum_{i=1}^{\text{rank}(\mathbf{K})} \frac{1}{\sigma_i^2(\mathbf{K})} \quad (4.14)$$

By this, a small value for ϵ should be considered to reduce the error: $\Phi_\epsilon(\mathbf{K}) \rightarrow \text{rank}(\mathbf{K})$ for all \mathbf{K} when $\epsilon \rightarrow 0$.

Step 2. Introduce a new variable $\mathbf{Y}_K \in \mathbb{S}^n$, where \mathbb{S}^n is the set of real symmetric matrices. Therefore, (4.13) can be approximated by a nonlinear optimization problem as follows:

$$\min\{\text{Tr}(\mathbf{Y}_K) : \mathbf{Y}_K \succeq \mathbf{K}(\mathbf{K}^T \mathbf{K} + \epsilon \mathbf{I})^{-1} \mathbf{K}^T\} \quad (4.15)$$

Applying the Schur complement theorem on (4.15) provides a result that remains a non-linear non-convex problem, where the minimization is taken over \mathbf{Y}_K and \mathbf{K} , as follows:

$$\min \left\{ \text{Tr}(\mathbf{Y}_K) : \begin{pmatrix} \mathbf{Y}_K & \mathbf{K} \\ \mathbf{K}^T & \mathbf{K}^T \mathbf{K} + \epsilon \mathbf{I} \end{pmatrix} \succeq 0 \right\} \\ \Leftrightarrow \begin{cases} (i) & \mathbf{Y}_K \succeq 0, \\ (ii) & \mathbf{K}^T (\mathbf{I} - \mathbf{Y}_K \mathbf{Y}_K^\dagger) = \mathbf{0}, \\ (iii) & (\mathbf{K}^T \mathbf{K} + \epsilon \mathbf{I}) - \mathbf{K}^T \mathbf{Y}_K^\dagger \mathbf{K} \succeq 0 \end{cases} \quad (4.16)$$

where \mathbf{Y}^\dagger denotes the Moore-Penrose pseudoinverse of \mathbf{Y} .

Step 3. Enter, therefore, a new variable $\mathbf{Z}_K = \mathbf{K}^T \mathbf{K}$. However, this hard

equality adds further difficulty in solving the problem. Hence, we relax the equality to $\mathbf{Z}_K \succeq \mathbf{K}^T \mathbf{K}$ and apply the Schur complement on it in order to convert problem (4.16) to an SDP one:

$$\min \left\{ \text{Tr}(\mathbf{Y}_K) : \begin{pmatrix} \mathbf{Y}_K & \mathbf{K} \\ \mathbf{K}^T & \mathbf{Z}_K + \epsilon \mathbf{I} \end{pmatrix} \succeq 0, \begin{pmatrix} \mathbf{I} & \mathbf{K} \\ \mathbf{K}^T & \mathbf{Z}_K \end{pmatrix} \succeq 0 \right\} \quad (4.17)$$

Step 4. Impose a penalty on \mathbf{Z}_K by appending the term $\frac{1}{\gamma} \text{Tr}(\mathbf{Z}_K)$ ($\gamma > 0$) to $\text{Tr}(\mathbf{Y}_K)$, so that \mathbf{Z}_K is restored to be near to $\mathbf{K}^T \mathbf{K}$. This is because, due to the relaxation $\mathbf{Z}_K \succeq \mathbf{K}^T \mathbf{K}$, \mathbf{Z}_K could deviate too much from $\mathbf{K}^T \mathbf{K}$, which affects on $\text{Tr}(\mathbf{Y}_K)$ by deviating it from $\Phi_\epsilon(\mathbf{K})$ ($\approx \text{rank}(\mathbf{K})$). For completeness, we apply the same above steps to \mathbf{E} to get the following mathematical model:

$$\begin{aligned} & \min \left(\text{Tr}(\mathbf{Y}_E) + \frac{1}{\gamma} \text{Tr}(\mathbf{Z}_E) \right) + \left(\text{Tr}(\mathbf{Y}_K) + \frac{1}{\gamma} \text{Tr}(\mathbf{Z}_K) \right) \\ \text{s.t. } & \begin{pmatrix} \mathbf{E} & \mathbf{X} \\ \mathbf{X}^T & \mathbf{K} \end{pmatrix} \succeq 0, \begin{pmatrix} \mathbf{Y}_E & \mathbf{E} \\ \mathbf{E}^T & \mathbf{Z}_E + \epsilon \mathbf{I} \end{pmatrix} \succeq 0, \begin{pmatrix} \mathbf{I} & \mathbf{E} \\ \mathbf{E}^T & \mathbf{Z}_E \end{pmatrix} \succeq 0, \\ & \begin{pmatrix} \mathbf{Y}_K & \mathbf{K} \\ \mathbf{K}^T & \mathbf{Z}_K + \epsilon \mathbf{I} \end{pmatrix} \succeq 0, \begin{pmatrix} \mathbf{I} & \mathbf{K} \\ \mathbf{K}^T & \mathbf{Z}_K \end{pmatrix} \succeq 0, \\ & X_{i,j} = M_{i,j}, (i, j) \in \mathcal{S} \end{aligned} \quad (4.18)$$

The problem above can be solved using SDP solvers. The variables are \mathbf{X} and the PSD matrices \mathbf{Y}_K , \mathbf{Y}_E , \mathbf{K} , \mathbf{E} , \mathbf{Z}_K , \mathbf{Z}_E . \mathbf{X} does not have necessarily to be symmetric due to the presence of \mathbf{X} and \mathbf{X}^T in the constraint. It is good to mention here that this rank approximation may still return a full rank diagonal matrix after replacing "*" in \mathbf{X} by zeros, since the resulting \mathbf{K} and \mathbf{E} may also be diagonal (the proof can be found in the Appendices A.1 and A.2). Consequently, additional constraints are needed to prevent these matrices from being diagonal. The following Lemma solves this issue.

4.2.2.1 Step 5. Solution for the Diagonal Issue

Lemma 2. Let \mathbf{K} and $\mathbf{E} \in \mathbb{R}^{n \times n}$ with $K_{i,i} < 2$ and $E_{i,i} < 2$ where $i = 1, \dots, n$. Let \mathbf{J} be a matrix of all ones. If $(\mathbf{K} - \mathbf{J})$ and $(\mathbf{E} - \mathbf{J})$ are PSD matrices then \mathbf{K} and \mathbf{E} are not diagonal.

Proof. We validate the above lemma for \mathbf{K} , and the same holds for \mathbf{E} . We prove that, if \mathbf{K} is a diagonal matrix, then $(\mathbf{K} - \mathbf{J})$ is not PSD. If \mathbf{K} is diagonal, then $(\mathbf{K} - \mathbf{J})$ becomes a matrix with diagonal entries equal to $K'_{i,i}$ where $K'_{i,i} = K_{i,i} - 1 < 1$ since $K_{i,i} < 2$, and the remaining entries equal to 1. To prove that $\mathbf{K} - \mathbf{J}$ is not PSD, it is sufficient to show that $\exists \mathbf{u} \in \mathbb{R}^{n \times 1}$ such that $\mathbf{u}^T (\mathbf{K} - \mathbf{J}) \mathbf{u} \leq 0$. For this, we consider a special case and let $u_1 = \dots = u_n$

(where $u_i \in \mathbb{R}$).

$$(u_1, \dots, u_n) \begin{pmatrix} K'_{1,1} & -1 & \dots & -1 \\ -1 & \ddots & \ddots & \vdots \\ \vdots & \ddots & \ddots & -1 \\ -1 & \dots & -1 & K'_{n,n} \end{pmatrix} \begin{pmatrix} u_1 \\ \vdots \\ u_n \end{pmatrix} \quad (4.19)$$

Recall that $K'_{i,i} < 1 \forall i$, then $\mathbf{u}^T(\mathbf{K} - \mathbf{J})\mathbf{u}$ is equal to

$$\begin{aligned} \sum_i K'_{i,i} u_i^2 - \sum_i \sum_{j \neq i} u_i u_j &= \left(\sum_i K'_{i,i} \right) \mathbf{u}^2 - \sum_i \sum_{j \neq i} \mathbf{u}^2 \\ &= \left(\sum_i K'_{i,i} \right) \mathbf{u}^2 - n(n-1) \mathbf{u}^2 < 0 \end{aligned} \quad (4.20)$$

since $\sum_i K'_{i,i} < n$. Hence, $\mathbf{u}^T(\mathbf{K} - \mathbf{J})\mathbf{u} < 0$ and $(\mathbf{K} - \mathbf{J})$ are not PSD. This concludes the proof. \square

Final Step. After proving this lemma, additional constraints should be added to (4.18) by forcing $(\mathbf{K} - \mathbf{J})$ and $(\mathbf{E} - \mathbf{J})$ to be PSD. Based on the above, this will oblige \mathbf{K} and \mathbf{E} *not* to be diagonal, and hence will solve the issue of the ”*” fields in \mathbf{X} . By this, the final objective function for the problem of the rank minimization of the TIM matrix (that we call *RM-TIM*) along with the constraints, can be written as follows:

$$\begin{aligned} \text{RM-TIM} \quad & \min \left(\text{Tr}(\mathbf{Y}_E) + \frac{1}{\gamma} \text{Tr}(\mathbf{Z}_E) \right) + \left(\text{Tr}(\mathbf{Y}_K) + \frac{1}{\gamma} \text{Tr}(\mathbf{Z}_K) \right) \\ \text{s.t.} \quad & \begin{pmatrix} \mathbf{E} & \mathbf{X} \\ \mathbf{X}^T & \mathbf{K} \end{pmatrix} \succeq 0, \begin{pmatrix} \mathbf{Y}_E & \mathbf{E} \\ \mathbf{E}^T & \mathbf{Z}_E + \epsilon \mathbf{I} \end{pmatrix} \succeq 0, \begin{pmatrix} \mathbf{I} & \mathbf{E} \\ \mathbf{E}^T & \mathbf{Z}_E \end{pmatrix} \succeq 0, \\ & \begin{pmatrix} \mathbf{Y}_K & \mathbf{K} \\ \mathbf{K}^T & \mathbf{Z}_K + \epsilon \mathbf{I} \end{pmatrix} \succeq 0, \begin{pmatrix} \mathbf{I} & \mathbf{K} \\ \mathbf{K}^T & \mathbf{Z}_K \end{pmatrix} \succeq 0, (\mathbf{K} - \mathbf{J}) \succeq 0, \\ & (\mathbf{E} - \mathbf{J}) \succeq 0, K_{i,i} < 2, E_{i,i} < 2, \forall i = 1, \dots, n, \\ & X_{i,j} = M_{i,j}, (i, j) \in \mathcal{S} \end{aligned} \quad (4.21)$$

The flow of the *RM-TIM* algorithm can be summarized in the figure below:

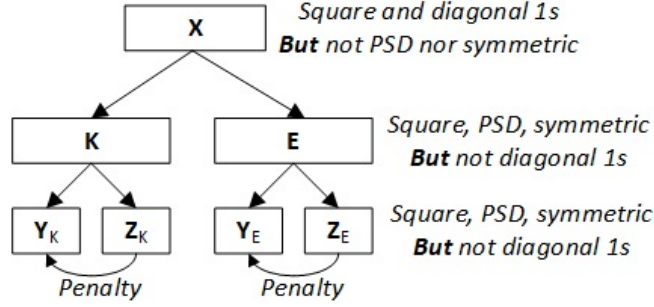


Figure 4.2: Flow of *RM-TIM* method

Therefore, comparing our work to Fazel’s work [101], the main difference resides in the rank relaxation of \mathbf{K} and \mathbf{E} , where we replaced the nuclear norm by a pseudo-inverse reformulation of the rank and added additional constraints, as shown in Eq. (4.21). Having all 1s in the diagonal entries of \mathbf{X} , which is the case of the TIM problem (multiple unicast setting), prohibited the direct use of the nuclear norm heuristic proposed by Fazel, knowing that it will always give an identity matrix (full rank matrix). It is good to recall here that in Fazel’s problem, \mathbf{X} was a general matrix (no hard constraint on the diagonal entries), which did not require a specific treatment to overcome this special structure.

4.2.2.2 Simulation Setup and Parameters

We implement problem (4.21) using the convex optimization toolbox CVX [146] in MATLAB R2016b on a desktop of 64 GB RAM with Intel Xeon CPU E5–2620 v4 working at 2.10 GHz. As for the constant factors, the γ value is chosen in a way to enforce the penalty terms $\text{Tr}(\mathbf{Z}_K)$ and $\text{Tr}(\mathbf{Z}_E)$ *not* to be negligible w.r.t $\text{Tr}(\mathbf{Y}_K)$ and $\text{Tr}(\mathbf{Y}_E)$, while still taking small values, so that \mathbf{Y}_K and \mathbf{Y}_E *do not deviate* from their exact rank: γ is found heuristically to be in the range [4, 20], (so we take $\gamma = 10$), while ϵ is set to 10^{-4} , for which the error in (4.14) is reduced.

4.2.2.3 Parameters Assumptions Justification

- γ parameter: $\gamma = 10$.

Justification: γ is chosen heuristically, and it is found to be in the range $4 \leq \gamma \leq 20$ after trying different topologies (and hence different matrices) and different dimensions. The value for γ should be chosen in such a way to enforce $\text{Tr}(\mathbf{Z}_K)$ and $\text{Tr}(\mathbf{Z}_E)$ *not* to be negligible with respect to $\text{Tr}(\mathbf{Y}_K)$ and $\text{Tr}(\mathbf{Y}_E)$ respectively in Eq. (4.21), and at the same time, γ should not take a very high value so that \mathbf{Y}_K and \mathbf{Y}_E do not deviate from their exact rank. If $\text{Tr}(\mathbf{Z}_K)$ and $\text{Tr}(\mathbf{Z}_E)$ dominate, this will impact the rank of \mathbf{X} by increasing it. Recall that $\frac{1}{\gamma}\text{Tr}(\mathbf{Z}_K)$ and $\frac{1}{\gamma}\text{Tr}(\mathbf{Z}_E)$ play the role of penalty functions that are necessary because $\text{Tr}(\mathbf{Y}_K) = \text{Tr}(\mathbf{K}(\mathbf{K}^T\mathbf{K} + \epsilon\mathbf{I})^{-1}\mathbf{K}^T) =$

$\text{Tr}(\mathbf{K}(\mathbf{Z}_K + \epsilon \mathbf{I})^{-1} \mathbf{K}^T)$ may significantly deviate from $\Phi(\mathbf{K})(\approx \text{rank}(\mathbf{K}))$. This can be justified by the fact that \mathbf{Z}_K gains too much freedom while $\mathbf{Z}_K = \mathbf{K}^T \mathbf{K}$ is relaxed to $\mathbf{Z}_K \succeq \mathbf{K}^T \mathbf{K}$, and thus \mathbf{Z}_K can deviate away from $\mathbf{K}^T \mathbf{K}$. The same analysis aforementioned holds for \mathbf{Z}_E .

It is worth mentioning that although some parameters should be fixed heuristically, we believe that this does not impact the interest of the proposed solution as the number of parameters is small and can be adjusted easily. Also fixing parameters heuristically is encountered in several existing / known optimization methods.

- **ϵ parameter:** $\epsilon = 10^{-4}$.

Justification: The error difference between the rank of \mathbf{K} and its approximation $\Phi_\epsilon(\mathbf{K})$ is upper bounded by $\epsilon \sum_{i=1}^{\text{rank}(\mathbf{K})} \frac{1}{\sigma_i^2(\mathbf{K})}$, as shown in (4.14) The interpretation of this bound derives from Zhao's paper [41], but to be precise, this is derived without taking into account the constraints in (4.21), i.e., $(\mathbf{K} - \mathbf{J}) \succeq 0, (\mathbf{E} - \mathbf{J}) \succeq 0, K_{i,i} \leq 2, E_{i,i} \leq 2$, etc. This upper bound helps in choosing the suitable value for the parameter ϵ . It turns out that one can check easily (two to three times) by starting with a small value for ϵ until Φ_ϵ becomes very close to the rank, i.e., the error tends to 0. For a given ϵ , one can solve the problem (e.g., using our method), and then easily compute the error by $\text{rank}(\mathbf{K}) - \Phi_\epsilon(\mathbf{K})$. If for a given ϵ , the error computed turns out to be large, ϵ should be reduced further and the process repeats. We have noticed from our simulations that the number of values for ϵ that should be tested is small (note that beyond a certain value, the decrease in the error becomes negligible and hence the improvement in the rank does not change, therefore the value of ϵ should be small, tending to 0 but not exactly 0 to not fall into convergence issues). A similar conclusion has been drawn in [41] (although the problem is different in our case with more constraints), where it was shown that by using the function Φ_ϵ , the rank can be minimized by testing only a small number of values for ϵ . For instance, for $\epsilon = 10^{-4}$, the singular values of \mathbf{K} are 2.4759, 1.9025, 0.8573, 0.0007, 0.0000 making the error between the exact rank and its approximation equal to the following: (for rank = 3, taking only the first 3 singular values)

$$\sum_{i=1}^{\text{rank}(\mathbf{K})} \frac{\epsilon}{\sigma_i^2(\mathbf{K}) + \epsilon} = 1.7998 \times 10^{-4}$$

As for $\epsilon = 10^{-1}$, the singular values σ_i of \mathbf{K} become equal to $\boldsymbol{\sigma} = [2.4570, 1.4754, 1.0372, 0.0136, 0.0168]$ and the value of the upper bound of the error reaches:

$$\sum_{i=1}^{\text{rank}(\mathbf{K})} \frac{\epsilon}{\sigma_i^2(\mathbf{K}) + \epsilon} = 0.1453$$

Moreover, one can look at it from another perspective: according to [147],

Zhao’s formulation of the rank function is considered as a pseudo-inverse reformulation. The equivalent formulation can be stated as follows :

$$\text{rank}(\mathbf{K}) = \text{rank}(\mathbf{K}^\dagger \mathbf{K}) = \text{Tr}(\mathbf{K}^\dagger \mathbf{K})$$

and these pseudoinverses are limits where

$$\mathbf{K}^\dagger = \lim_{\epsilon \rightarrow 0} (\mathbf{K}^T \mathbf{K} + \epsilon \mathbf{I})^{-1} \mathbf{K}^T = \lim_{\epsilon \rightarrow 0} \mathbf{K}^T (\mathbf{K} \mathbf{K}^T + \epsilon \mathbf{I})^{-1}, \quad \epsilon > 0$$

However, similar to matrix rank, the pseudo-inverse function is not continuous but it can be approximated by using a Tikhonov regularization technique. Inspired by this fact, the work of Zhao proves that rank minimization can be approximated to any level of accuracy via continuous optimization controlled by ϵ . The optimal value of this parameter ϵ is specific to each problem and is usually unknown. In practical problems, it is determined by an ad hoc method [44]. For instance, in our problem, ϵ is found through heuristic methods to be equal to 10^{-4} .

4.2.2.4 Results and Analysis

Toward showing the relevance of our technique *RM-TIM*, we test it on a moderate D2D network (which is translated into a square TIM matrix of size n) and compare the result to the known Directional Alternating Projection via eigenvalue decomposition (dirAP) algorithm [36] in terms of rank reduction, and matrix perturbation and decoding error. The dirAP method, which converges the fastest, is usually used for index coding problems where all the diagonal entries of the matrix are equal to 1, the (i, j) th entry of the matrix is equal to 0 if user i does not have packet j and the remaining entries should be set to NaN or represented by stars “*” in the literature. More details about index coding can be found in Section 2.1.3 of Chapter 2. In order to accomplish this comparison, we give the TIM adjacency matrix as input to our algorithm and its complement (the index coding matrix) to the dirAP algorithm. For evaluation, we particularly choose the $n = 5$ example shown in Fig. 2.1 (also studied in other papers [26] and [19]), knowing its historical significance, as it turns out that it is an index coding problem that was considered originally by Birk and Kol in [2], and was the first known example of interference alignment. We also evaluate our proposed method on another example with larger dimension ($n = 12$), illustrated in Fig. 4.1.

Rank achieved: In this subsection, we compare the performance of our proposed algorithm, *RM-TIM* to the dirAP method, in terms of the minimum rank achieved. In Table 4.3, we show the resulting matrices after applying both methods on Birk and Kol example, illustrated in Fig. 2.1. Note that we choose here

Table 4.3: Resulting \mathbf{X} (a) from *RM-TIM*

1	0.6962	0	0	0.8689
0.8689	1	0	0	0.5191
0	0.4284	1	1	0
0	0.4284	1	1	0
0.6962	0	0.4284	0.4284	1

(b) from *dirAP*

1.0004	$9.3993e^{-7} + 7.4649e^{-16}i$	$-3.2122e^{-4} + 1.6199e^{-14}i$	$-3.2122e^{-4} - 1.6231e^{-14}i$	1.0004
$9.3993e^{-7} + 7.4649e^{-16}i$	1	$-8.7635e^{-4} + 5.2482e^{-15}i$	$-8.7635e^{-4} - 5.2517e^{-15}i$	$9.3993e^{-7} - 1.1367e^{-17}i$
$-3.2122e^{-4} + 1.6199e^{-14}i$	$-8.7635e^{-4} + 5.2536e^{-15}i$	1	-2.3545	$-3.2122e^{-4} + 1.6200e^{-14}i$
$-3.2122e^{-4} - 1.6231e^{-14}i$	$-8.7635e^{-4} - 5.2462e^{-15}i$	-2.3545	1	$-3.2122e^{-4} + 1.6229e^{-14}i$
1.0004	$9.3993e^{-7} - 1.1364e^{-17}i$	$-3.2122e^{-4} - 1.6200e^{-14}i$	$-3.2122e^{-4} + 1.6229e^{-14}i$	1.0004

to show the output of the $n = 5$ topology as an example, due to space constraint.

In order to assess the minimum rank achieved in both methods, we apply the rank approximation decision algorithm (Algorithm 1) discussed in Section 4.1.4. In the following, we consider *RM-TIM*'s output of Table 4.3a as an example to explain the procedure of applying Algorithm 1. However, the same strategy can be applied on any other matrix, e.g., Table 4.3b. We start here by applying the singular value decomposition (SVD) on Table 4.3a, which delivers three matrices: \mathbf{Y} , \mathbf{S} and \mathbf{Z} , as shown in Table 4.4.

As we can see in Table 4.4b, the two last singular values (in bold) are so small and can be neglected. Therefore, we approximate \mathbf{S} by another matrix $\hat{\mathbf{S}}$ after zeroing these two singular values as in Table 4.5 and we compute the approximated $\hat{\mathbf{X}}_k$ as $\hat{\mathbf{X}}_k = \mathbf{Y}\hat{\mathbf{S}}\mathbf{Z}^T$, represented in Table 4.6. According to (4.7), the approximation error is equal to 0.0228% (much less than 10%). Thus, *RM-TIM* reduced the rank of the TIM matrix of Fig. 2.1 from 5 to 3.

On the other hand, after applying the same procedure on Table 4.3b, we deduce that *dirAP* reduces the rank of the TIM matrix of Fig. 2.1 from 5 to 4 only. By this, *RM-TIM* achieves a minimum rank lower than the one attained

Table 4.4: Applying SVD on the resulting \mathbf{X}

(a) Resulting \mathbf{Y}

-0.4842	0.4706	0.0402	-0.7365	-7.182e-13
-0.4516	0.3872	0.5617	0.5750	5.590e-13
-0.4168	-0.5534	0.1212	-0.0730	-0.7071
-0.4168	-0.5534	0.1212	-0.0730	0.7071
-0.4628	0.1265	-0.8084	0.3410	3.338e-13

(b) Resulting \mathbf{S}

2.4756	0	0	0	0
0	1.9020	0	0	0
0	0	0.8579	0	0
0	0	0	0.0007	0
0	0	0	0	1.681e-05

(c) Resulting \mathbf{Z}

-0.4842	0.4706	-0.0402	0.7365	6.5003e-13
-0.4628	0.1265	0.8084	-0.3410	-3.0223e-13
-0.4168	-0.5534	-0.1212	0.0730	-0.7071
-0.4168	-0.5534	-0.1212	0.0730	0.7071
-0.4516	0.3872	-0.5617	-0.5750	-5.059e-13

Table 4.5: Approximate \mathbf{S} by $\hat{\mathbf{S}}$ after zeroing the two smallest singular values

2.4756	0	0	0	0
0	1.9020	0	0	0
0	0	0.8579	0	0
0	0	0	0	0
0	0	0	0	0

Table 4.6: $\hat{\mathbf{X}}$: Approximated \mathbf{X}

1.0004	0.6960	3.964e-05	3.964e-05	0.8686
0.8686	1.0001	-3.095e-05	-3.095e-05	0.5193
3.964e-05	0.4283	1.0000	1.0000	-3.095e-05
3.964e-05	0.4283	1.0000	1.0000	-3.095e-05
0.6960	8.573e-05	0.4283	0.4283	1.0001

by dirAP. Moreover, Birk and Kol have shown that the symmetric capacity of the index coding problem is 0.5 per message [2], meaning the minimum rank achieved was 2 (as previously discussed, the minimum rank cannot be 1, since the matrix has predefined 1s (diagonal) and 0s). Therefore, *RM-TIM* outperforms dirAP by delivering a solution that is closer to the optimal one. In all, this shows the effectiveness of *RM-TIM* in increasing the DoF of a network containing 5 D2D pairs from 1/5 to 1/3, and hence boosting its throughput. With this, the interference can be roughly concentrated into one half of the signal space at each receiver, leaving the other half available for the desired signal and free of interference.

Decoding error: As for the decoding error at the receiver side, *RM-TIM* performs better than dirAP, since it stays consistent with the given 0s and 1s as inputs in the adjacency matrix, while dirAP changes these initial values (0s replaced by relatively small numbers in the resulting matrix, as shown in Table 4.3), leading to a matrix perturbation [36]. This perturbation may probably cause a small decoding error at the user’s side. In this regard, an additional point concerns the practicality of the decoding and precoding matrices ($\mathbf{U} = [\mathbf{u}_i]$ and $\mathbf{V} = [\mathbf{v}_j]$ respectively) resulting from the QR decomposition of the resulting matrix from the dirAP method. To apply the solution, each transmitter j needs to know the precoding vector \mathbf{v}_j by which it should multiply its information symbol, and each receiver i should be aware of the decoding vector \mathbf{u}_i , so that it only decodes its intended signal. However, if we apply QR decomposition on the output matrix of the dirAP algorithm, we find that the factors \mathbf{Q} and \mathbf{R} (i.e. \mathbf{U} and \mathbf{V} respectively) contain very small entries, in the range of 10^{-7} or even 10^{-16} , which cannot be implemented in practice, knowing that it requires a very high precision at the UEs’ side. Therefore, these very small entries in these matrices will be replaced in practice by 0s, and hence the resulting matrix multiplication $\mathbf{X}_{\text{new}} = \mathbf{U}_{\text{new}}\mathbf{V}_{\text{new}}$ (where \mathbf{U}_{new} and \mathbf{V}_{new} are the matrices after the substitution by 0s) will have a higher rank than the one previously found.

Moreover, it is applicable here to stress the fact that the resulting matrix from our method respects the special structure required (being not symmetric), in contrast to the output matrix resulting from dirAP that deviated from the specified model by being symmetric. Note that having a symmetric matrix should have increased the possibility of having higher dependency between the rows (and hence decreasing the rank), which did not happen in the dirAP output.

In Table 4.7, we summarize the results that correspond to both topologies $n = 5$ and $n = 12$ in terms of the minimum rank achieved and the matrix perturbation.

Getting \mathbf{U} and \mathbf{V} : In this subsection, we also consider the TIM matrix that corresponds to Birk and Kol example illustrated in Table 4.3a as an applied

Table 4.7: Comparison of *RM-TIM* against dirAP

Matrix	Min Rank		Matrix Perturbation	
	dirAP	<i>RM-TIM</i>	dirAP	<i>RM-TIM</i>
$n = 5$ (Fig. 2.1)	4	3	Yes	No
$n = 12$ (Fig. 4.1)	9	7	Yes	No

example. To get the corresponding precoding and decoding matrices, \mathbf{V} and \mathbf{U} , respectively, (as in Table 4.8) we apply the QR algorithm on \mathbf{X} , which delivers two matrices \mathbf{Q} and \mathbf{R} .

Table 4.8: Applying QR decomposition on \mathbf{X} resulting from *RM-TIM*(a) Original \mathbf{Q}

0.6682	-0.0030	-0.1038	-9.7945e-07	0.7367
0.5806	0.4512	-0.3583	-3.3801e-06	-0.5753
0	0.4920	0.5026	-0.7071	0.0729
0	0.4920	0.5026	0.7071	0.0729
0.4652	-0.5588	0.5963	5.6257e-06	-0.3402

(b) Original \mathbf{R}

1.4965	1.0458	0.1993	0.1993	1.3472
0	0.8706	0.7447	0.7447	-0.3272
0	0	1.2606	1.2606	0.3201
0	0	0	2.3785e-05	3.020e-06
0	0	0	0	0.0013

As proved above, the rank of \mathbf{X} is minimized to 3, then the originals \mathbf{Q} and \mathbf{R} should be truncated by removing the last two columns of \mathbf{Q} and the last two rows of \mathbf{R} , as represented in Table 4.9. To show that this truncation is valid, we multiply the truncated \mathbf{Q} and \mathbf{R} . This multiplication gives an approximation of \mathbf{X} in Table 4.10, which is almost equal to the original \mathbf{X} in Table 4.3a.

4.2.2.5 *RM-TIM*'s Complexity

Concerning time comparison, *RM-TIM* requires a higher CPU time than dirAP to solve the optimization problem. For instance, *RM-TIM* spends around 0.8s (seconds) to fill the matrix example of Fig. 4.1 ($n = 12$), while dirAP takes 0.4s. This difference arises partially from our use of the general-purpose CVX toolbox (with its built-in SDPT3 solver), where it is hard to exploit the semantics of the program to direct the search inside the solver and to control the encoding of process interleavings. CVX solves the problem based on the interior point

Table 4.9: Truncating \mathbf{Q} and \mathbf{R} (a) $\mathbf{U}:=$ Truncated \mathbf{Q}

0.6682	-0.0030	-0.1038
0.5806	0.4512	-0.3583
0	0.4920	0.5026
0	0.4920	0.5026
0.4652	-0.5588	0.5963

(b) $\mathbf{V}:=$ Truncated \mathbf{R}

1.4965	1.0458	0.1993	0.1993	1.3472
0	0.8706	0.7447	0.7447	-0.3272
0	0	1.2606	1.2606	0.3201

Table 4.10: Approximated \mathbf{X} with $r=3$

1	0.6962	-6.025e-18	2.329e-11	0.8679
0.8689	1	8.0913e-17	8.0396e-11	0.5198
0	0.4284	1	1	-9.128e-05
0	0.4284	1	1	-9.555e-05
0.6962	-4.088e-17	0.4284	0.4284	1.0004

algorithm in at most $\mathcal{O}(\sqrt{n}\log(1/\eta))$ iterations (n is the matrix dimension and η is related to the solution precision), while maintaining a polynomial complexity per iteration [148] (roughly $\mathcal{O}(n^6)$, without considering the special structure of the constraints in (13) which can reduce the complexity further).

As for dirAP, although it requires more iterations, it has less complexity per iteration, leading to a lower CPU time. Indeed, there is a tradeoff between complexity and performance, but the former becomes critical when the update of the adjacency matrix configuration (the run of the algorithm) should be done in each timeslot. However, this is not the case of TIM, knowing that it is not based on the instantaneous CSI, but only on the network topology (i.e., connectivity). This topology changes very slowly over time (once each few seconds), especially in a D2D scenario, since the D2D communication is well-known to be more suitable for static and low speed environment (i.e., coffee shop, campus university), where the D2D pairs have interest in staying connected after completing the relatively long discovery process [3]. This is because, if the D2D pairs move rapidly, the connection between them will be broken, and hence they should repeat the discovery step before being able to exchange files and photos or play games. Therefore, with the above in mind, 0.8s can be considered an acceptable time duration to run our algorithm (with polynomial complexity) and minimize

the rank. It is worth reminding here that, although our algorithm may require higher CPU time, but it outperforms the dirAP method in terms of rank reduction, consistency with given 0s and 1s as inputs, while still respecting the TIM special structure, as previously discussed.

4.2.2.6 Summary

In the first part of this chapter, we model the Topological Interference Management (TIM) problem, in the context of D2D, as a low-rank matrix completion problem. We show that the lack of vector space structure of the adjacency matrix resulting from TIM when optimizing its rank can be mitigated through a novel scheme that we propose, based on semi-definite programming (SDP). The complexity of the problem resides in the special structure of the TIM matrix in which all the diagonal entries must be equal to 1 and some other entries must be equal to 0. This special structure is due to the interference topology of the D2D network. To the best of our knowledge, this is the first work that develops an SDP solution for TIM to fill the matrix missing entries. The proposed approximation method follows in several steps: it starts by dividing the general matrix for which its rank should be minimized into two symmetric and positive semi-definite (PSD) matrices related to it via its Schur complement, and then replace the rank function for each of these matrices by a continuous generic approximation function controlled by a parameter ϵ . A key step is the development of a novel mathematical result to force each of these matrices *not* to be diagonal, and hence avoiding obtaining full rank matrices. This result combined with the other rank approximation steps derived in this subsection allows us to reduce the rank of the TIM matrix using an SDP solver. Our simulations show a matrix rank reduction ability that outperforms other existing methods. This is translated as reducing interference in the network.

This part of this chapter, which is related to RM-TIM rank minimization method, has been published in IEEE Wireless Communication Letters [28].

4.2.3 *eRM-TIM*: "Tweaked" Nuclear Norm-Rank Approximation Method

Although the TIM rank minimization method that we developed (also using SDP), *RM-TIM*, gave good results in terms of the minimum rank achieved, however, it suffers from a relatively high complexity due to the five linear matrix inequalities (LMI) present in the constraints. This motivates us to propose, in the following, a less complex rank approximation method, while still achieving the same performance, but with much lower complexity. In this subsection, we provide details of this an enhanced TIM rank minimization method, that we call

eRM-TIM.

In this method, we also build on (4.9), and we replace the non-convex rank function by the trace function as in (4.10). However, knowing that this will also lead to a full rank diagonal matrix (as previously discussed in Section 4.2.1), then we develop another Lemma that forces \mathbf{K} and \mathbf{E} not to be diagonal, while keeping the trace function in the objective function.

4.2.3.1 Solution for the Diagonal Issue

Lemma 3. *Let \mathbf{K} and $\mathbf{E} \in \mathbb{R}^{n \times n}$ with $K_{i,i} \leq a$ and $E_{i,i} \leq a$ where $i = 1, \dots, n$, and let \mathbf{F} be a matrix with diagonal entries $F_{i,i} \leq b$ and the remaining values equal to c , where $a, b, c > 0$. If $(\mathbf{K} - \mathbf{F})$ and $(\mathbf{E} - \mathbf{F})$ are PSD matrices, such that a, b , and c satisfy the condition $(a - b) \leq (n - 1)c$, then \mathbf{K} and \mathbf{E} are not diagonal.*

Proof. For space constraint, we validate the above lemma for \mathbf{K} , and the same holds for \mathbf{E} . We prove that, if \mathbf{K} is a diagonal matrix, then $(\mathbf{K} - \mathbf{F})$ is not PSD, i.e., if \mathbf{K} is diagonal, then $(\mathbf{K} - \mathbf{F})$ becomes a matrix with $K'_{i,i}$ on the diagonal entries, where $K'_{i,i} = K_{i,i} - F_{i,i} \leq a - b$. To prove that $\mathbf{K} - \mathbf{F}$ is not PSD, it is sufficient to show that $\exists \mathbf{u} \in \mathbb{R}^{n \times 1}$ such that $\mathbf{u}^T(\mathbf{K} - \mathbf{F})\mathbf{u} \leq 0$. To this end, we consider a special case and let $u_1 = \dots = u_n$ (where $u_i \in \mathbb{R}$). Recall that $K'_{i,i} \leq a - b, \forall i$, which leads to $\sum_i K'_{i,i} \leq n(a - b)$ since the maximum value of \mathbf{K} is a ($\text{diag}(\mathbf{K}) \leq a$). By this, $\mathbf{u}^T(\mathbf{K} - \mathbf{F})\mathbf{u}$ becomes equal to:

$$\sum_i K'_{i,i} u_i^2 - \sum_i \sum_{j \neq i} c u_i u_j = \left(\sum_i K'_{i,i} \right) \mathbf{u}^2 - \sum_i \sum_{j \neq i} \mathbf{u}^2 \leq \mathbf{u}^2 (n(a - b) - n(n - 1)c)$$

Hence, $\mathbf{u}^T(\mathbf{K} - \mathbf{F})\mathbf{u} \leq 0$ relates the variables as $(a - b) \leq (n - 1)c$, which forces $(\mathbf{K} - \mathbf{F})$ to *not* be PSD. This concludes the proof. \square

After proving this lemma, additional constraints should be added to (4.10) by forcing $(\mathbf{K} - \mathbf{F})$ and $(\mathbf{E} - \mathbf{F})$ to be PSD. Based on the above, this will force \mathbf{K} and \mathbf{E} *not* to be diagonal, and hence will solve the issue of the "*" fields in \mathbf{X} . By this, the final objective function for the problem of the rank minimization of the TIM matrix (that we name *enhanced RM-TIM*, *eRM-TIM*) along with the constraints, can be written as follows:

$$\begin{aligned} \mathbf{eRM-TIM} \quad & \min \frac{1}{2}(\text{Trace}(\mathbf{K}) + \text{Trace}(\mathbf{E})) \\ \mathbf{W} = \begin{pmatrix} \mathbf{E} & \mathbf{X} \\ \mathbf{X}^T & \mathbf{K} \end{pmatrix} \succeq 0, \mathbf{X}_{i,j} = \mathbf{M}_{i,j}, (i, j \in \mathcal{S}, (\mathbf{K} - \mathbf{F}) \succeq 0, \\ & (\mathbf{E} - \mathbf{F}) \succeq 0, K_{i,i} \leq a, E_{i,i} \leq a, \forall i = 1, \dots, n \end{aligned} \quad (4.22)$$

One can notice that the resulting optimization problem is much simpler than the one for *RM-TIM* in (4.21) due to the reduction of the number of linear matrix inequality (LMIs) from five to only one.

4.2.3.2 Simulation Setup

To show the performance of *eRM-TIM*, we test it on a D2D network (which is translated into a square TIM matrix of size n), with different topologies, i.e., different interference patterns, while keeping the same number n of D2D pairs. We compare the symmetric DoF achieved per user (and hence the minimum rank attained) using our proposed method to the classical time-division multiple access (TDMA) scheme (when no TIM is applied) and to our previous rank minimization method *RM-TIM* in Section 4.2.2, as well as to other existing methods in the literature (i.e., Alternating Projections via singular value decomposition (SVDAP), and directional Alternating Projections via SVD (dirSVDAP) [36]), nine different topologies: 1) $n = 5$ in Fig. 2.1, 2) $n = 6$, illustrated as T_{17} to T_{22} in Fig. 4.3 (chosen to conserve space), 3) $n = 12$ in Fig. 4.1, 4) $n = 15$, topology showed in [32] and in Fig. 5.1, and 5) $n = 30$, the whole topology in Fig. 4.3(a), which is one sketch of different topologies (with different interfering links) that we tried. The remaining four topologies represent sparse uniformly-distributed random matrices, where 50% of the entries are 0s. We implemented *eRM-TIM* using the convex optimization toolbox CVX [146] in MATLAB R2016b also on a desktop of 16 GB RAM with Intel(R) Core(TM) i7-7700 HQ CPU, working at 2.8 GHz.

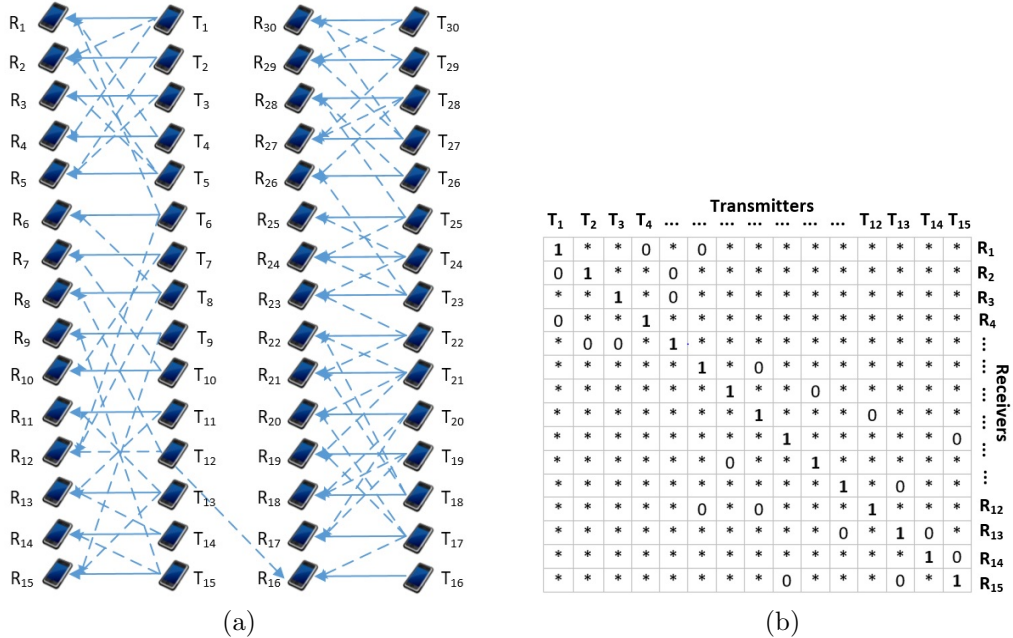


Figure 4.3: (a) Topology pattern of an example network of 30 D2D pairs, (b) interference representation matrix of the first 15 D2D pairs

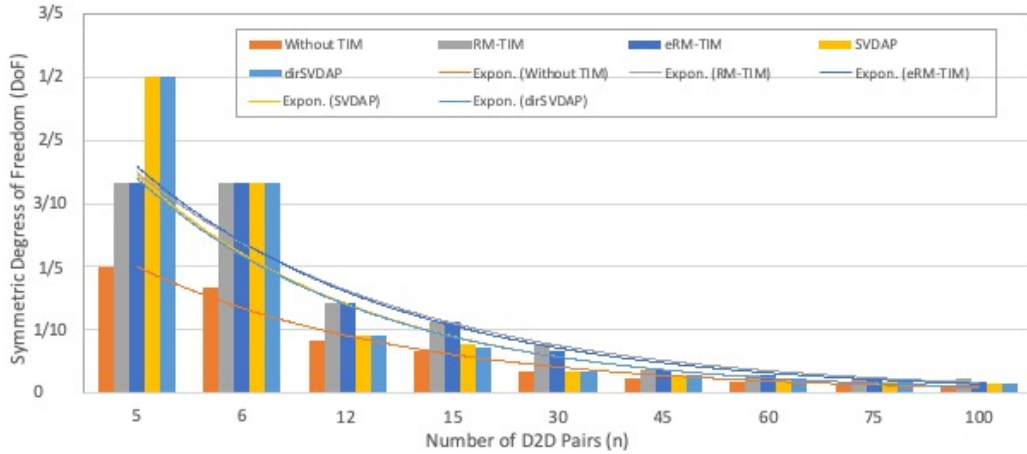


Figure 4.4: The achieved symmetric DoF by different rank minimization methods

4.2.3.3 Results and Analysis

Fig. 4.4 shows that applying TIM using any method, whether from our proposed ones (*RM-TIM/eRM-TIM*) or the existing ones in the literature (*SVDAP/dirSVDAP*), performs always better than TDMA (without TIM) which can only achieve a DoF of $1/n$ per user. Comparing among the TIM rank minimization methods, although SVDAP and dirSVDAP achieved lower rank than our methods after applying them on the $n = 5$ example [2], *eRM-TIM* behaved much better for larger n values. For instance, for the 15×15 network, *eRM-TIM* was able to minimize the rank to 9, while SVDAP and dirSVDAP, were only able to reduce it to 13 and 14, respectively. Although the large number of pairs highlights the scalability issue of the LRMC approach in formulating TIM, but still, our proposed methods are able to decrease the rank even further than other existing works. Its efficiency appears better while applying it on moderate networks than on large ones. That is, using *eRM-TIM*, the rank reduces to 57 for a 100×100 matrix, but it goes down to half for a 30×30 matrix. This is due to the interference that worsens when the number of devices increases, which also makes the adjacency matrix sparser, prohibiting the rank flexibility. Such results motivate our work in developing a clustering technique that cuts the big matrix into several less sparse sub-matrices, as will be shown in Chapter 5.

4.2.3.4 eRM-TIM's Complexity

As previously discussed in Section 4.2.2.5, solving one Linear Matrix Inequality (LMI) using the general-purpose CVX toolbox has a complexity of around $\mathcal{O}(n^6)$, where n is the matrix dimension. Then, the complexity of executing *eRM-TIM* method is in the same range of $\mathcal{O}(n^6)$. This can be explained by the fact that

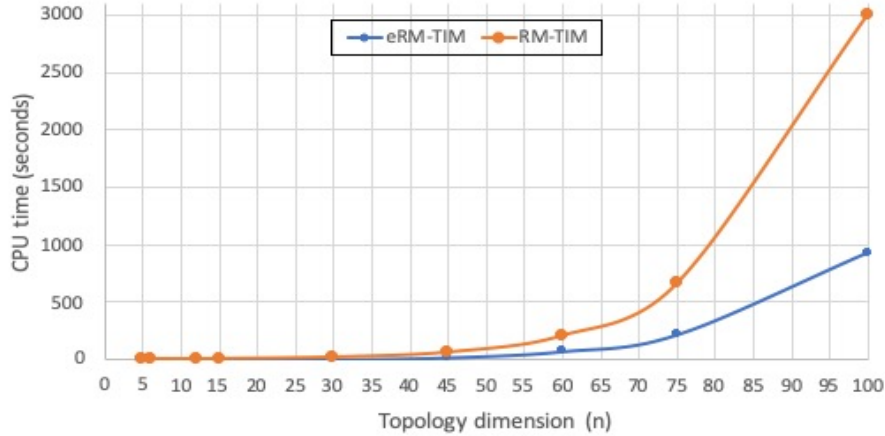


Figure 4.5: CPU time comparison between $RM-TIM$ and $eRM-TIM$

the SDP problem in (4.22), that corresponds to $eRM-TIM$, has only one LMI in the constraint. This is in contrast to $RM-TIM$, which includes five LMIs in its SDP optimization problem represented in (4.21). This difference in complexity is then translated to the processing time spent while solving each of these methods. As an illustration, we show in Fig. 4.4 the CPU time spent in function of the topology dimensions. It is clear that the gap between both methods becomes larger as the network’s dimension increases. For instance, for a 60×60 D2D network, $RM-TIM$ requires around 203.75 s to be solved, while $eRM-TIM$ needs 71.86 s only.

4.2.3.5 Summary

In the second part of this chapter, we propose an enhanced LRMC-based TIM rank minimization method, as its name (enhanced RM-TIM, $eRM-TIM$) implies. This method is different in its formulation from the previous one, i.e., $RM-TIM$ on many levels: 1) in the objective function, where the continuous generic approximation function used in [28] is replaced by a tweaked nuclear norm heuristic, and 2) in the constraints, where the five LMIs in [28] are reduced to only one LMI here, while still achieving the same performance, but with much lower complexity (and hence less processing time).

This part of this chapter, which is related to $eRM-TIM$ rank minimization method, has been published in IEEE Transactions on Communications [29].

4.2.4 Summary

All the proposed rank minimization methods in this chapter, i.e., $RM-TIM$ and $eRM-TIM$ have proved their efficiency in reducing the rank of the TIM adjacency

matrix, while respecting its special structure. These rank minimization methods can then guarantee that the interference subspaces collapse to the minimum dimensions possible.

4.3 Extending TIM using SIC

We recognize that applying TIM in D2D networks makes it more challenging, since D2D communications occur in close proximity, along with heterogeneous path losses among the users, and the use of different levels of transmit powers [149]. Hence, there may be scenarios in which the interference may be stronger than the desired signal, and therefore cannot be managed by TIM, which does not differentiate among the different levels of interference. To this end, we propose to combine TIM with a technique that separates the superimposed information, so that each receiver can retrieve its signal and decode its own data. This can be achieved by non-linear receivers that employ maximum likelihood detection (ML) or Successive Interference Cancellation (SIC). In this work, we choose to rely on SIC whose complexity is much less than that of ML detection [66]. Firstly introduced in [150], SIC is employed to decode the stronger signal, subtract it from the combined signal, and then extract the weaker one from the residue. Here appears the importance of our proposed approach that involves interference level classification while building the adjacency matrix, so that SIC can process the desired signals. Although one might question the practicality of SIC in cellular networks due to its demanding computational requirements, it is expected that the capacity of the wireless channel can be improved significantly with the aid of SIC [151]. Moreover, by the time 5G is widespread, the computational capacity of both handsets and access points is expected to be high enough to run such algorithms [152].

The main contributions of the second part of this chapter are:

- Formulating a novel rank minimization method, *cRM-TIM*, while building on the characteristic polynomial function of the TIM adjacency matrix, and combining this with a physical layer interference management technique, i.e., the successive interference cancellation (SIC) technique, in the same framework of LRMC in order to reduce the matrix rank even further.
- Integrating the notion of interference classification into Topological Interference Management (TIM), by differentiating between two levels: strong and very strong interference, which are likely to occur in D2D networks.
- Handling the very strong interference component using successive interference cancellation (SIC), while depending on TIM to manage the strong one.

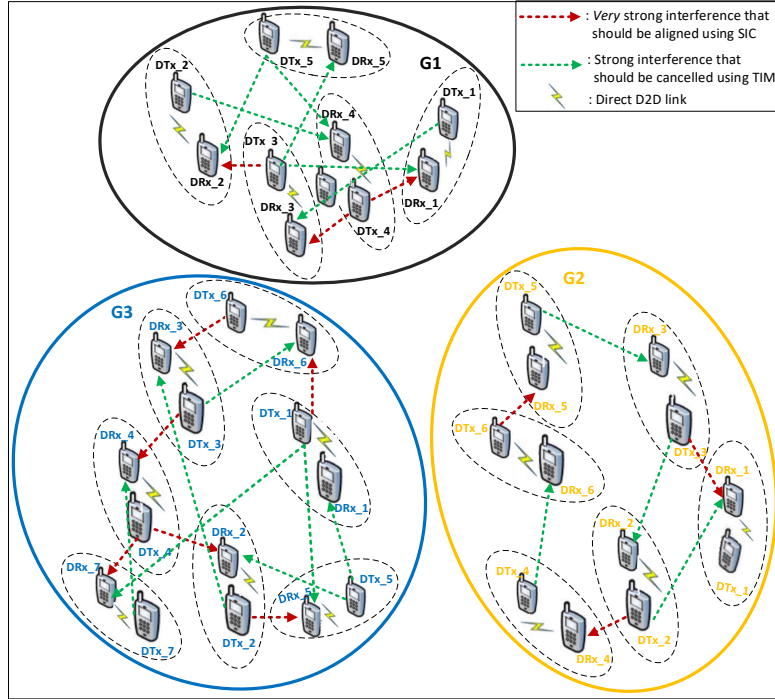


Figure 4.6: A network of 18×18 D2D-enabled devices with SIC capabilities

4.3.1 System Model for Joint TIM-SIC

We consider the architecture shown in Fig. 4.6, and composed of $d = 18$ D2D pairs (with SIC capability), communicating in a multiple unicast setting. We assume that these pairs (which are only aware of the network topology, and not of the instantaneous CSI) are divided into three groups $G1$, $G2$ and $G3$, (after applying the clustering algorithm which we describe in Chapter 5) where each cluster operates at a different frequency (illustrated by a circle with a different color). As will be shown later, our objective in Chapter 5 (in brief) is to cluster the D2D pairs with mutual interference into different groups (assigned orthogonal frequencies), and to apply the LRMC-based TIM to manage the remaining interferences (which are one-sided and hence asymmetric in the resulting sub-matrices) within the different groups. The rank minimization solution developed in this section builds on the clustering work we are presenting in Chapter 5, by classifying the remaining interference *within* each cluster into two levels: *strong* and *very strong* (after comparing it to a certain threshold): the first type is managed using the traditional TIM, while the second type is handled using the new capability provided to each D2D device in 5G networks, namely SIC.

Back to Figure 4.6, it illustrates a scenario of D2D communications in which

some of the communicating devices are in very close proximity, leading to very strong interferences that can be even stronger than the desired signal. Consequently, as shown in the figure, a D2D-receiver could receive the sum of the desired signal (yellow arrow), a very strong interference component (red arrow), a strong interference component (green arrow), and some weak interferences from far transmitters that could be neglected (and hence deleted from the figure for simplicity). Without loss of generality, we assume one very strong interference component in the received signal, but the method we integrate in our approach, can manage (i.e., cancel) multiple very strong interference components, as long as there are significant differences in their strengths. Managing all these kinds of interferences (specially the very strong one that overwhelms the desired signal) through TIM is not doable, since TIM cares only about the presence or absence of interference, not its strength. We consequently propose to combine TIM with the Successive Interference Cancellation (SIC) method. We should note that our work is inline with the one in [151] in that our clustering part of our framework keeps the number of D2D devices within the cluster relatively small, given that they will be assigned the same subchannel (frequency range). This in turn keeps the receiver complexity low as was described in [62, 63, 65, 153]. This is attributed to the fact that the hardware complexity and processing delay increase with the number of receivers that are multiplexed on the same subchannel [65]. Our framework, a finer classification of interference takes place, where a strong interference can be managed by TIM while the very strong one is handled by SIC. In pure SIC, the signal separation is typically performed sequentially: each receiver decodes the strongest signal first, and then subtracts the decoded signal from the received signal to find its own signal. In this work, we assume that all receivers are equipped with SIC which operates ideally, in that it makes perfect cancellation of the signals in the iteration steps. We remind here that the previously mentioned assumptions related to the absence of the instantaneous channel state information at the transmitter and at the receiver remain valid in the SIC scheme [154]. This results in a very smooth and successful combination of TIM and SIC.

Practically, each transmitter T_i in a cluster sends a signal $\mathbf{v}_i s_i$ to its corresponding receiver R_i (\mathbf{v}_i is the i^{th} column of the precoding matrix \mathbf{V} extracted via QR decomposition from the adjacency matrix \mathbf{X}). To recover its desired message, R_i decodes s_i by multiplying the received signal \mathbf{y}_i (combined with other undesired signals like s_j and s_k) by \mathbf{u}_i (\mathbf{u}_i is the i^{th} row of the decoding matrix \mathbf{U} , similarly extracted from \mathbf{X}). Recall that the clusters are using orthogonal frequencies and hence the inter-cluster interference is absent. The input-output relationship within each cluster can be then written as:

$$\mathbf{u}_i \mathbf{y}_i = \mathbf{u}_i (\mathbf{v}_i h_{i,i} s_i + \sum_{k, (i,k) \in \mathcal{S}'} \mathbf{v}_k h_{i,k} s_k + \sum_{j, (i,j) \in \mathcal{S}} \mathbf{v}_j h_{i,j} s_j + z_i) \quad (4.23)$$

where $h_{i,i}$ and $h_{i,j}$ are the channel coefficients between $T_i - R_i$ and $T_j - R_i$ respectively, $z_i \sim \mathcal{N}(0, 1)$ is the noise, and \mathcal{S} is the set of all pairs (i, j) such that R_i has strong interference from T_j , e.g., in group $G2$ in Fig. 4.6, \mathcal{S} includes $(1, 2)$ since R_1 desires a signal from T_1 , but it is suffering from the interference resulting from T_2 . We define here a new set \mathcal{S}' containing the indices of the nodes (T_k, R_i) with a *very strong* interference element (even stronger than the desired signal) that should be cancelled using SIC, e.g., \mathcal{S}' includes $(1, 3)$ in group $G2$ in Fig. 4.6 since R_1 is also suffering from a *very strong* interference coming from T_3 . Thus, to preserve the wanted signal, we start by following the original TIM framework conditions on the precoding and decoding matrices, $\mathbf{V} = [\mathbf{v}_i]$ and $\mathbf{U} = [\mathbf{u}_j]$, respectively, as in [26]:

$$\begin{aligned} \mathbf{u}_i \mathbf{v}_j &= 0, \quad \text{for } \forall i \neq j, (i, j) \in \mathcal{S}, \text{ and} \\ \mathbf{u}_i \mathbf{v}_i &= 1, \quad \text{otherwise} \end{aligned} \quad (4.24)$$

These TIM strategies allow a part of the undesired signals, i.e., the strong interference to be removed ($\mathbf{u}_i \sum_{(i,j) \in \mathcal{S}, i \neq j} \mathbf{v}_j h_{i,j}$), as in (4.25). We therefore employ SIC to remove the other *very strong* interference, and recover the intended signal.

$$\begin{aligned} \mathbf{u}_i \mathbf{y}_i &= \mathbf{u}_i \mathbf{v}_i h_{i,i} s_i + \sum_{k, (i,k) \in \mathcal{S}'} \mathbf{u}_i \mathbf{v}_k h_{i,k} s_k + \sum_{j, (i,j) \in \mathcal{S}} \underbrace{\mathbf{u}_i \mathbf{v}_j}_{0} h_{i,j} s_j + \mathbf{u}_i z_i \\ &= \mathbf{u}_i \mathbf{v}_i h_{i,i} s_i + \sum_{k, (i,k) \in \mathcal{S}'} \mathbf{u}_i \mathbf{v}_k h_{i,k} s_k + \mathbf{u}_i z_i \end{aligned} \quad (4.25)$$

According to [26], the conditions in (4.24) can be rewritten in a matrix form such as $\mathbf{X}_{G\ell} = [X_{i,j/k}] = \mathbf{u}_i \mathbf{v}_{j/k}$ is an $n \times n$ real matrix ($n < d$ since it corresponds to the sub-matrix that results after clustering) and ℓ refers to the ℓ^{th} cluster. As for its entries in (4.26), we add a new symbol \dagger denoting that the interference coming from T_k should be cancelled using SIC. This \dagger value is well-defined, and computed in the following subsections.

$$\mathbf{X}_{G\ell} = [X_{i,j/k}] = \mathbf{u}_i \mathbf{v}_{j/k} = \begin{cases} 1 & \text{if } i = j = k \\ & \text{the desired signal} \\ 0 & \text{if } (i, j) \in \mathcal{S} \text{ \& } i \neq j \\ & \text{interference cancelled by TIM} \\ \dagger & \text{if } (i, k) \in \mathcal{S}' \text{ \& } i \neq k \\ & \text{interference cancelled by SIC} \\ * & \text{otherwise} \\ & \text{not affecting interference} \end{cases} \quad (4.26)$$

Note that the \dagger value is kept general here since it can vary from one topology to another, but in all cases, \dagger is greater than 2, to show that it is stronger

than the desired signal ($X_{i,i} = \mathbf{u}_i \mathbf{v}_i = 1$). This can be hence considered as an LRMC approach for the joint TIM-SIC problem. The rank of the resulting matrix \mathbf{X} is related to DoF, knowing the equivalence between TIM and index coding with linear schemes (as previously discussed in Section 2.1.3 of Chapter 2). More specifically, we consider, in this work, the symmetric DoF (DoF_{sym}) of the network (the largest DoF that can be achieved by all users simultaneously) as our main figure of merit [26]. We assume for convenience a single data stream transmission per D2D pair, and so, DoF_{sym} that is attainable at high signal-to-noise ratio (SNR) will be $\text{DoF}_{\text{sym}} = \frac{1}{\text{rank}(\mathbf{X}^*)} = \frac{1}{r}$ per user. Thus, our objective is to minimize the matrix rank, and hence maximize the DoF. Back to (4.25), replacing the values of $X_{i,j}$ in this equation gives:

$$\tilde{\mathbf{y}}_i = \mathbf{u}_i \mathbf{v}_i h_{i,i} s_i + \dagger h_{i,k} s_k + \mathbf{u}_i z_i \quad (4.27)$$

Thus, to cancel the *very strong* interference, R_i can use SIC. However, prior to SIC, users should be ordered according to their signal strengths, so that the SIC-enabled receivers can work properly [155]. Reordering (4.27) accordingly leads to:

$$\tilde{\mathbf{y}}_i = \dagger h_{i,k} s_k + \mathbf{u}_i \mathbf{v}_i h_{i,i} s_i + \mathbf{u}_i z_i \quad (4.28)$$

By this, SIC can decode first signal x_k by extracting s_k (where s_k was defined in (4.25) to belong to \mathcal{S}'), considering its own signal as noise, and subtracting the estimate \hat{x}_k from the output of the TIM block (which cancels the strong interference signal component), $\tilde{\mathbf{y}}_i$, so that it can decode its own signal \hat{x}_i :

$$\begin{aligned} \text{First stage: } \hat{x}_k &= \dagger h_{i,k} s_k \\ \text{Second stage: } \hat{x}_i &= \tilde{\mathbf{y}}_i - \dagger h_{i,k} s_k = \mathbf{u}_i \mathbf{v}_i h_{i,i} s_i \end{aligned} \quad (4.29)$$

The block diagram in Fig. 4.7 illustrates the process of cancelling the interference using the joint TIM-SIC approach. The top block shown in the figure is detailed in the next section, but as shown, its purpose is to produce the decoding vector \mathbf{u}_i .

4.3.2 Two-Stage Rank Minimization

To solve the joint TIM-SIC problem, we rely on the low-rank matrix completion (LRMC) approach. Based on (4.26), we can write the adjacency matrices \mathbf{X}_{G1} , \mathbf{X}_{G2} and \mathbf{X}_{G3} that correspond to each of the groups present in Fig.4.6, as follows:

$$\mathbf{X}_{G1} = \begin{pmatrix} 1 & a_1 & 0 & \dagger_{1,1} & b_1 \\ c_1 & 1 & \dagger_{2,1} & d_1 & 0 \\ 0 & e_1 & 1 & \dagger_{3,1} & f_1 \\ g_1 & 0 & h_1 & 1 & 0 \\ i_1 & j_1 & 0 & k_1 & 1 \end{pmatrix}, \mathbf{X}_{G2} = \begin{pmatrix} 1 & 0 & \dagger_{1,2} & a_2 & b_2 & c_2 \\ d_2 & 1 & 0 & e_2 & f_2 & g_2 \\ h_2 & i_2 & 1 & j_2 & 0 & k_2 \\ l_2 & \dagger_{2,2} & m_2 & 1 & n_2 & o_2 \\ p_2 & q_2 & r_2 & s_2 & 1 & \dagger_{3,2} \\ t_2 & u_2 & v_2 & 0 & w_2 & 1 \end{pmatrix}, \mathbf{X}_{G3} = \begin{pmatrix} 1 & a_3 & b_3 & c_3 & 0 & d_3 & e_3 \\ f_3 & 1 & g_3 & \dagger_{1,3} & 0 & h & i \\ j_3 & 0 & 1 & k_3 & l_3 & \dagger_{2,3} & m_3 \\ n_3 & o & \dagger_{3,3} & 1 & p_3 & q_3 & 0 \\ 0 & \dagger_{4,3} & r_3 & s_3 & 1 & t_3 & u_3 \\ \dagger_{5,3} & v_3 & 0 & w_3 & x_3 & 1 & y_3 \\ 0 & z_3 & aa_3 & \dagger_{6,3} & bb_3 & cc_3 & 1 \end{pmatrix} \quad (4.30)$$

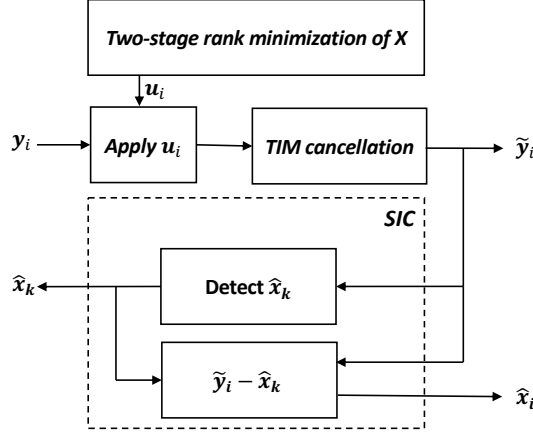


Figure 4.7: Interference cancellation at the receiver using TIM and SIC

where \mathbf{X}_{G1} , \mathbf{X}_{G2} and \mathbf{X}_{G3} have all ones on their diagonals to represent the desired communication between the D2D pairs, and predefined values as 0s to denote the strong interferences within each cluster. As for $\{a_\ell, \dots, w_\ell\}$ where $\ell = \{1, 2, 3\}$ and $\{aa_3, bb_3, cc_3\} \in \mathcal{T}$, they represent the missing values ”*” (don’t care values) of (4.26). As for $\dagger_{\bullet, \ell}$, its place in the matrix indicates the source of the *very strong* interference. In this framework, we start in Stage 1 by computing the adequate value of $\dagger_{\bullet, \ell}$ for each of the groups, so that it can be used in Stage 2, where we apply *eRM-TIM* (the rank minimization method that we developed in Section 4.2.3).

4.3.2.1 Stage 1: *cRM-TIM*

To determine the appropriate value of \dagger_ℓ (recognizing that the interference should be cancelled using SIC), we rely on the characteristic polynomial of a square $n \times n$ matrix $\mathbf{X}_{G\ell}$ (having the eigenvalues λ_i as roots of this polynomial) [56], given by:

$$\begin{aligned}
 p(\lambda) &= \det(\mathbf{X}_{G\ell} - \lambda \mathbf{I}) = (-1)^n (\lambda - \lambda_1)(\lambda - \lambda_2) \dots (\lambda - \lambda_n) \\
 &= (-1)^n [\lambda^n + c_1 \lambda^{n-1} + c_2 \lambda^{n-2} + \dots + c_{n-1} \lambda + c_n] \\
 &= (-1)^n [\lambda^n - \lambda^{n-1} \text{Trace}(\mathbf{X}_{G\ell}) + c_2 \lambda^{n-2} + \dots \\
 &\quad + (-1)^{n-1} c_{n-1} \lambda + (-1)^n \det(\mathbf{X}_{G\ell})]
 \end{aligned} \tag{4.31}$$

where \mathbf{I} is the identity matrix, and the coefficients c_2, \dots, c_{n-1} can be expressed in terms of traces of powers of $\mathbf{X}_{G\ell}$ (as c_m in (4.32)):

$$\begin{aligned}
 c_m &= -\frac{t_m}{m} + \frac{1}{2!} \underbrace{\sum_{i=1}^{m-1} \sum_{j=1}^{m-1} \frac{t_i t_j}{ij}}_{i+j=m} - \frac{1}{3!} \underbrace{\sum_{i=1}^{m-2} \sum_{j=1}^{m-2} \sum_{k=1}^{m-2} \frac{t_i t_j t_k}{ijk}}_{i+j+k=m} + \dots + \frac{(-1)^m t_1^m}{m!}, \\
 &\text{where } m = 1, 2, \dots, n, \text{ and } t_k = \text{Trace}((\mathbf{X}_{G\ell})^k)
 \end{aligned} \tag{4.32}$$

or in terms of its eigenvalues (as c_k in (4.33)):

$$c_k = (-1)^k \sum_{i_1 < i_2 < \dots < i_k}^n \sum_{i_2=1}^n \dots \sum_{i_k=1}^n \underbrace{\lambda_{i_1} \lambda_{i_2} \dots \lambda_{i_k}}_{k \text{ factors}}, \text{ for } k = 1, 2, \dots, n \quad (4.33)$$

Recall that our objective is to minimize the rank of each sub-matrix that corresponds to a cluster, or, equivalently, to minimize the number of non-zero eigenvalues of $\mathbf{X}_{G\ell}$, knowing that the number of non-zero eigenvalues of $\mathbf{X}_{G\ell}$ is at most the rank of $\mathbf{X}_{G\ell}$. Building on the relation between the c_k coefficients and the eigenvalues of $\mathbf{X}_{G\ell}$ in (4.33), we recognize that the matrix rank ($\text{rank}(\mathbf{X}_{G\ell}) = n$ when it is full rank) gets reduced by z , if and only if:

$$c_n = 0, c_{n-1} = 0, \dots, \text{ and } c_{n-(z-1)} = 0 \rightarrow c_n^2 + c_{n-1}^2 \dots + c_{n-(z-1)}^2 = 0 \quad (4.34)$$

To this end, for each sub-matrix, we define a vector \mathbf{f}_ℓ that contains all the c_k coefficients, such that $\mathbf{f}_\ell = [c_n, \dots, c_2]$ (where $k = (n-1), \dots, 2$). Note here that the c_k coefficients, which are included in \mathbf{f}_ℓ , are the ones that contain variables, excluding by this the c_k factors that represent constant values (e.g., $c_1 = -\text{Trace}(\mathbf{X}_{G\ell}) = \text{cst}$, since the TIM adjacency matrix always has 1 on its diagonal entries). We have also chosen to work with the square of these values since the c_k factors belong to \mathbb{R} , i.e., c_k can take positive or negative values. The objective then becomes to minimize the square of the ℓ_2 -norm of \mathbf{f}_ℓ that corresponds to each sub-matrix, i.e., $\|\mathbf{f}_\ell\|_2^2 = c_n^2 + c_{n-1}^2 + \dots + c_2^2$ (the dimension of \mathbf{f}_ℓ is then $1 \times (n-1)$). As for the constraints, on one hand, \dagger should be greater than 2, so that $X_{i,k} = \mathbf{u}_i \mathbf{v}_k = \dagger$, representing a *very strong* interference, should be greater than the desired one $X_{i,i} = \mathbf{u}_i \mathbf{v}_i = 1$ (as previously mentioned) to be placed first in (4.28). On the other hand, the variables $\{a_\ell, \dots, w_\ell\}$ and $\{aa_3, bb_3, cc_3\} \in \mathcal{T}$ that are assigned "*" (don't care values) in (4.26) are not subjected to any constraint, since their effect do not appear in the received signal in (4.23). The optimization problem (that refers to the method that we call *cRM-TIM*) can hence be written as:

$$\begin{aligned} \text{cRM-TIM} \quad \min \quad & \|\mathbf{f}_\ell\|_2^2 \\ \text{s.t.} \quad & \dagger_{\bullet, \ell} \geq 2 \end{aligned} \quad (4.35)$$

This problem is a strictly convex one, since the vector 2-norm squared is a strictly convex function. Note also that (4.35) can be linearized and written in trace format, as follows:

$$\begin{aligned} \text{cRM-TIM} \quad \min \quad & \text{Tr}(\mathbf{f}_\ell \mathbf{f}_\ell^T) \\ \text{s.t.} \quad & \dagger_{\bullet, \ell} \geq 2 \end{aligned} \quad (4.36)$$

since $\text{Tr}(\mathbf{f}_\ell \mathbf{f}_\ell^T) = \|\mathbf{f}_\ell\|_2^2$. Knowing this equivalence, we solve the optimization problem in (4.35) using the Matlab optimization toolbox (and more specifically

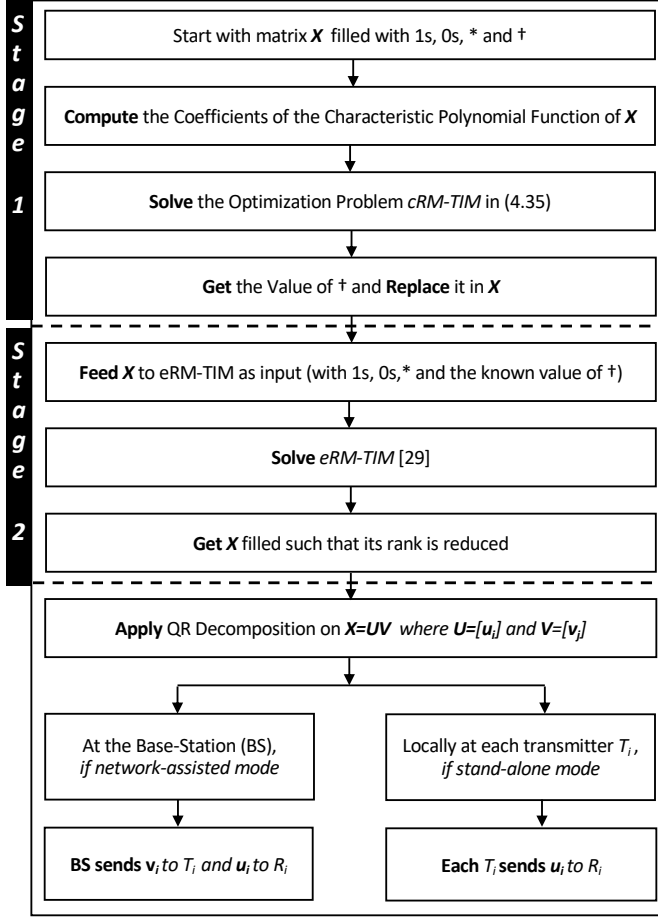


Figure 4.8: Two-stage rank minimization of \mathbf{X}

the 'fmincon' function, i.e., minimum of constrained nonlinear multi-variable function) in order to compute the appropriate value of \dagger that should be adopted. This is because $\dagger_{\bullet,\ell}$ is dependent on the topology (i.e., each topology is represented by a different matrix, with different entries). Therefore, each of the adjacency sub-matrices \mathbf{X}_{G1} , \mathbf{X}_{G2} and \mathbf{X}_{G1} will have its own $\dagger_{\bullet,\ell}$ value.

4.3.2.2 Stage 2: *eRM-TIM*

Once the value of $\dagger_{\bullet,\ell}$ is known, the rank optimization method *eRM-TIM* that we proposed in Section 4.2.3 can be applied to get the appropriate * entries (or represented as variables in (4.30)) that minimize the rank of matrix $\mathbf{X}_{G\ell}$. The solution \mathbf{X}^* can be then factorized using QR decomposition to get the precoding and decoding matrices, \mathbf{V} and \mathbf{U} , respectively.

Based on our experimental results (as will be shown later) and for the scenarios

that we have tested, we made some observations: 1) solving (4.30) by using *eRM-TIM* only (without feedback) gives a higher rank than when we combine both methods ((4.30) and *eRM-TIM*), and 2) when \dagger is replaced by a 0 value, it reverts back to the previous minimization problem, while giving a higher rank. This implies that there is a benefit behind doing a classification (by using a threshold) of the experienced interferences and distinguishing between two levels of interference: strong and *very strong*.

4.3.3 Joint TIM-SIC Framework's Complexity

The overall complexity of our proposed framework results from solving TIM, and from implementing SIC, after computing the coefficients of the characteristic polynomial function.

To calculate the polynomial function in Stage 1, many algorithms were proposed. One of those is Berkowitz's algorithm [156], which is widely used in simulation software like Matlab. It computes the coefficients by calculating iterated matrix products and performing $\mathcal{O}(n^4)$ multiplications in \mathbb{R} [157], where n is the dimension of the matrix which in our case corresponds to the average cluster size. Both rank minimization methods used in Stage 1 and Stage 2 use the interior point method: on one hand, our *eRM-TIM* method (proposed in Section 4.2.3 and [29]) which is used in Stage 2 requires $\mathcal{O}(n^6)$, while on the other hand, the built-in function "fmincon", used in Stage 1, is part of the optimization tool for nonlinear optimization programming of Matlab, and is based on the interior point method [158]. In this regard, Newton's method is often used to approximate the central path for non-linear programming, as it requires at most $\mathcal{O}(\sqrt{n} \log \epsilon^{-1})$ iterations, where ϵ is the desired accuracy [159]. The most computationally expensive step in each iteration here is the LDL factorization of the $p \times p$ system matrix, where p is the number of constraints [160] present in the optimization problem (4.35), which we had called the *cRM-TIM method*. In the worst case, this LDL factorization could take $\mathcal{O}(p^3)$ time [161–163]. The total complexity of this step will become $\mathcal{O}(n^{\frac{1}{2}}p^3)$. As for the implementation complexity of SIC at the receiver, it increases with the number of interfering users, m , i.e., $\mathcal{O}(m^3)$ [63].

Thus, the overall complexity resulting from the combination of TIM and SIC becomes equal to $\mathcal{O}(n^6) + \mathcal{O}(n^4) + \mathcal{O}(m^3) + \mathcal{O}(n^{\frac{1}{2}}p^3) = \mathcal{O}(n^6)$, where, again, n is the total number of D2D pairs *within* a cluster, m represents the number of interfering D2D users ($m < n$) and p denotes the number of constraints present in *cRM-TIM*. It is worth mentioning here that the joint TIM-SIC framework is executed in parallel across all sub-matrices that correspond to the different clusters, and hence this complexity is computed per cluster. This certainly leads to a gain in the computation because if the network was not divided into ℓ clusters, then the value of n above would have been substituted by d , where d is the total

number of D2D pairs in the whole network, i.e., $d = n \times \ell$.

Finally, it is worth commenting on the overall complexity of the proposed two-stage interference mitigation framework of this part of this chapter. First, it is not worse than the complexity of *eRM-TIM* proposed in Section 4.2.3 and [29], and second, by being a function of the number of D2D pairs (n) within each cluster, the runtime is kept under check. For example, a cluster with 20 D2D pairs (moderately large), the number of iterations is upper-bounded by 64 Millions. Moreover, we note that even if we factor in our clustering method which we proposed in Chapter 5 and [29], the overall complexity will not increase. In other words, no matter how the network size increases, the complexity will always depend on the number of D2D pairs *within* the cluster and not on the whole network.

4.3.4 Experimental Results

We implement the combination of TIM and SIC using the built-in Optimization Toolbox [164], as well as the convex optimization toolbox CVX [146] in Matlab R2016b on a desktop of 64GB RAM with Intel Xeon CPU E5-2620 v4 working at 2.10 GHz. To demonstrate the relative performance gains of the proposed algorithm, we consider, as an example, the three different clusters G_1 , G_2 and G_3 (with 5×5 , 6×6 , and 7×7 topologies, respectively) of the 18×18 D2D network represented in Fig. 4.6 in the following three various scenarios. It is good to mention here that, regardless of how large the network is, the cluster size can be made not to surpass 14 devices (i.e., 7×7 topology), and hence, there is no need to consider larger cluster sizes.

4.3.4.1 Scenario 1: No differentiation among the interferences

In this scenario, we consider that all interferences within the same cluster are recognized in the same fashion, i.e., no difference between strong and *very strong* interferences, and hence $\dagger_{\bullet, \ell} = 0$. Consequently, the SIC role vanishes. We consider this scenario as a performance baseline. In this context, if the built-in function "fmincon" of Matlab is used to solve (4.35), with the matrices \mathbf{X}_{G_1} , \mathbf{X}_{G_2} and \mathbf{X}_{G_3} in (4.30) as inputs (each one at a time), then the ranks of the 5×5 , 6×6 , and 7×7 topologies get minimized only to 3, 5, and 4, respectively, as shown in Table 4.11. On the other hand, if the same matrices are provided as inputs for our previous rank minimization *eRM-TIM* in [29], then the ranks get reduced to 4, 4, and 4, respectively. However, for these specific topologies, the obtained values have not reached the optimal values yet (which is equal to 2 for all). Recall that this optimal rank can be deduced from (4.8), with $n = 5, 6, 7$ and the numbers of c_k factors which are variables in the corresponding characteristic polynomial functions are equal to 4, 5 and 6 respectively. These results show

that an additional step can be added to decrease the rank further, namely by distinguishing between two levels of interference: strong and *very strong*, where the former is managed by TIM, while the latter is resolved using SIC. This is covered by the following two scenarios.

4.3.4.2 Scenario 2: Rank minimization without feedback

In this scenario, we adopt the interference classification approach, which we denote mathematically by putting $\dagger_{\bullet,\ell}$ back in the adjacency matrix, and setting it to a value that is strictly greater than 2 (to differentiate it from the desired signal, as previously discussed). In this step, we test the importance of having a feedback between the two rank minimization methods, by showing the effect of its non-existence. Hence, we measure the achieved rank while using each method independently. Results have shown that applying *cRM-TIM* reduces the ranks only to 2, 3 and 5, respectively, for the considered topologies of Fig. 4.6. When *eRM-TIM* in [29] is applied, however, (without feedback) and after defining the input $\dagger_{\bullet,\ell} \geq 2$, the ranks are minimized to 3, 3 and 4, respectively. This demonstrates the effectiveness of working with interference classification. From an LRMC perspective, differentiating between the levels of interference gives more flexibility to the matrix by removing the 0s, and hence reduces the rank further (in both rank minimization methods). From a communication perspective, it allows for making use of the SIC function, which, by the way, is a capability implemented in hardware in 5G devices [152]. As with the previous scenario, the optimal rank is still not reached while using each method separately. For this, we try to combine both rank minimization methods, while implementing a feedback from *cRM-TIM* to *eRM-TIM* to pass the value of $\dagger_{\bullet,\ell}$, which leads us to the third scenario.

4.3.4.3 Scenario 3: Running the rank minimization method with feedback

Finally, we test here the whole framework represented in Fig. 4.7. For ease of discussion, we refer to *cRM-TIM* as Stage 1 or *S1*, and to our *eRM-TIM* method as Stage 2 or *S2*. We start by solving the problem in (4.35) in order to get the appropriate value of $\dagger_{\bullet,\ell}$ for each sub-matrix of (4.30). Once obtained, the value is inserted in the corresponding entries of $\mathbf{X}_{G\ell}$. Next, the matrix $\mathbf{X}_{G\ell}$ is fed to *eRM-TIM*. As a result, the rank $\mathbf{X}_{G\ell}$ attained the optimal value of 2 in the tested networks of sizes $n = 5$ and $n = 6$. This proves that establishing a feedback step between the two rank minimization methods is beneficial. We remind here that both scenarios 1 and 2, apply either *S1* or *S2* alone. In this regard, applying *S1* alone does not always achieve the minimum rank as in the case of the 5×5 and 6×6 topologies, and the same goes for *S2*. Moreover, it is not only about the rank achieved, but also about the value of \dagger it is achieving. More specifically, *S1* forces $\dagger_{\bullet,\ell}$ to be much greater than 2, whereas the *eRM-TIM*

Table 4.11: Rank minimization performance with different values for \dagger

Scenario		Rank Achieved for the network of size		
		5×5	6×6	7×7
No interference classification ($\dagger = 0$)	Stage 1- <i>only</i>	3	5	4
	Stage 2- <i>only</i>	4	4	4
Rank minimization <i>without</i> feedback	Stage 1- <i>only</i>	2	3	5
	Stage 2- <i>only</i>	3	3	4
Rank minimization <i>with</i> feedback	Stage 1 + Stage 2	2(optimal)	2(optimal)	3

formulation has a tendency to make $\dagger_{\bullet,\ell}$ close to 2. In this regard, having a $\dagger_{\bullet,\ell}$ value much greater than 2 makes more sense since while sorting the factors in the input-output relation, some gap needs to exist between the desired signal and the *very strong* interference, so that the latter can be detected and managed by SIC.

As for the order of the rank minimization methods, one can ask if the order of the stages can be swapped, i.e., Stage 1 can become the one corresponding to *eRM-TIM* followed by *cRM-TIM*. In this case, the initial guess for $\dagger_{\bullet,\ell}$ will always be very close to 2, which makes this step unnecessary. On the other hand, if we start by *cRM-TIM*, then it can give the value of $\dagger_{\bullet,\ell}$ that helps in the rank minimization while applying *eRM-TIM*. In this case, *eRM-TIM* will have the value of $\dagger_{\bullet,\ell}$ adequately computed, and not assigned a value very close to 2. Table 4.11 summarizes all the aforementioned results, showing a remarkable improvement in terms of the minimum rank achieved (and hence in terms of DoF), as compared to the conventional TIM.

4.3.5 Summary

In this part of this chapter, the application of topological interference management (TIM) along with successive interference cancellation (SIC) to device-to-device (D2D) communications has been studied. A novel algorithm involving the combination of these two techniques has been proposed for tackling the interference management problem in a D2D framework, after classifying the interference intensity into two classes: strong and *very strong*. The first type is managed by TIM, while the latter is cancelled using the SIC technique. Numerical results showed that introducing SIC in the TIM scheme provides a good performance in terms of DoF as compared to the one obtained by the TIM method alone.

This part of this chapter has been submitted to IEEE Transactions on Communications [30].

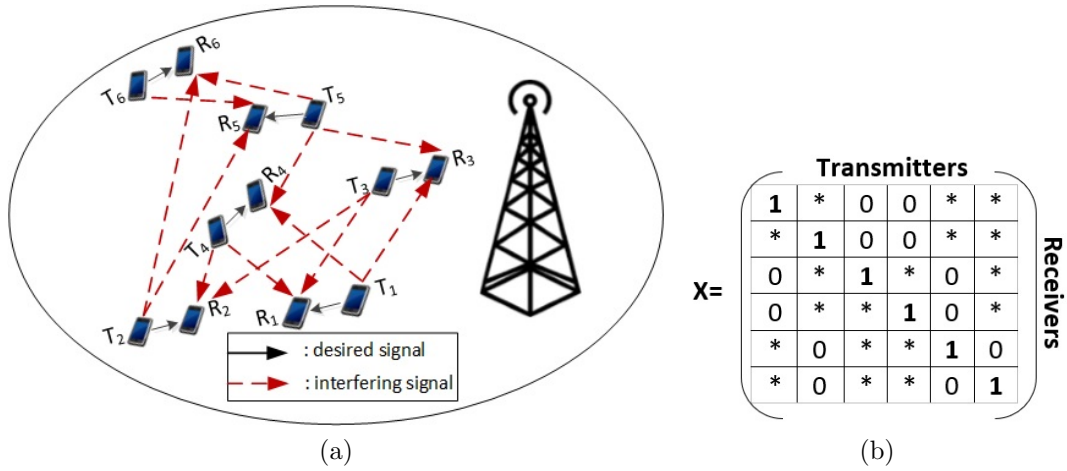


Figure 4.9: (a) Topology pattern of an example network of 6 D2D pairs, and its (b) interference representation matrix

4.4 Adapting TIM to Work for Practical Scenarios with Pathloss and Mobility

All the existing works in the literature (even our proposed methods in the previous sections of this chapter) that study the topological interference management (TIM) problem ignored the most critical aspect of interference management in practice, namely the variations in the signal strengths due to path loss. It is also important to note that the wireless networks are typically not partially connected as considered in TIM.

The main contributions of third part of this chapter can be summarized as follows:

- We extend the application of TIM from partially connected networks to ones operating in real scenarios, concerning accounting for path loss and device mobility.
- We identify the conditions when to re-run the rank minimization method in order to save processing time.

4.4.1 System Model for Pathloss and Mobility

While a variety of topologies are possible, we show in Fig. 4.9(a) the setting of an example of a 6×6 network with its corresponding adjacency matrix in (b) that reflects the connectivity among these devices. These D2D pairs operate in a network-assisted mode, and are communicating via a single-hop transmission. The devices are only aware of the network topology, and not of the instantaneous CSI [19].

4.4.2 TIM with Path Loss

In this part of this chapter, we render TIM more practical by accounting for physical phenomena, most importantly, the propagation path loss. This will help us in presenting how DoF results translate to practical signal-to-noise ratio (SNR), and how it is affected when geometrically-placed transmitters and receivers are studied.

We start by studying the D2D network of Fig. 4.9(a). Over r time slots, each transmitter T_i is communicating with its corresponding receiver R_i by sending its intended signal s_i (via the sidelink channel of the PC5 interface, as defined in the 3GPP standards [145]) after multiplying it by \mathbf{v}_i , the corresponding precoding vector. As for R_i , it decodes symbol s_i (corrupted by interfering signals) by projecting the received vector \mathbf{y}_i into the space \mathbf{u}_i , which represents its decoding vector. The input-output relationship can be written as:

$$\mathbf{u}_i \mathbf{y}_i = \mathbf{u}_i \mathbf{v}_i \sqrt{\gamma_{i,i}} h_{i,i} s_i + \mathbf{u}_i \sum_{(i,j) \in \mathcal{S}} \mathbf{v}_j \sqrt{\gamma_{i,j}} h_{i,j} s_j + \mathbf{u}_i \mathbf{z}_i \quad (4.37)$$

where $h_{i,i}$ and $h_{i,j}$ are the channel coefficients between $T_i - R_i$ and $T_j - R_i$ respectively, $z_i \sim \mathcal{N}(0, 1)$ is the noise, and \mathcal{S} is the set of indices (i, j) , where i and j correspond to the i^{th} receiver R_i and the j^{th} transmitter T_j , respectively. For instance, in Fig. 4.9(a), \mathcal{S} includes (1,1), (1,3), and (1,4) since R_1 desires a signal from T_1 , but it is suffering from the interference resulting from T_3 and T_4 . As for $\gamma_{i,i}$ and $\gamma_{i,j}$, they represent the path loss components between $T_i - R_i$ and $T_j - R_i$, respectively. For simplicity, we adopt the distance-based path loss model [165]:

$$\gamma_{i,i} = A d_{i,i}^{-\alpha} ; \quad \gamma_{i,j} = A d_{i,j}^{-\alpha} \quad (4.38)$$

where A and α are the path loss coefficient and exponent, respectively, and $d_{i,i}$ and $d_{i,j}$ are the distances between $T_i - R_i$ and $T_j - R_i$, respectively. Now to succeed in decoding the intended signal in the regime of asymptotically high SNR, without knowing the exact values of the channel coefficients, the TIM strategies should be designed such as [26]:

$$\begin{aligned} \mathbf{u}_i \mathbf{v}_j &= 0, \quad \text{for } \forall i \neq j, (i, j) \in \mathcal{S}, \text{ and} \\ \mathbf{u}_i \mathbf{v}_i &= 1, \quad \text{for } \forall i = j, (i, j) \in \mathcal{S} \end{aligned} \quad (4.39)$$

These conditions can be then written as $\mathbf{X} = [X_{i,j}] = \mathbf{u}_i \mathbf{v}_j$, which is an $n \times n$ matrix in \mathbb{R} , with entries:

$$X_{i,j} = \begin{cases} 1 & \text{if } i = j \\ 0 & \text{if } (i, j) \in \mathcal{S} \text{ and } i \neq j \\ * \times \sqrt{\gamma_{i,j}} = * \text{ (cst)} & \text{otherwise} \end{cases} \quad (4.40)$$

Note that the appearing "don't care" values ("*") represent missing entries in the matrix and implicitly include the path loss component $\gamma_{i,j}$ to highlight its impact. As an illustration, we show in Fig. 4.9(b) the TIM adjacency matrix that corresponds to the 6×6 network in (a). Now to learn about the D2D network topology in practice, and consequently build the adjacency matrix, any scheme of Section 4.1.2 (whether the network-assisted or the stand-alone mode) can be used. The above allows us to formulate the LRMC-based TIM approach as follows:

$$\begin{aligned} \min_{\mathbf{X} \in \mathbb{R}^{n \times n}} \quad & \text{rank}(\mathbf{X}) \\ \text{s.t.} \quad & X_{i,j} = M_{i,j}, (i,j) \in \mathcal{S} \\ & \sum_{j,j \neq i} \gamma_{i,j} X_{i,j}^2 \leq \theta_i, \forall i = 1, \dots, n \end{aligned} \quad (4.41)$$

where the missing entries of \mathbf{X} constitute the optimization variable and $\mathbf{M} = [M_{i,j}]$ is the $n \times n$ matrix in \mathbb{R} that includes 1s in the diagonal and 0s in the positions designated in (4.40). The last constraint limits the summation of the "don't care" values in each row (corresponding to a certain receiver) to be below a threshold θ_i (θ_i definition will be discussed later). Related to this, some links in the original TIM problem were identified as *weak* (and hence neglected) when the received signal power fell below a certain threshold. However, although each channel by itself may be negligible, the collective effect of such channels may be significant, and thus corrupt the desired signal.

The objective is then to fill \mathbf{X} with values for "*" from \mathbb{R} such that its rank is minimized so that the system DoF, at high SNR, increases [19]. Knowing that we also assume here for convenience a single data stream transmission per D2D pair, then $\text{DoF} = \frac{1}{\text{rank}(\mathbf{X})}$. Many challenges arise when solving (4.41): \mathbf{X} has a special structure in terms of 1) its dimensionality as a square matrix (due to pairwise links in D2D), 2) its entries have all ones in the diagonal and 0s in some positions, and 3) its characteristic as a general matrix, i.e., not necessarily symmetric nor positive semi-definite (PSD). In this chapter, we were able to solve the first challenge by developing several rank minimization methods. On the other hand, the modified LRMC-based TIM problem in (4.41) has a new constraint on the summation of the missing values to be less than θ_i , which limits the flexibility while choosing the values from \mathbb{R} . This will affect the dependency among the rows, and hence the matrix rank.

Now to define θ_i mathematically, we start from the fact that the ratio between the desired signal and the interfering ones should be greater than a certain threshold for signal-to-interference ratio (SIR), $SIR_{\text{threshold}}$ (usually $SIR_{\text{threshold}} > 0$ dB)

in order to be able to decode the intended message successfully:

$$\frac{\gamma_{i,i}|\mathbf{u}_i\mathbf{v}_i|^2}{\sum_{i \neq j} \gamma_{i,j}|\mathbf{u}_i\mathbf{v}_j|^2} \geq SIR_{\text{threshold}} \quad (4.42)$$

However, since $|\mathbf{u}_i\mathbf{v}_i|^2 = 1$ according to (4.39), then

$$\begin{aligned} \sum_{j,j \neq i} \gamma_{i,j}|\mathbf{u}_i\mathbf{v}_j|^2 &\leq \frac{\gamma_{i,i}}{SIR_{\text{threshold}}} \text{ and } \sum_{j,j \neq i} \gamma_{i,j}|\mathbf{u}_i\mathbf{v}_j|^2 \leq \theta_i, \\ \rightarrow \theta_i &= \frac{\gamma_{i,i}}{SIR_{\text{threshold}}} \end{aligned} \quad (4.43)$$

Thus, θ_i depends on the value of the pathloss $\gamma_{i,i}$ of the desired link and on $SIR_{\text{threshold}}$. Now to simplify (4.41), we can write it in ℓ_2 norm as follows:

$$\begin{aligned} \min_{\mathbf{X} \in \mathbb{R}^{n \times n}} \quad &\text{rank}(\mathbf{X}) \\ \text{s.t.} \quad &X_{i,j} = M_{i,j}, \quad (i,j) \in \mathcal{S} \\ &\|\mathbf{X}_i\|_2^2 \leq 1 + \theta_i \end{aligned} \quad (4.44)$$

Proof. The last constraint in (4.41) which includes the summation of squares can be written in ℓ_2 norm as follows:

$$\begin{aligned} \|\mathbf{X}_i\|_2 &= \sqrt{\gamma_{i,1}X_{i,1}^2 + \cdots + \gamma_{i,n}X_{i,n}^2} \\ \text{in our TIM problem, for } i &= j, X_{i,i} = 1, \text{ then} \\ \|\mathbf{X}_i\|_2^2 &= 1 + \gamma_{i,1}X_{i,1}^2 + \cdots + \gamma_{i,n}X_{i,n}^2 \leq 1 + \theta_i \quad (\forall i \neq j) \\ \|\mathbf{X}_i\|_2^2 &= 1 + \sum_{j,j \neq i} \gamma_{i,j}X_{i,j}^2 \leq 1 + \theta_i \end{aligned} \quad (4.45)$$

Then, we can replace the sum of squares by the ℓ_2 norm squared, which is a convex function. This concludes the proof. \square

Now once (4.41) is solved and \mathbf{X}^* is obtained, the maximum achievable DoF can be calculated as the inverse of the rank of the resulting \mathbf{X}^* . Moreover, the decoding and precoding matrices \mathbf{U} and \mathbf{V} , respectively can be also designed by factorizing the solution as $\mathbf{X}^* = \mathbf{UV}$ using QR decomposition based on the Gram-Schmidt process [27].

4.4.3 TIM with Mobility

Knowing that any TIM rank minimization method (including our proposed methods in Chapter 4) requires processing time and battery resources, we propose to re-run the algorithm *only* under certain conditions:

- when a 0 in \mathbf{X} is replaced by a "don't care" ("*"), i.e., this transmitter is no more an interfering source,

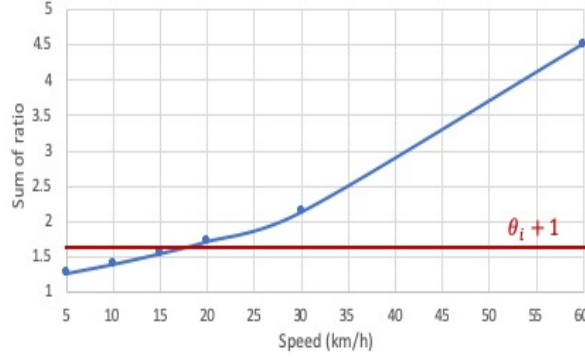


Figure 4.10: Effect of speed on re-running TIM algorithm

- when a "*" value in \mathbf{X} is replaced by a 0, i.e., this receiver is suffering from a new strong interfering link,
- when the "*" values change in such a way that:

$$\sum_j \text{ratio}_{\text{change}} > \theta_i + 1 (\forall i = 1, \dots, n), \text{ where} \quad (4.46)$$

$$\text{ratio}_{\text{change}} = \frac{\gamma_{i,j}(\text{new})}{\gamma_{i,j}(\text{old})} \times |X_{i,j}|_{\text{old}}$$

These changes occur more frequently when the devices' speeds increase. This affects the distances between the D2D pairs and their interferers, by approaching them or moving away. Hence, this will be translated in the matrix entries by turning "*" values into 0s, and vice versa. This will also appear in the $\gamma_{i,j}(\text{new})$, such that $(d_{i,j})_{\text{new}} = (d_{i,j})_{\text{old}} \pm (c_j \times \cos(\beta) \times t)$ where c_j is the speed of the j^{th} transmitter in the surrounding, β represents the direction of the movement relative to the old distance vector and t stands for the elapsed time. As an example, we consider the 6×6 topology in the system model, and we change the devices' speeds between 5 and 60 km/h. Hence, the distances between a specific D2D pair and the remaining devices (that were not initially interfering) also change. We consider here the worst case scenario when the devices are approaching which increases the probability of having interference. Then, we compute $\sum_i \text{ratio}_{\text{change}}$ in (4.46) and plot it in function of the speed in Fig. 4.10. As we can see, for a speed less than 20km/h, the sum of ratio is below the threshold $(\theta_i + 1)$, then re-running the rank minimization method is not useful here.

4.4.4 Mathematical Model of TIM in Such Real Scenario

The constraint in (4.44) can be seen as a second-order cone program (SOCP) convex optimization problem, due to the presence of the last constraint which is quadratic. Therefore, this SOCP constraint should be linearized and written as a linear matrix inequality (LMI) in order to formulate the problem as an instance

of semi-definite program as follows:

$$\begin{aligned}
& \min_{\mathbf{X} \in \mathbb{R}^{n \times n}} \text{rank}(\mathbf{X}) \\
& \text{s.t.} \quad X_{i,j} = M_{i,j}, (i,j) \in \mathcal{S} \\
& \quad \begin{pmatrix} \sqrt{\theta_i + 1} & X_{i\bullet} \\ X'_{i\bullet} & (\sqrt{\theta_i + 1})\mathbf{I} \end{pmatrix} \succeq 0, \forall i = 1, \dots, n
\end{aligned} \tag{4.47}$$

For the relaxation form, we can replace the rank function in the objective function by any method we developed earlier in this chapter and add the constraints in (4.47). Since the complexity of our rank minimization method *eRM-TIM* in [29] is lower than *RM-TIM*, the one proposed in [28], (having only one LMI), then we chose to adopt *eRM-TIM*. Therefore, we can write:

$$\begin{aligned}
& \min \frac{1}{2}(\text{Trace}(\mathbf{K}) + \text{Trace}(\mathbf{E})) \\
& \mathbf{W} = \begin{pmatrix} \mathbf{E} & \mathbf{X} \\ \mathbf{X}^T & \mathbf{K} \end{pmatrix} \succeq 0, \mathbf{X}_{i,j} = \mathbf{M}_{i,j}, (i,j) \in \mathcal{S} \\
& (\mathbf{K} - \mathbf{F}) \succeq 0, (\mathbf{E} - \mathbf{F}) \succeq 0, K_{i,i} < a, E_{i,i} < a, \\
& \begin{pmatrix} \sqrt{\theta_i + 1} & X_{i\bullet} \\ X'_{i\bullet} & (\sqrt{\theta_i + 1})\mathbf{I} \end{pmatrix} \succeq 0, \forall i = 1, \dots, n
\end{aligned} \tag{4.48}$$

4.4.5 Complexity

The complexity of solving the SDP problem in (4.48) is in the order of $\mathcal{O}(n^6)$ due to the two LMIs in the constraints. As previously discussed, this results from our use of the general-purpose CVX toolbox which solves the problem based on the interior point algorithm in at most $\mathcal{O}(\sqrt{n} \log(1/\eta))$ iterations (n is the matrix dimension and η is related to the solution precision), while maintaining a polynomial complexity per iteration [148]. Note that this complexity is computed without considering the special structure of the constraints in (4.48) which can reduce the complexity further. Although this complexity can be seen as relatively high, but it remains a polynomial one. Moreover, if the mobility conditions in Section 4.4.3 are considered, then solving the SDP problem is not frequently performed since the topology does not change very often in D2D scenarios.

4.4.6 Experimental Results

Numerical results are provided to demonstrate the performance of TIM in managing interference in D2D networks in real scenarios. The n D2D pairs are communicating at 2GHz in a cell of radius 500m. For the simulation, we consider the nine different topologies (with different number of D2D pairs) that exist in Section 4.2.3. The distances between the D2D-Txs and their corresponding D2D-Rxs are considered uniformly distributed between 5 and 50 m, in line with the work in [166]. As for the path loss model in (4.38), we select $A = 28.03$ dBs and $\alpha = 4$, in agreement with [167].

4.4.6.1 DoF Achieved

We now study how the rank r (and hence $DoF = \frac{1}{r}$) of the considered matrices corresponding to the different topologies behave when the path loss component is considered. For each receiver R_i , we compute θ_i according to (4.43), where $SIR_{\text{threshold}}$ is fixed at 2dB [167] and the path loss $\gamma_{i,i}$ in (4.38) changes relative to the distance $d_{i,i}$ between T_i and R_i . Then, we solve the LRMC problem in (4.48) to get \mathbf{X} , and thus calculate its rank r . For comparison, we adopt the scheme where the original *eRM-TIM* of [29] is applied, without considering the path loss component. The results are captured in Table 4.12, where we see that the achieved DoF when the path loss factor is accounted for, is lower than the one achieved by *eRM-TIM*. For instance, in the 45×45 topology, the DoF resulting from *eRM-TIM* attains $\frac{1}{28}$, while it only reaches $\frac{1}{32}$ when the path loss factor intervenes. This can be explained by the fact that in the second case, a new constraint is added, which limits the flexibility of the choice of the "*" values, while filling the missing entries of \mathbf{X} .

Table 4.12: Path loss effect on the achieved DoF

n	DoF achieved using	
	original <i>eRM-TIM</i>	<i>eRM-TIM</i> (with pathloss)
5×5 (Fig. 2.1)	$\frac{1}{3}$	$\frac{1}{5}$
6×6 (Fig. 4.9(a))	$\frac{1}{3}$	$\frac{1}{5}$
12×12 (Fig. 4.1)	$\frac{1}{7}$	$\frac{1}{10}$
15×15 (Fig. 5.1)	$\frac{1}{9}$	$\frac{1}{13}$
30×30 (Fig. 4.3(a))	$\frac{1}{15}$	$\frac{1}{28}$
45×45	$\frac{1}{28}$	$\frac{1}{32}$
60×60	$\frac{1}{37}$	$\frac{1}{42}$
75×75	$\frac{1}{45}$	$\frac{1}{52}$
100×100	$\frac{1}{57}$	$\frac{1}{70}$

4.4.6.2 CPU Time

Here, we report the required CPU time to resolve the rank minimization as a function of the topology dimension in Fig. 4.11. We see that triggering this method only when the conditions discussed in Section 4.4.3 are satisfied saves significant processing time. For instance, for a 30×30 network, it takes around 5.43s to run the rank minimization method. Hence, if the topology does not change, i.e., no variations in the sources of interference, and no disturbances in the path losses occur, then there is no need to spend another 5.43s to run the algorithm.

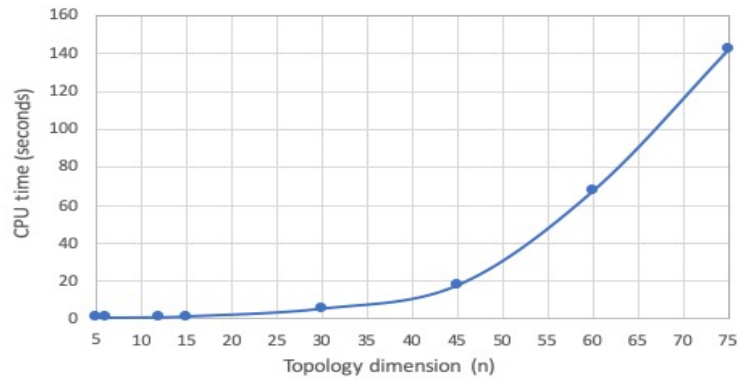


Figure 4.11: CPU time function of the topology dimensions

4.4.7 Summary

In this chapter, we study the effect of path loss and mobility on the topological interference management (TIM) method for D2D networks. We also define the conditions under which TIM should be launched, leading to significant savings in the used resources. The results show that the TIM scheme is suitable for small to medium networks, when realistic conditions are considered.

The work of this chapter has been accepted at the 15th International Conference on Wireless and Mobile Computing, Networking and Communications (WiMob 2019) [31].

Chapter 5

Providing Scalability through TIM-tailored Clustering Method

We recognize that adopting the low-rank matrix completion (LRMC) approach to solve TIM has some limitations: 1) the scalability (growing network size) [19], which hinders its application to large D2D networks, and 2) the predefined 0 entries in the adjacency matrix (denoting interference), which prevents matrix rank reduction. This can be explained by the fact that a larger number of devices in the network gives rise to a bigger interference, and makes the adjacency matrix larger and sparser, which in turn decreases its flexibility in terms of row dependency. For instance, the rank flexibility of the TIM adjacency matrix of Fig. 4.3(b) is constrained by the presence of the predefined 0s in different entry positions, where each 0 indicates the transmitter (the column index) from which the interference should be aligned at a specific receiver (the row index). More specifically, we observe that a 0 value appears in two symmetric positions when it denotes a mutual interference (e.g., the 0 entries in $X_{1,4}$ and $X_{4,1}$ correspond to $(T-R)_1$ and $(T-R)_4$ pairs that are interfering with each other). Thus, there is a need to break the original matrix into several sub-matrices to exclude the undesired 0s in these double positions.

For this, we propose to combine TIM with a corresponding clustering technique to 1) manage the interference among multiple D2D pairs communicating in a network with multiple available frequencies, and 2) group the D2D devices in a way that increases the system DoF by applying the LRMC approach of TIM on clustered devices (whereby each cluster operates with a different frequency). This can be achieved by clustering the D2D devices that are mutually interfering into different clusters, so that their corresponding sub-matrices include less 0 entries and more "*" values, and hence improve the TIM rank minimization method performance. By minimizing the rank of the sub-matrix associated with each cluster (operating at a different frequency), the total system DoF increases, multiple *interference-free* D2D simultaneous transmissions can now occur, and

hence the throughput gets boosted. Simulations results show that combining the LRMC approach of TIM with clustering is advantageous in terms of increasing the total system DoF and reducing the complexity of LRMC-based TIM. Our results suggest that even if the network has only one frequency band, dividing this frequency band into multiple sub-bands, such that each sub-band is assigned to a cluster and LRMC is applied inside each cluster, may provide DoF and processing time gains especially for high number of devices. To the best of our knowledge, this is the first work that studies *how* to apply clustering so that LRMC-based TIM can be used for larger D2D networks.

The contributions of this chapter can be summarized as follows:

- Developing a clustering algorithm specific to the LRMC approach of TIM that cuts the original adjacency matrix into sub-matrices in a way that increases the system DoF: this algorithm eliminates the "double" 0s in the matrix and replaces them by "*" (don't care values) to enhance the rank flexibility, based on the observation that two 0s in symmetric positions designate a mutual interference. This formulation is different from classical clustering techniques, in that from a communication perspective, users with mutual interference are placed in different groups. For this, we formulate the clustering scheme (using graph theory) as a relaxed SDP problem, while building on the max-k-cut formulation, but with adding a constraint on the cluster's size. To solve it, a heuristic algorithm with polynomial complexity was developed. Hence, combining the LRMC-based TIM with the proposed clustering technique overcomes the scalability issue of LRMC (which is only suitable for a limited number of users [111]), and reduces its computation time, since the resource allocation problem is divided into smaller sub-problems, on which LRMC-based TIM is applied, in a parallel way.
- Providing extensive analysis of the clustering model in [32], by deriving a novel relatively tight upper bound for its SDP relaxation using Laplacian Algebra and matrix diagonal perturbation method. This allows to determine the performance guarantee of our proposed heuristic algorithm relative to the optimal method. We have also analyzed the randomized clustering method and derived mathematically its performance w.r.t. the optimal method.
- Adding numerical results that evaluate the effectiveness of the proposed approach further.

In the below, we start by detailing the formulation of our proposed clustering model, using graph theory.

5.1 System Model for Joint TIM-Clustering

In this chapter, we build on the system model described in Section 4.1 of Chapter 4, and we consider a multiuser interference D2D network with n transmitters and

intended receivers (where n could be a moderately large number) operating in a single-hop transmission and in a multiple unicast setting. As an illustration, we show in Fig. 5.1(a), the connectivity pattern of 15 D2D enabled devices working in pairs, where solid lines denote intended signals, whereas dashed lines represent interference links. For instance, receiver R_1 is suffering from interference resulting from two transmitters T_4 and T_6 , while receiving its desired signal from T_1 . Note that we consider here an asymmetric attenuation interference network to keep the problem more general, where the received signals could have differences in strengths, due to the network topology (i.e., presence/absence of obstacles) and physical phenomena (i.e., path loss). For example, T_1 is interfering to R_2 , however T_2 does not hurt R_1 while transmitting its signal. In 5.1(b), we show the corresponding TIM adjacency matrix of the 15×15 network of 5.1(a). For instance, in Fig. 5.1(b), $X_{1,2}$ must be 0 as it represents the equivalent interference channel from T_1 to R_2 , while $X_{2,1}$ can take any value (indicated by a star "**"), as there is no interference from T_2 to R_1 .

Moreover, we assume that a set of frequencies (in the licensed or unlicensed band) $\mathcal{K} = \{Fr_1, \dots, Fr_k\}$ is available (Fr not necessarily adjacent), and that a base station (BS) clusters the D2D pairs into multiple groups, each of which with a different frequency. By clustering the devices, and assigning k orthogonal resources for the k clusters (i.e., one orthogonal resource to each cluster), the major interference among devices is eliminated. For illustration, we show in Fig. 5.2 the clustering (resulting from our proposed clustering algorithm that will be detailed later) of the 15×15 network of Fig. 5.1(a) into three different clusters ($k = 3$), and each color defines an orthogonal frequency resource. As we can see, the strong interference is eliminated here, e.g., the two pairs ($T_1 - R_1$) and ($T_4 - R_4$) interfering the one on the other are separated into two different clusters: ($T_1 - R_1$) in the cluster filled in yellow, whereas ($T_4 - R_4$) is in the blue one. Hence, ($T_1 - R_1$) and ($T_4 - R_4$) can send now simultaneously without interference.

Mapping this to the TIM model, the interference elimination will be translated in the TIM sub-matrices of Fig. 5.1(c) that relate the transmitters and receivers inside the same cluster. These sub-matrices are filled according to the connectivity pattern: the rows in \mathbf{X}_{P_2} in Fig. 5.1(c) refer to the receivers $R_2, R_3, R_4, R_6, R_{10}$ and the columns indicate $T_2, T_3, T_4, T_6, T_{10}$. We observe that each interference cut corresponds to an *eliminated* 0, which will be replaced by a "**" (don't care value), making the matrix rank subject to further minimization (further row dependency). The LRMC-based TIM scheme can hence be applied on each sub-matrix corresponding to a cluster, in a parallel way, to manage the intra-cluster interference. For instance, applying rank minimization (using any method of Chapter 4) to each sub-matrix in Fig. 5.1(c) can minimize its rank by replacing the "**" by 1s for \mathbf{X}_{P_2} and \mathbf{X}_{P_3} , and transforming them into rank-1 matrices. As for \mathbf{X}_{P_1} , which has 0 entry at $X_{5,6}$, we expect that its rank can be

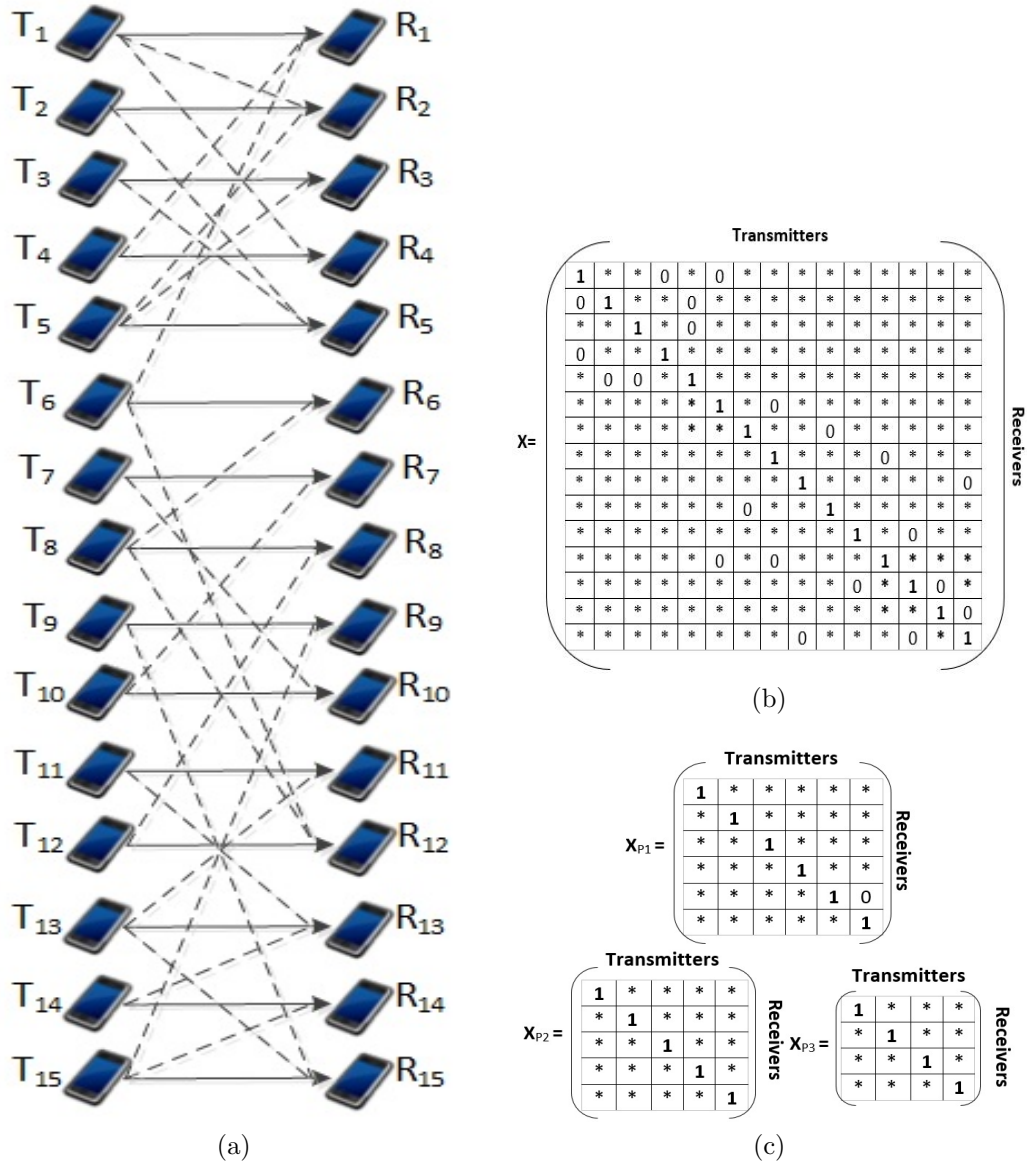


Figure 5.1: (a) TIM pattern of a 15 × 15 D2D network, (b) its corresponding matrix, and (c) sub-matrices (after clustering)

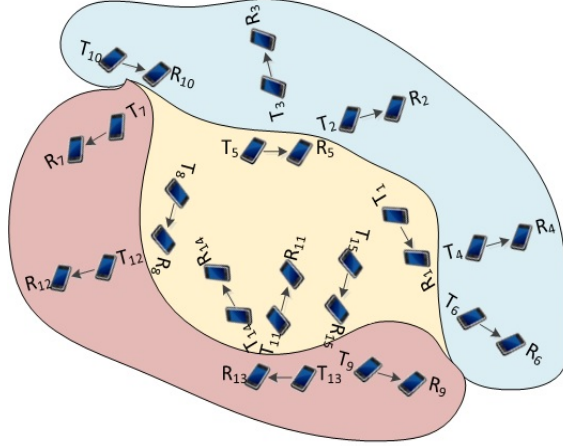


Figure 5.2: TIM clustering of the 15×15 D2D network

reduced to 2.

Comparing this system model to the one we formulated in Section 4.1 of Chapter 4, the difference resides in the clustering model, which was not present in that chapter. That is, in Section 4.1, the TIM rank minimization method was applied to the whole network (e.g., matrix of Fig. 5.1(b)), while here, it is applied to each resulting cluster (e.g., each of the three sub-matrices in Fig. 5.1(c)).

By this, the complete model of this chapter is to group D2D pairs that are mutually interfering into k clusters, to which we assign the k frequencies available in \mathcal{K} , and thus enable the devices in different clusters to send simultaneously. As for the intra-cluster interference that may reside despite the cut, translated into 0s in the sub-matrices as in \mathbf{X}_{P_1} of Fig. 5.1(c), it is eliminated using any proposed rank minimization method of Chapter 4 applied on each cluster's sub-matrix. We thus expect to increase the total sum of symmetric DoF over the whole D2D network. For consistency, we define $(\text{DoF}_{\text{sym}})_{\text{cluster}} = \frac{1}{k \times r}$ to be the symmetric DoF achieved per user per cluster, since each cluster is using $\frac{1}{k}$ of all the frequency resources. Note that when there is no clustering ($k = 1$), this metric reverts back to the symmetric DoF per user: $(\text{DoF}_{\text{sym}})_{\text{cluster}}|_{k=1} = \text{DoF}_{\text{sym}} = \frac{1}{r}$. Then, the total sum of symmetric DoF (with clustering) is:

$$\begin{aligned}
 (\text{DoF}_{\text{sym}})_{\text{total}}^{wc} &= \sum_{i=1}^k n_i \times (\text{DoF}_{\text{sym}})_{\text{cluster}} \\
 &= \frac{n_1}{k \times r_1} + \dots + \frac{n_k}{k \times r_k} = \frac{1}{k} \left(\frac{n_1}{r_1} + \dots + \frac{n_k}{r_k} \right) \quad (5.1)
 \end{aligned}$$

where n_k is the number of D2D pairs inside each cluster. Note here that the number of clusters increases by the network size, and so the orthogonal resources,

which could affect the achievable proposed scheme, since $(\text{DoF}_{\text{sym}})_{\text{total}}^{wc}$ in (5.1) is inversely proportional to k : this could lead to a smaller value of $\text{DoF}_{\text{system}}$ than the TIM case without clustering (where $(\text{DoF}_{\text{sym}})_{\text{cluster}}|_{k=1} = \text{DoF}_{\text{sym}}$ is simply equal to $\frac{1}{r}$). To avoid this, a frequency reuse pattern can be applied among non-adjacent clusters. This will improve the cellular network efficiency by serving a large number of D2D subscribers using a limited radio spectrum, and hence, will enhance the system capacity.

5.1.1 Interpreting the Interference Network as a Graph

We consider clustering as a partitioning problem for a conflict graph $\mathcal{G} = (\mathcal{V}, \mathcal{E}, w)$, where $\mathcal{V} = \{1, \dots, n\}$ is the set of vertices, each of which represents a $(T-R)_i$ pair, and \mathcal{E} designates the set of edges. We define this conflict graph to be with assigned weights $w_{i,j}$, such as $w_{i,j} = w_{j,i}$ for $1 \leq i, j \leq n$, and $w_{i,i} = 0$ for all $i = j$ (i.e., no self-looping, meaning no self-interference). Knowing that there is no knowledge about CSI in TIM, we associate the edges' weights in (5.2) to the number of 0s that appear in the TIM matrix, indicating by this the interference relationship among the D2D pairs. For instance, on a hand, $w_{i,j} = 2$ is seen as two 0s in the matrix, and hence signifies a mutual interference (e.g., pairs $(T-R)_2$ and $(T-R)_5$) of Fig. 5.1's network, and on the other hand, $w_{i,j} = 1$ is translated as one 0 in the matrix, and thus denotes a one-directional interference (e.g., pairs $(T-R)_1$ and $(T-R)_6$ of Fig. 5.1's network). For completeness, we assume $w_{i,j} = 0$ to denote a missing edge, i.e., when the two D2D pairs are not interfering with each other, making then the graph \mathcal{G} a complete one.

$$w_{i,j} = \begin{cases} 0 & \text{if no edge between pair } i \text{ and } j \\ & \text{(no interference)} \\ 1 & \text{if } \exists \text{ edge between pair } i \text{ and } j \mid i \rightarrow j \vee j \rightarrow i \\ & \text{(one-directional interference)} \\ 2 & \text{if } \exists \text{ edge between pair } i \text{ and } j \mid i \rightarrow j \wedge j \rightarrow i \\ & \text{(mutual interference)} \end{cases} \quad (5.2)$$

As an illustration, we show, in Fig. 5.3, the conflict graph of the D2D network example of Fig. 5.1(a). We introduce here the notion of a conflict graph "with assigned weights", where a bold link replaces the incoming and outgoing links of two particular nodes present in any traditional conflict graph (such as in [19]) to denote mutual interference ($w_{i,j} = 2$). On the other hand, a light link replaces the one link between them to designate a one-directional ($w_{i,j} = 1$) interference. Recall that this work's objective is to group the D2D devices into k groups in such a way that maximizes the inter-cluster interference by keeping the edges with large weights ($w_{i,j} = 2$) as inter-cluster edges (this interference is managed

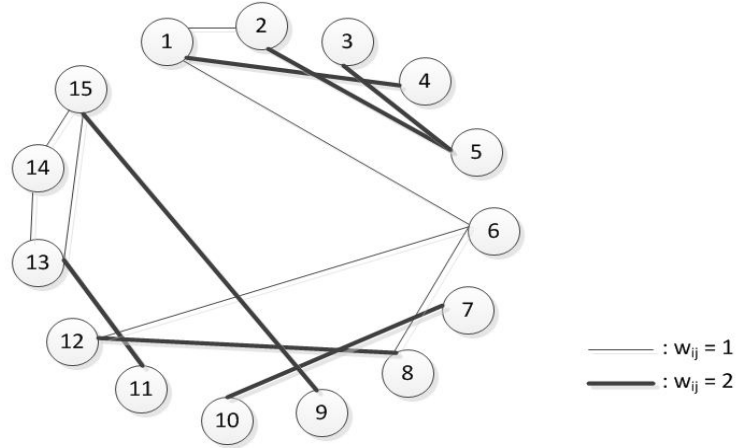


Figure 5.3: TIM conflict graph with assigned weights for the 15×15 network

by assigning k orthogonal frequencies among the k groups), and minimizes the intra-cluster interference, by including the edges with smaller weights ($w_{i,j} = 1$) within the cluster (this interference is managed by TIM). This is because when mutual interference is cut, more 0s in the TIM matrix are eliminated and replaced by "*" values, allowing more dependency among the rows, and hence improving the rank. Thus, to achieve this partitioning objective, we build on the max- k -cut problem (as will be shown in Section 5.2), which attempts to divide the vertex set \mathcal{V} into at most k subsets, such that the sum of edge weights that join nodes in the different subsets is maximized [57].

5.1.2 Clustered TIM

To model the clustering problem, we name $\mathcal{P} = \{P_1, \dots, P_k\}$ as the set of disjoint partitions, where P_k denotes the k^{th} cluster, and k refers to the number of clusters. We consider that $(T-R)_i$ pair should belong to only one cluster at a time and that the dimension of each cluster should not exceed the maximum number $L_{\max} \geq \frac{n}{k}$ (where $\frac{n}{k}$ is the smallest value for which this problem is solvable). This capacity constraint reduces hence the complexity (as well as the computation time) of solving TIM using LRMC, since it will be applied (in a parallel way) on sub-matrices with reduced sizes.

With this in mind, the clustering problem can be modeled as:

$$P_k \subseteq \mathcal{V}, \quad \forall k, \quad (5.3)$$

$$\bigcup_{i=1}^k P_k = \mathcal{V}, \quad (5.4)$$

$$P_q \cap P_s = \emptyset, \quad q \neq s \quad (5.5)$$

$$|P_q| \leq L_{\max}, \quad \forall q \in \{1, \dots, k\} \quad (5.6)$$

where the first constraint in Eq. (5.3) denotes that each resulting partition belongs to the whole set of partitions, Eq. (5.4) means that the union of all vertices constitute the whole set of vertices, Eq. (5.5) indicates that each pair of devices belongs to only one cluster at a time and Eq. (5.6) refers to the maximum number of pairs allowed in each cluster.

The objective is thus to maximize the aggregated inter-cluster interference by capturing as many edges with large weights as inter-cluster edges, and minimize the intra-cluster interference by keeping the edges with small weight as intra-cluster edges. This is because when strong interference is cut, more 0s in the TIM matrix are eliminated and replaced by "*" values, allowing more flexibility in terms of row dependency, i.e., the matrix rank. Using our clustering approach, more D2D pairs will be allowed to transmit simultaneously *across* clusters which are assigned orthogonal frequency resources. We rely here on the *maximum-k-cut problem*, since it satisfies our objective by partitioning the vertex set \mathcal{V} into at most k subsets, such that the sum of the weighted edges (defined in (5.2)) that join the nodes in the different k subsets is maximized [57]. By this, the max-k-cut algorithm will choose the edges with larger weights ($w_{i,j} = 2$) as inter-cluster edges to maximize the inter-cluster interference.

Note here that we assume that the number of clusters is determined from the set of frequencies $\mathcal{K} = \{Fr_1, \dots, Fr_k\}$ that is available (not necessarily adjacent, in the licensed or unlicensed band) in the network, constituting the network's design parameters, and that these two numbers are equal. On the other hand, even if the system has only one frequency, our results (as will be shown later) imply that it would be better to divide the frequency band into multiple sub-bands, such that each sub-band is assigned to one cluster, and LRMC is applied separately (and in parallel) within each cluster. In this context, finding the optimal number of sub-bands is an interesting question for future work. As a first tentative to address this issue is to solve the problem for several values of k , and then select the k value that gives the best performance, in terms of DoF and processing time.

5.1.3 Parameters and Variables

Throughout this chapter, here is the list of parameters and variables used:

Table 5.1: Parameters and variables used in Chapter 5

Parameter	Description
$(T - R)_i$	i^{th} D2D pair
n	Number of D2D pairs
\mathcal{K}	Set of available frequencies
F_{r_k}	k^{th} frequency
k	Number of clusters
$(\text{DoF}_{\text{sym}})$	Symmetric DoF achieved per user
$(\text{DoF}_{\text{sym}})_{\text{cluster}}$	Symmetric DoF achieved per user per cluster
$(\text{DoF}_{\text{sym}})_{\text{total}}^{wc}$	Total sum of symmetric DoF (with clustering)
n_k	Number of D2D pairs inside each cluster
$w_{i,j}$	Assigned weight between nodes i and j
\mathcal{G}	Conflict graph with assigned weights
\mathcal{V}	Set of vertices
\mathcal{E}	Set of edges
\mathcal{P}	Set of disjoint partitions
P_k	k^{th} cluster
L_{max}	Maximum number of D2D pairs allowed within each cluster
$w(\mathcal{P})$	Weight of the edges among the different clusters
$\mathbf{L} = [L_{i,j}]$	Laplacian matrix
$\mathbf{H} = [H_{i,j}]$	k -partition matrix
m_ℓ	ℓ^{th} cluster's size
\mathbf{Y}_{RS}	Matrix used in the matrix lifting method, as defined in (5.11)
\mathbf{Y}_{FJ}	Matrix such that its entries are defined in (5.14)
\mathcal{M}	Convex combinations of the feasible set
\mathbf{b}_i	i^{th} column of \mathbf{B} resulting from the Cholesky decomposition of \mathbf{Y}_{FJ}
\mathcal{S}_{gt}	Set of the clusters having a size exactly greater than the bound L_{max}
\mathcal{S}_{lt}	Set of the clusters having a size exactly less than the bound L_{max}
\mathcal{S}_{eq}	Set of the clusters having a size exactly equal to the bound L_{max}
$\mathbf{Q}_{(C_g)}$	The entries of this matrix represent the summation of the dot product of \mathbf{b}_i 's between each node of a cluster in \mathcal{S}_{gt} and each node in each cluster in \mathcal{S}_{lt}
C	Cluster's capacity
m	Number of subsets $m = \lfloor \frac{n}{L_{\text{max}}} \rfloor$
λ	Eigenvalue of \mathbf{L}
$\lambda_d(\mathbf{L})$	Largest eigenvalue of \mathbf{L}
\mathbf{A}_i	Matrix whose columns form an orthonormal basis of the eigenspace corresponding to the i^{th} eigenvalue λ_i
\mathbf{F}_i	Matrix defined as $\mathbf{F}_i = \mathbf{A}_i \mathbf{A}_i^T$
f_i	Rank of \mathbf{F}_i
\mathbf{d}	Correcting vector for the diagonal perturbation method
\mathbf{Z}	M-matrix
\mathbf{B}	Non-negative matrix such that $\mathbf{B} = \mathbf{L} + \text{diag}(\mathbf{d}) \geq 0$
$\rho(\mathbf{B})$	Spectral radius of \mathbf{B}
$\sigma(\mathbf{B})$	Spectrum of \mathbf{B} (the set of its eigenvalues)
$w(E_{\text{cut}})_{\text{clust. alg.}}$	Total weight of edges that are cut
T	Number of timeslots
q	Number of constraints

5.2 Mathematical Model

5.2.1 Original Problem

Recall that the objective of this work is to partition the D2D devices into clusters such that the devices having mutual interference are separated into different groups. From our aforementioned formulation based on graph theory, our aim

is to cut the edges with large weights. This can be considered as a max-k-cut problem, which targets to partition the vertices of a weighted graph into k blocks, so as to maximize the weight of crossing edges [57]. Given the weighted graph $\mathcal{G} = (\mathcal{V}, \mathcal{E}, w)$, then the original problem can be formulated in (5.7), where $w(\mathcal{P})$ represents the weight of the edges among the different clusters. As for the constraints, the first one binds the number of clusters, and the second one restricts each cluster's capacity to L_{\max} .

$$\begin{aligned} \max_{\mathcal{P}} \quad & w(\mathcal{P}) = \sum_{1 \leq r \neq s \leq k} \sum_{i \in P_r, j \in P_s} w_{i,j} \\ \text{s.t.} \quad & |\mathcal{P}| = k, \\ & |P_i| \leq L_{\max} \end{aligned} \tag{5.7}$$

This problem turns out to be the NP-hard capacitated max-k-cut problem (since it is not efficient to solve the problem directly by evaluating all possible partitions) [57], for which we develop, in the following subsection, a new SDP relaxation method, with a heuristic algorithm to solve it. Note here that one can also reformulate the original problem as a partial clique covering, used in index coding [2]. However, the capacity constraint in (5.7) makes it different, since, to the best of our knowledge, this constraint is not considered in the existing index coding works, where the optimality of the partial clique covering in terms of coding rate is studied, and some bounds on the achievable rate are found. Our work differs also from [2], since we derive here a polynomial sub-optimal solution of the formulated capacitated max-k-cut problem and we find a performance guarantee to the proposed solution.

5.2.2 SDP Relaxation

This chapter's objective is to group the D2D devices that are mutually interfering with each other into different clusters while satisfying each group's capacity, and thus to cut the edges with large weights in the conflict graph with assigned weights. Knowing that the problem in (5.7) is NP-hard, we derive its SDP relaxation, and then we develop a heuristic algorithm to solve it.

We base our work on the Laplacian method [57], where the quadratic optimization problem is a function of the Laplacian matrix $\mathbf{L} = [L_{i,j}]$ (more details about the Laplacian method and the Laplacian matrix can be found in Section 2.3 of Chapter 2). We construct \mathbf{L} (with PSD characteristics) in terms of the edges' weights in (5.7), such that $L_{i,j} = -w_{i,j}$ for $i \neq j$ and $L_{i,i} = \sum_{k=1}^n w_{i,k}$. We introduce an $n \times k$ matrix $\mathbf{H} = [H_{i,j}]$ as the k-partition matrix, denoting the decision variable:

$$H_{i,\ell} = \begin{cases} 1 & i \in P_\ell, \ell \in \{1, 2, \dots, k\} \text{ and} \\ 0 & i \notin P_\ell \end{cases} \tag{5.8}$$

By this, the feasible set \mathcal{P} can be defined as follows:

$$\mathcal{P} = \{\mathbf{H} \in \mathbb{R}^{n \times k} : \mathbf{H} = [\mathbf{h}_1, \dots, \mathbf{h}_k], \mathbf{H}\mathbf{u}_k = \mathbf{u}_n, \mathbf{H}^T \mathbf{u}_n = \mathbf{m}, H_{i,\ell} \in \{0, 1\}, \forall i = 1, \dots, n, \ell = 1, \dots, k\} \quad (5.9)$$

where \mathbf{u}_k (\mathbf{u}_n) is the all-ones vector of length k (and n , respectively), and $m_\ell \in \mathbf{m} = [m_\ell, \dots, m_k]^T$ is the ℓ^{th} cluster's size. The quadratic form in \mathbf{H} is related to the objective function in (5.7), since for each $\mathbf{H} \in \mathcal{P}$, $\mathbf{h}_\ell^T \mathbf{L} \mathbf{h}_\ell$ gives the weight of edges joining P_ℓ to the other partitions in \mathcal{P} , and $\frac{1}{2} \text{Tr}(\mathbf{H}^T \mathbf{L} \mathbf{H})$ gives the total weight of the edges cut by \mathbf{H} (those joining different partitions):

$$\frac{1}{2} \text{Tr}(\mathbf{H}^T \mathbf{L} \mathbf{H}) = \frac{1}{2} \sum_{\ell=1}^k \mathbf{h}_\ell^T \mathbf{L} \mathbf{h}_\ell = \frac{1}{2} \sum_{\ell=1}^k \sum_{v \in P_\ell, w \notin P_\ell} w_{v,w} \quad (5.10)$$

Note that the reward in (5.10) is equal to half of the one in (5.7) because the outer summation in (5.7) is only over $i < j$. To construct the SDP relaxation of (5.7), we start by introducing a new matrix \mathbf{Y}_{RS} , which is linked to \mathbf{H} , following the convex combinations of the feasible set \mathcal{M} :

$$\mathcal{M} := \text{conv}\{\mathbf{Y}_{\text{RS}} : \exists \mathbf{H} \in \mathcal{P} \text{ s.t. } \mathbf{Y}_{\text{RS}} = \mathbf{H} \mathbf{H}^T\} \quad (5.11)$$

Hence, $\frac{1}{2} \text{Tr}(\mathbf{H}^T \mathbf{L} \mathbf{H})$ can be linearized to $\text{Tr}(\mathbf{L} \mathbf{Y}_{\text{RS}})$ (using the matrix lifting method), which will constitute the objective function of the SDP relaxation of (5.7). As for the constraints, it is clear that $\text{diag}(\mathbf{Y}_{\text{RS}}) = \mathbf{u}_n$, (where "diag" maps an $n \times n$ matrix to the n vector given by its diagonal), $\mathbf{Y}_{\text{RS}} \succeq 0$, and $\mathbf{Y}_{\text{RS}} \succeq 0$. However, this last constraint will be replaced by a stronger PSD one $k\mathbf{Y}_{\text{RS}} - \mathbf{J} \succeq 0$, where \mathbf{J} is the all ones $n \times n$ matrix (as proven in [168]), improving by this the relaxation performance. As for the cluster size constraint, it can be written as:

$$\text{Tr}(\mathbf{J} \mathbf{Y}_{\text{RS}}) = \text{Tr}(\mathbf{H} \mathbf{H}^T \mathbf{u}_n \mathbf{u}_n^T) = \text{Tr}(\mathbf{m}^T \mathbf{m}) = \sum_{\ell=1}^k m_\ell^2 \quad (5.12)$$

The optimization problem can be formulated then in (5.13.a) by compiling the objective function in (5.10) and the aforementioned constraints. It is proven in [168] that this problem is equivalent to a trace formulation [57] as in (5.13.b) by doing simple changing of variables $\left(\mathbf{Y}_{\text{RS}} = \frac{(k-1)\mathbf{Y}_{\text{EJ}} + \mathbf{J}}{k}\right)$.

Original Matrix Lifting

$$\begin{aligned}
& \max_{\mathbf{Y}_{\text{RS}}} \frac{1}{2} \text{Tr}(\mathbf{L}\mathbf{Y}_{\text{RS}}) \\
& \text{s.t. } \text{diag}(\mathbf{Y}_{\text{RS}}) = \mathbf{u}_n \\
& \quad k\mathbf{Y}_{\text{RS}} - \mathbf{J} \succeq 0 \\
& \quad \mathbf{Y}_{\text{RS}} \succeq 0 \\
& \text{Tr}(\mathbf{J}\mathbf{Y}_{\text{RS}}) = \sum_{\ell=1}^k m_\ell^2
\end{aligned} \tag{5.13a}$$

Original Trace Formulation

$$\begin{aligned}
& \max_{\mathbf{Y}_{\text{FJ}}} \frac{k-1}{2k} \text{Tr}(\mathbf{L}\mathbf{Y}_{\text{FJ}}) \\
& \text{s.t. } \text{diag}(\mathbf{Y}_{\text{FJ}}) = \mathbf{u}_n \\
& \quad \mathbf{Y}_{\text{FJ}} \succeq 0 \\
& \quad (Y_{i,j})_{\text{FJ}} \geq \frac{-1}{k-1}, i \neq j \\
& \text{Tr}(\mathbf{J}\mathbf{Y}_{\text{FJ}}) = \frac{1}{k-1} (k \sum_{\ell=1}^k m_\ell^2 - n^2)
\end{aligned} \tag{5.13b}$$

where \mathbf{Y}_{RS} is defined in (5.11) and $\mathbf{Y}_{\text{FJ}} = [(Y_{i,j})_{\text{FJ}}]$ is a matrix variable, $(i, j \in \mathcal{V})$ such that:

$$(Y_{i,j})_{\text{FJ}} = \begin{cases} \frac{-1}{k-1} & \text{if } i \text{ and } j \text{ are in different partitions of the } k\text{-cut of } \mathcal{G} \\ 1 & \text{otherwise} \end{cases} \tag{5.14}$$

However, the problem in (5.13) which was developed in [168] cannot be directly applied here, because the cluster size m_ℓ in this work is bounded by L_{max} , while in [168] the size of each cluster was a priori known. Based on this, we adapt the last constraint in (5.13) to be compliant with L_{max} such that each group size m_ℓ should be less than or equal to L_{max} , i.e., $m_\ell m_q \leq L_{\text{max}}^2$:

$$\text{We know that } \left(\sum_{\ell=1}^k m_\ell \right)^2 = n^2 = \sum_{\ell=1}^k m_\ell^2 + \sum_{\ell \neq q} m_\ell m_q, \text{ and} \tag{5.15}$$

$$\sum_{\ell \neq q} m_\ell m_q \leq k(k-1)L_{\text{max}}^2, \text{ then} \tag{5.16}$$

$$\sum_{\ell=1}^k m_\ell^2 = n^2 - \sum_{\ell \neq q} m_\ell m_q \geq n^2 - k(k-1)L_{\text{max}}^2 \tag{5.17}$$

Replacing (5.17) in (5.13) leads to the final form of the SDP relaxation of our clustering problem:

Adapted Matrix Lifting

$$\begin{aligned}
& \max_{\mathbf{Y}_{\text{RS}}} \frac{1}{2} \text{Tr}(\mathbf{L}\mathbf{Y}_{\text{RS}}) \\
& \text{s.t. } \text{diag}(\mathbf{Y}_{\text{RS}}) = \mathbf{u}_n \\
& \quad k\mathbf{Y}_{\text{RS}} - \mathbf{J} \succeq 0, \\
& \quad \mathbf{Y}_{\text{RS}} \succeq 0 \\
& -\text{Tr}(\mathbf{J}\mathbf{Y}_{\text{RS}}) \leq k(k-1)L_{\text{max}}^2 - n^2
\end{aligned} \tag{5.18a}$$

Adapted Trace Formulation

$$\begin{aligned}
& \max_{\mathbf{Y}_{\text{FJ}}} \frac{k-1}{2k} \text{Tr}(\mathbf{L}\mathbf{Y}_{\text{FJ}}) \\
& \text{s.t. } \text{diag}(\mathbf{Y}_{\text{FJ}}) = \mathbf{u}_n \\
& \quad \mathbf{Y}_{\text{FJ}} \succeq 0 \\
& \quad (Y_{i,j})_{\text{FJ}} \geq \frac{-1}{k-1}, i \neq j \\
& -\text{Tr}(\mathbf{J}\mathbf{Y}_{\text{FJ}}) \leq k^2 L_{\text{max}}^2 - n^2
\end{aligned} \tag{5.18b}$$

Since the entries of \mathbf{Y}_{FJ} and \mathbf{Y}_{RS} (i.e., the optimization variables of the SDP relaxation problem in (5.18)) are relaxed and do not give clear insights regarding which vertices belong to the same partition, a rounding heuristic algorithm is proposed. For this, we present next Algorithm 2, which divides the nodes into groups, while considering the cluster’s capacity.

5.3 Heuristic Clustering Algorithm

To cluster the D2D pairs into k groups, each with a capacity of L_{max} , and operating at a different frequency from \mathcal{K} , we propose Algorithm 2, a rounding algorithm, since the entries of the matrix \mathbf{Y}_{FJ} resulting from (5.18.b) are relaxed. Technically, we extend the SDP relaxation of the max-k-cut problem [57] (Steps 1-7) to account for the cluster’s size constraint. To solve the problem, we decompose the matrix \mathbf{Y}_{FJ} in (5.18.b) into $\mathbf{B}^T \mathbf{B}$ using Cholesky decomposition, where \mathbf{Y}_{FJ} represents the Gram matrix of $\{\mathbf{b}_1, \dots, \mathbf{b}_n\}$, and each \mathbf{b}_i (the i^{th} column of \mathbf{B}) corresponds to a node. To partition these vertices into different subsets with a bounded size L_{max} , we compare each \mathbf{b}_i against k independent vectors from a normal distribution with 0 mean and variance 1, and we group together the nodes having \mathbf{b}_i ’s similar to the same vector in $\mathcal{N}(0, 1)$. This result is collected in Step 7. At this level, L_{max} is not yet taken into account, and hence more steps are required to check the satisfaction of this constraint. Thus, our contribution appears starting at Step 8. If the sizes of the partitions collected in Step 7 are less than or equal to L_{max} , then it becomes the final output (Step 11). Else, we develop

an algorithm (Steps 13-30) to designate the *appropriate nodes* to be re-clustered and the *adequate clusters* to be joined. For this, we divide the clusters into two sets \mathcal{S}_{gt} and \mathcal{S}_{lt} , where they are collected based on their sizes (greater and lower than L_{max} , respectively). As for the clusters having a size exactly equal to the bound, they are captured in a set \mathcal{S}_{eq} , since they are not candidates for admitting new nodes (Step 13), and hence this set is excluded from the re-assignment algorithm. Now, to determine the *potential cluster* that each node in each cluster in \mathcal{S}_{gt} can join (if re-assigned), we compute the summation of the dot product of \mathbf{b}_i 's between each node of a cluster in \mathcal{S}_{gt} and each node in each cluster in \mathcal{S}_{lt} , and collect these values in a matrix $\mathbf{Q}_{(C_g)}$ defined as:

$$\mathbf{Q}_{(C_g)} = \begin{pmatrix} q_{(g_1, C_{l1})} & q_{(g_1, C_{l2})} & \cdots & q_{(g_1, C_{l|\mathcal{S}_{\text{lt}}|})} \\ q_{(g_2, C_{l1})} & q_{(g_2, C_{l2})} & \cdots & q_{(g_2, C_{l|\mathcal{S}_{\text{lt}}|})} \\ \vdots & \vdots & \cdots & \vdots \\ q_{(g_{|\mathcal{S}_{\text{gt}}|}, C_{l1})} & q_{(g_{|\mathcal{S}_{\text{gt}}|}, C_{l2})} & \cdots & q_{(g_{|\mathcal{S}_{\text{gt}}|}, C_{l|\mathcal{S}_{\text{lt}}|})} \end{pmatrix} \quad (5.19)$$

where its minimum entry $q_{(g, C_l)}$ identifies *which node(s)* should be moved *to which cluster* (while satisfying the cluster's size constraint), so that it has the least effect on $\sum_j (Y_{i,j})_{\text{FJ}}$, which should be less than or equal to $(L_{\text{max}} - \frac{n-L_{\text{max}}}{k-1})$. This is because the summation over all j within a cluster should give a value less than or equal to L_{max} from which the $(n - L_{\text{max}})$ nodes that belong to the other clusters should be subtracted (in $(Y_{i,j})_{\text{FJ}} = -\frac{1}{k-1}$ if i and j belong to different clusters, and $(Y_{i,j})_{\text{FJ}} = 1$ if i and j are within the same cluster Eq. (5.14)). Once the appropriate reassignment is achieved, the final partition will be the union of the *updated* clusters in \mathcal{S}_{gt} and \mathcal{S}_{lt} , and the existing ones in \mathcal{S}_{eq} .

5.4 Bounds Analysis

In this section, we derive the performance guarantee of our proposed heuristic algorithm (relatively to the optimal method), after determining some interesting bounds which served in the computation. We also analyze the performance of the randomized clustering algorithm.

5.4.1 Randomized Policy

One of the obvious methods for our clustering problem is the randomized clustering algorithm, which starts by arbitrarily partitioning the n vertices into m subsets with a capacity $C = L_{\text{max}}$ each, where $m = \lfloor \frac{n}{L_{\text{max}}} \rfloor$. As for the residual nodes, they are randomly assigned to the remaining $(k - m)$ clusters, where the cluster's size can vary from one subset to another, but the capacity is equal to L_{max} , i.e., $C < L_{\text{max}}$. Note that the nodes here are randomly chosen, i.e.,

Algorithm 2: Clustering devices into k partitions with bounded subset sizes

Input : $\mathcal{G} = (\mathcal{V}, \mathcal{E}), k, n, \mathbf{L}, L_{\max}$
Output: $\mathcal{P} = P_1, P_2, \dots, P_k$

- 1 Solve Problem (5.18.b) to get $\mathbf{Y}_{\text{FJ}} = [Y_{i,j}]$
- 2 Find unit vectors $\mathbf{b}_1, \dots, \mathbf{b}_n \in \mathbb{R}^{n \times 1}$ satisfying $\mathbf{b}_i^T \cdot \mathbf{b}_j = Y_{i,j}$ ($1 \leq i, j \leq n$) by computing the Cholesky factorization $\mathbf{B}^T \mathbf{B}$ of \mathbf{Y}_{FJ} where $\mathbf{B} = [\mathbf{b}_1, \dots, \mathbf{b}_n]$
- 3 Choose k independent random vectors $\mathbf{z}_1, \dots, \mathbf{z}_k \in \mathbb{R}^{n \times 1}$ where its elements $\sim \mathcal{N}(0, 1)$
- 4 Partition \mathcal{V} into P_1, \dots, P_k where P_h consists of the nodes $i \in \mathcal{V}$ for which $\mathbf{b}_i^T \mathbf{z}_h = \max_{m=1, \dots, k} \mathbf{b}_i^T \mathbf{z}_m$
- 5 // now that we know to which cluster each node belongs
- 6 // validate against L_{\max} , and reassign if necessary
- 7 Capture $\mathcal{P}_{\text{initial}} = P_1, \dots, P_k$
- 8 **foreach** $P_h \in \mathcal{P}_{\text{initial}}$ **do**
- 9 **if** $\|P_h\| \leq L_{\max}$ **then**
- 10 $\mathcal{P} = \mathcal{P}_{\text{initial}} = P_1, \dots, P_k$
- 11 **else**
- 12 Form three sets $\mathcal{S}_{\text{gt}} = \{C_g \mid \|C_g\| > L_{\max}\}$, $\mathcal{S}_{\text{lt}} = \{C_l \mid \|C_l\| < L_{\max}\}$,
 $\mathcal{S}_{\text{eq}} = \{C_e \mid \|C_e\| = L_{\max}\}$
- 13 **foreach** $C_g \in \mathcal{S}_{\text{gt}}$ **do**
- 14 // Compute for cluster C_g and each cluster C_l a set of product vectors
- 15 **foreach** $C_l \in \mathcal{S}_{\text{lt}}$ **do**
- 16 **foreach** $g \in C_g$ **do**
- 17 $q_{(g, C_l)} = 0$
- 18 **foreach** $l \in C_l$ **do**
- 19 // $\mathbf{q}_{(g, C_l)}$ is a product vector corresponding to node g and cluster C_l
- 20 $\mathbf{q}_{(g, C_l)}$ where $q_{(g, C_l)} = \sum \mathbf{b}_{(g)}^T \cdot \mathbf{b}_{(l)}$
- 21 // where $\mathbf{b}_{(p)}$ is the vector $\mathbf{b} \in \mathbf{B}$ that corresponds to node p
- 22 **end**
- 23 **end**
- 24 // we now have a matrix $\mathbf{Q}_{(C_g)} = [q_{(g, C_l)}]$ for all clusters in \mathcal{S}_{lt} whose dimension is $\|C_g\| \times \|\mathcal{S}_{\text{lt}}\|$
- 25 **end**
- 26 Identify according to $\mathbf{Q}_{(C_g)}$ nodes $\{g^o \in C_g\}$ and clusters $\{C_l^p \in \mathcal{S}_{\text{lt}}\}$ such that $q_{(g^o, C_l^p)}$ is minimum and moving $\{g^o\}$ to $\{C_l^p\}$, $\|C_g\| = L_{\max}$ and $\|C_l^p\|$ remains $\leq L_{\max}$
- 27 **end**
- 28 // \mathcal{P} is the union of updated clusters
- 29 $\mathcal{P} = \mathcal{S}_{\text{gt}} \cup \mathcal{S}_{\text{lt}} \cup \mathcal{S}_{\text{eq}}$
- 30 **end**
- 31 // Reuse frequency among clusters if they are not adjacent
- 32 $\forall i \in C_l, \forall j \mid j$ is adjacent to $i \wedge j \in C_m,$
- 33 **if** $\exists k \in C_n$ adjacent to j and not adjacent to $i,$
- 34 **then** C_l and C_n can reuse the same frequency bands

the selected nodes to be grouped in the same group do not necessarily have the lowest edges' weights. Hence, this method constitutes the lower bound of the capacitated max-k-cut problem, which can be written in (5.20), while its detailed derivations are in Appendix B.1.

$$\text{MC}_{k,\text{cap}} \geq \begin{cases} \left[\frac{m(m-1)L_{\max}^2}{n^2} + \left(1 - \frac{mL_{\max}}{n}\right) \times \right. & \text{if } k > m \\ \left. \left(\frac{2mL_{\max}}{n} + \left(1 - \frac{mL_{\max}}{n}\right) \binom{k-m-1}{k-m} \right) \right] \times \left(\sum_{i \neq j} w_{i,j} \right)_{\text{total}} & \\ \frac{m(m-1)L_{\max}^2}{n^2} \times \left(\sum_{i \neq j} w_{i,j} \right)_{\text{total}} & \text{if } k = m \end{cases} \quad (5.20)$$

where $\left(\sum_{i \neq j} w_{i,j} \right)_{\text{total}}$ is the total sum of weights of *all* the edges connecting *all* vertices.

5.4.2 Upper Bound (SDP Relaxation)

We derive three eigenvalue-based bounds for our clustering problem: the first one is the solution of an SDP relaxation that is weaker than the original problem (5.7), the second one is a strengthened version, and the third one is an improvement of all the previous versions, where the diagonal of the Laplacian matrix is perturbed, leading to a stronger bound. We mention here that although the first bound may be a loose upper bound, we use it here for clarity purpose to help the reader understand the derivations corresponding to the upper bounds that follow.

5.4.2.1 Eigenvalue Bound

To derive the first eigenvalue bound, we rely on the the Laplacian algebra \mathcal{L} , as in [60] and [61] but with some modifications: the eigenvalue bound 1) in [60] is found for the max-k-cut problem with *no* restriction on the sizes of the subsets (in contrast to our work, which corresponds to its capacitated version), and 2) in [61] is determined for the graph partition problem, where the size of each subset is already given and fixed (while in this work, the size is not apriori known, but is upper bounded by L_{\max}).

Recall that \mathcal{L} is a set of matrices that is closed under addition, scalar and matrix multiplication, and conjugate transposes [60], [61]. The orthonormal basis of eigenvectors corresponding to the eigenvalues of the Laplacian matrix \mathbf{L} constitute the basis of \mathcal{L} matrices. In particular, we consider $0 = \lambda_0 \leq \lambda_1 < \dots < \lambda_d =: \lambda_{\max}(\mathbf{L})$ to be the distinct eigenvalues of \mathbf{L} , and \mathbf{A}_i be a matrix whose columns form an orthonormal basis of the eigenspace corresponding to the i^{th} eigenvalue λ_i , constituting $\mathbf{F}_i = \mathbf{A}_i \mathbf{A}_i^T$ for $i = 0, \dots, d$. We define $f_i = \text{rank}(\mathbf{F}_i)$ as the corresponding multiplicities. Hence, \mathcal{L} is now described by the span of $\{\mathbf{F}_0, \dots, \mathbf{F}_d\}$. This span is called the basis of idempotents of \mathcal{L} , and $\mathbf{L} = \sum_{i=0}^d \lambda_i \mathbf{F}_i$ [60], [61].

For more details about Laplacian Algebra \mathcal{L} , the reader can refer back to Section 2.3.2 of Chapter 2.

To find these derivations, we rely on the matrix lifting formulation in (5.18.a) and not on the trace formulation in (5.18.b) 1) to avoid the problem of the negative values that may appear in the relaxed version of \mathbf{Y}_{FJ} in (5.18.b), and 2) to stay conformant with the idempotent property of \mathcal{L} basis, which is satisfied in the matrix lifting formulation, where the entries of \mathbf{H} in (5.8) are 0 or 1, in contrast to the trace formulation, where the square of \mathbf{Y}_{FJ} 's entries in (5.14) do not give the same values due to $(Y_{i,j})_{\text{FJ}} \geq \frac{-1}{k-1}$. Since the SDP relaxation of the original problem cannot be restricted to feasible points in \mathcal{L} , we adapt it accordingly by the following relaxation:

$$\begin{aligned}
& \mathbf{Adapted\ Matrix\ Lifting} \\
& \max_{\mathbf{Y}_{\text{RS}}} \frac{1}{2} \text{Tr}(\mathbf{L}\mathbf{Y}_{\text{RS}}) \\
& \text{s.t. } \text{diag}(\mathbf{Y}_{\text{RS}}) = \mathbf{u}_n \\
& \quad k\mathbf{Y}_{\text{RS}} - \mathbf{J} \succeq 0 \\
& -\text{Tr}(\mathbf{J}\mathbf{Y}_{\text{RS}}) \leq k(k-1)L_{\text{max}}^2 - n^2 \\
& \quad \mathbf{Y}_{\text{RS}} \geq 0
\end{aligned} \tag{5.21a}$$

Adapted & *Relaxed* Matrix Lifting

$$\begin{aligned}
& \max_{\mathbf{Y}_{\text{RS}}} \frac{1}{2} \text{Tr}(\mathbf{L}\mathbf{Y}_{\text{RS}}) \\
& \text{s.t. } \text{Tr}(\mathbf{Y}_{\text{RS}}) = n \\
& \quad k\mathbf{Y}_{\text{RS}} - \mathbf{J} \succeq 0 \\
& -\text{Tr}(\mathbf{J}\mathbf{Y}_{\text{RS}}) \leq k(k-1)L_{\text{max}}^2 - n^2
\end{aligned} \tag{5.21b}$$

By restricting the optimization problem of (5.21) to feasible points in \mathcal{L} , we obtain the following.

Proposition 1. *We let \mathcal{G} be a graph on n vertices, and k an integer such that $2 \leq k \leq n$. Then, the upper bound of the SDP relaxation (5.21.b) becomes equal to:*

$$MC_{k,\text{cap}} \leq \frac{k(k-1)L_{\text{max}}^2}{2n} \times \lambda_d \tag{5.22}$$

where $\lambda_d(\mathbf{L})$ is the largest eigenvalue of the Laplacian matrix \mathbf{L} of \mathcal{G} .

Proof. The conversion of (5.21.b) into the Laplacian algebra \mathcal{L} domain and the derivation of the upper bound expressed in (5.22) can be found in Appendix B.2. \square

5.4.2.2 Strengthened Eigenvalue Bound

The bound in (5.22) is considered a loose one, especially in the case when some clusters are of full capacity. For this scenario, we determine a strengthened bound, after deriving an interesting Lemma related to the summation of the product of the clusters' sizes. To the best of our knowledge, this is the first time that this bound is established.

Theorem 4. *In the case of at least one cluster is of full capacity (i.e., equal to L_{max}) is derived, the upper bound of our clustering problem can be improved to be equal to :*

$$MC_{k,cap} \leq \frac{k(n^2 - L_{max}^2) + 2n(L_{max} - n)}{2n(k - 1)} \times \lambda_d \quad (5.23)$$

Proof. The derivation of the strengthened upper bound can be found in Appendices B.3 and B.4. \square

Although (5.23) is a better bound than (5.22), we can enhance it further by perturbing the diagonal.

5.4.2.3 Perturbed Bound

We improve the eigenvalue bound that we derived above in (5.23) by applying on it the diagonal perturbation method [60]. We note that perturbing the cost matrix by a diagonal matrix with zero trace does not change the optimal value of our optimization problem, but has an effect on the maximal eigenvalue of the Laplacian matrix. Thus, we can express the perturbation of the diagonal entries of (5.23) by the following optimization problem:

$$\min_{\mathbf{d}^T \mathbf{u}_n = 0} \frac{k(n^2 - L_{max}^2) + 2n(L_{max} - n)}{2n(k - 1)} \lambda_d(\mathbf{L} + \text{diag}(\mathbf{d})) \quad (5.24)$$

where the vector \mathbf{d} is known as the correcting vector and \mathbf{d} is chosen such that $\sum_{1 \leq i \leq n} d_i = 0$. However, problem (5.24) does not have a closed form expression, so we can formulate it as SDP using the concept of M-matrices [38] (detailed in Section 2.2.1.4 of Chapter 2): we let \mathbf{Z} be an M-matrix such that $\mathbf{Z} = \mu \mathbf{I} - \mathbf{B}$, where \mathbf{B} is a non-negative matrix such that $\mathbf{B} = \mathbf{L} + \text{diag}(\mathbf{d}) \geq 0$, and $\mu \in \mathbb{R}$ such that $\mu \geq \rho(\mathbf{B})$, where $\rho(\mathbf{B})$ is the spectral radius of \mathbf{B} (the largest absolute value of its eigenvalues), i.e., $\rho(\mathbf{B}) := \max\{|\lambda| \mid \lambda \in \sigma(\mathbf{B})\}$ and $\sigma(\mathbf{B})$ denotes the spectrum of \mathbf{B} (the set of its eigenvalues) [38]. Thus, minimizing μ reduces the eigenvalues of \mathbf{B} (particularly, its maximum value λ_d):

Primary Problem of the Perturbed Bound

$$\begin{aligned} \min \quad & \frac{k(n^2 - L_{\max}^2) + 2n(L_{\max} - n)}{2n(k-1)} \mu \\ \text{s.t.} \quad & \mu \mathbf{I}_n - (\mathbf{L} + \text{diag}(\mathbf{d})) = \mathbf{Z}, \quad \mathbf{Z} \succeq 0, \\ & \mathbf{d}^T \mathbf{u}_n = 0 \end{aligned} \tag{5.25a}$$

Dual Problem of the Perturbed Bound

$$\begin{aligned} \max_{\mathbf{Y}_{\text{RS}}} \quad & \frac{1}{2} \text{Tr}(\mathbf{L}\mathbf{Y}) \\ \text{s.t.} \quad & \text{diag}(\mathbf{Y}) = \frac{k(n^2 - L_{\max}^2) + 2n(L_{\max} - n)}{n^2(k-1)} \mathbf{u}_n \\ & \mathbf{Y}_{\text{RS}} \succeq 0 \end{aligned} \tag{5.25b}$$

By solving the SDP relaxation in (5.25.b), we get the optimal value of the eigenvalue problem in (5.24), knowing its equivalence. Finally, we summarize the relations among the presented SDP relaxations for the clustering problem and their corresponding bounds as follows:

$$\text{SDP in (5.21)} \succ \text{SDP in (B.16)} \succ \text{Original Problem}$$

$$\begin{aligned} \lambda_{\max} \text{bound (5.22)} &\geq \text{Strengthened bound (5.23)} \geq \text{Perturbed bound (5.25.b)} \\ &\geq \text{Optimal solution of the original problem} \end{aligned} \tag{5.26}$$

where $(X) \succ (Y)$ means that Problem (X) is more relaxed than Problem (Y) and $(a) \geq (b)$ refers to the fact that the solution's value in (a) is greater than or equal to the one in (b) .

5.4.3 Performance Guarantee

To assess a clustering algorithm's performance, we define the "ratio" metric which relates the average cost (in terms of the resulting total weight of edges that are cut $w(E_{\text{cut}})_{\text{clust. alg.}}$) to the upper bound of the optimal solution. This indicates the accuracy level of the considered policy's solution against the optimal one in (5.7). Numerically, the tightest upper bound of the SDP relaxation of the original problem can be directly calculated by only plugging the values of n , k , L_{\max} , and λ_d in (5.25.b), which is not a complex SDP problem to be solved. As for the total weight of the edges that are cut after partitioning ($w(E_{\text{cut}})_{\text{clust. alg.}}$ in (5.27)), it is related to the clustering algorithm considered. For instance, for the randomized policy, the ratio's numerator in (5.27) is replaced by $w(E_{\text{cut}})_{\text{rand. alg.}} = \text{MC}_{k, \text{cap}}$ in (5.20). Note here that the output of the randomized policy constitutes the lower

bound of the optimal solution of our clustering problem.

$$\text{ratio} = \frac{w(E_{\text{cut}})_{\text{clust. alg.}}}{\text{upper bound of the SDP relaxation of the original problem}},$$

$$\text{where } w(E_{\text{cut}})_{\text{clust. alg.}} = \frac{1}{2} \sum_{1 \leq r \neq s \leq k} \sum_{i \in P_r, j \in P_s} w_{i,j} \quad (5.27)$$

However, if this ratio is high enough, then there is no need to solve the SDP problem in (5.18), and the randomized policy can be directly applied, saving by this the CPU resources. On the other hand, if the performance of our proposed heuristic algorithm (Algorithm 2) is to be analyzed, then $w(E_{\text{cut}})_{\text{clust. alg.}}$ is replaced by $w(E_{\text{cut}})_{\text{Alg.2}}$, which is equal to the total sum of weighted edges that are cut (i.e., those joining different partitions). Thus, this ratio affirms that the considered clustering algorithm can be used to partition the network into different groups with a performance guarantee of at least ($\text{ratio} \times 100\%$) w.r.t to the optimal solution. Note that we expect that the value of the ratio (i.e., the performance guarantee) of our algorithm is more likely to be higher than the one for the randomized policy, and the experimental results in Section 5.5.2 (last two columns of Table 5.2) confirm this expectation. The reason is that our algorithm groups the nodes in a more intelligent way: the resultant \mathbf{Y}_{FJ} maximizes the objective function in (5.18.b), and the nodes that are grouped together are the ones with the vectors that have the highest dot product with the same random vector, which leads to a higher summation of edges' weights across the different partitions. In contrast, in the randomized policy, the nodes are randomly chosen to fill the clusters, without accounting for the edges' weights.

5.5 Experimental Results

To show the scalability of our approach, we consider the large network of 30 D2D pairs represented in Fig. 4.3 in Section 4.2.3 of Chapter 4, which also includes the associated matrix to this network representing the relationship among the first 15 D2D pairs. In Fig. 5.4, we show the conflict graph with assigned weights, that corresponds to the 30×30 topology, such that the blue edge stands for a link with a weight of 1, and the red one has a weight of 2.

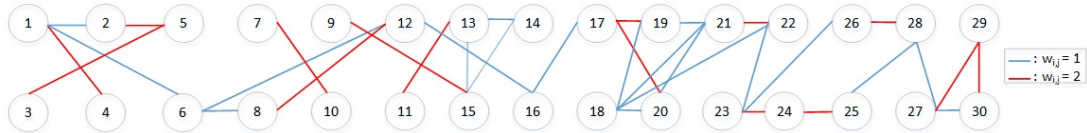


Figure 5.4: TIM conflict graph with assigned weights for the 30×30 network



Figure 5.5: The effect of the number of D2D pairs on the interference intensity

5.5.1 Clustering Algorithm Evaluation

We apply Algorithm 2 on the D2D network of Fig. 4.3(a) to cluster the 30 pairs into $k = 6$ groups with $L_{\max} = 6$. Although the number of users is typically higher in reality, this scenario is intended as a simple example meant to shed light on the potentials of the proposed scheme. An example of the algorithm’s output clusters is: $P_1 = \{5, 7, 25, 26, 27, 30\}$, $P_2 = \{1, 2, 3, 4, 6, 9\}$, $P_3 = \{8, 16, 19, 20, 22, 24\}$, $P_4 = \{12, 15, 17, 18, 21, 23\}$, $P_5 = \{10, 11, 14\}$, and $P_6 = \{13, 28, 29\}$. The cumulative weight of the edges connecting these partitions is 45 (with the sum of edges in the graph of Fig. (5.4) being 50), i.e., our algorithm was able to maximize the total sum of the cut edges, where only 5 zeros remained and appeared in some of the cluster sub-matrices. Fig. 5.5 shows the interference reduction for Fig. 4.3(a)’s topology, before and after clustering, where interference intensity refers to the sum of edge weights that signify the interference levels. We mention here that the presented algorithms are not tied to the example topologies, and can be applied to *any* topology. TIM is next applied in Section 5.6 to each cluster to cancel the intra-cluster interference that may remain after the cut.

5.5.1.1 Comparison against the Exhaustive Search Method

To study our algorithm’s performance, we consider partitioning the network of 6 vertices (T_{17} to T_{22} in Fig. 4.3) into $k = 3$ clusters with $L_{\max} = 3$. We assume here a small network size to make the exhaustive search method tractable, which produces the partitions $P_1 = \{T_{19}, T_{20}, T_{22}\}$, $P_2 = \{T_{17}, T_{18}\}$, and $P_3 = \{T_{21}\}$ with $w(E_{\text{cut}})_{\text{exhaustive search}} = 12$. This method leads to the optimal solution since the total sum of edges’ weights is equal to the value of the largest cut found, i.e., when all edges are cut. As for our algorithm, it gives $P_1 = \{T_{17}, T_{18}, T_{21}\}$, $P_2 = \{T_{19}, T_{20}, T_{22}\}$, and $P_3 = \emptyset$ as output, with $w(E_{\text{cut}})_{\text{Alg.2}} = 11$. On the other hand, the randomized policy divides the network into $P_1 = \{T_{17}, T_{19}, T_{20}\}$, $P_2 = \{T_{18}, T_{21}\}$, and $P_3 = \{T_{22}\}$, where $w(E_{\text{cut}})_{\text{rand. alg.}} = 5$. Hence, the naive

randomized algorithm is not the best possible method for this problem, and our algorithm performs better by being closer to the optimal solution in terms of total sum of edges' weights.

5.5.2 Clustering Bounds Evaluation

To give a flavor of the behavior of the various bounds, we consider two different topologies for $n = 15$ network, such that the interfering links per receiver were chosen randomly and their numbers are on average 5 in topology #1 and 6 in topology #2. This makes the total sum of weights of *all* edges, corresponding to each topology, equal to $\left(\sum_{i \neq j} w_{i,j}\right)_{\text{total}} = n \times \#$ of interfering links/receiver (i.e., equal to 75 and 90, respectively). Note here that, in all topologies, we consider the D2D network to be divided into $k = 3$ groups with $L_{\max} = 6$. In topology #1, there exist no edges with a weight of 2, e.g., while T_1 is communicating with R_1 , it interferes with R_2, R_3, R_4 and R_5 , but T_2 is not interfering with R_1 , and hence the connecting edge between nodes 1 and 2 has a weight of 1. Taking the mutual interference into account, we consider another scenario (topology #2) but with different number of interferes, e.g., in topology #2, T_3 is interfering with $T_1, T_2, T_4 \rightarrow T_7$, and T_4 is interfering with $T_2, T_3, T_5 \rightarrow T_8$. By this, T_3 and T_4 are mutually interfering, and the edge connecting nodes 3 and 4 has a weight of 2.

To numerically show the upper bound improvement, we illustrate in Table 5.2 the upper bound values for the two different topologies we discussed earlier. The results showed that the proposed methods in Section 5.4.2 were successful in tightening the upper bound. For instance, the tightest upper bound corresponding to topology #1 (equal to 66.55) is much less than the total sum of weights of *all* edges equal to 75. We can see that in practice these bounds can provide good approximations to the actual optimal solution in terms of the value of the sum of the edges that are cut. We mention here also that these results meet our expectations while comparing the upper bounds of the max-k-cut problem to the existing ones in the literature: when the clusters are bounded in size, the upper bound should get smaller. Numerically, we evaluate the tightest upper bound in (5.25.b) that corresponds to topology #1 with $\lambda_d = 13.445$ (recall that λ_d is the maximum eigenvalue of the Laplacian matrix), and we find it equal to 66.55. This value is less than the upper bound of the original max-k-cut problem in [60] that is equal to $\left(\frac{n(k-1)}{2k}\lambda_d\right) = 67.225$.

As for the total weight of the cut edges, we compute $w(E_{\text{cut}})_{\text{rand. alg.}}$ and $w(E_{\text{cut}})_{\text{Alg.2}}$ after applying the randomized algorithm and our proposed heuristic algorithm (Algorithm 2), respectively on the two different topologies. We also calculate the ratio metric of these two clustering algorithms (based on (5.27)) to assess their performance, and we summarize the results in the last two columns

Table 5.2: Lower and upper bounds for different topologies for the 15×15 D2D pairs network

	Topology #1	Topology #2
# of interferers	5	6
$\left(\sum_{i \neq j} w_{i,j}\right)_{\text{total}}$	75	90
Upper bound (5.22)	96.8047	108
Upper bound (5.23)	66.55	74.25
Upper bound (5.25.b)	66.55	74.25
$w(E_{\text{cut}})_{\text{rand. alg.}}$	48	57.6
$w(E_{\text{cut}})_{\text{Algorithm 2}}$	58	67
$(\text{ratio})_{\text{rand. alg.}}$	72.13 %	77.58 %
$(\text{ratio})_{\text{Alg.2}}$	87.15 %	90.23 %

of Table 5.2. As we can see, using our proposed heuristic algorithm improves the ratio achieved, as compared to the randomized policy (e.g., for topology #2, the ratio resulting from applying Algorithm 2 is equal to 90.23%, while it is only equal to 77.58% in the randomized policy case). One can argue that the attained ratio value is still high (above 70%) while using the randomized policy, and hence it can be directly applied in these two different topologies, without solving the SDP relaxation in (5.18). However, this decision is not valid in all cases. For instance, in the example mentioned in Section 5.5.1.1, the exhaustive search method cuts the network, with $w(E_{\text{cut}})_{\text{exhaustive search}} = 12$ (optimal solution, i.e., all edges are cut). Computing the upper bound of the SDP relaxation of the original problem, the solution (relaxed value of the total sum of the edges that were cut) is 12.5. As for our algorithm, the total of the edges that were cut is $w(E_{\text{cut}})_{\text{Alg.2}} = 11$, and for the randomized policy, $w(E_{\text{cut}})_{\text{rand. alg.}} = 5$. Consequently, calculating the performance guarantee based on (5.27), such that $(\text{ratio} \times 100)$, then $(\text{ratio})_{\text{Alg.2}} = \frac{11}{12.5} \times 100 = 88\%$ and $(\text{ratio})_{\text{rand. alg.}} = \frac{5}{12.5} \times 100 = 40\%$. Hence, the naive randomized algorithm is not the best possible method for this problem, and our algorithm performs better by being closer to the optimal solution in terms of total sum of edges' weights.

5.6 Clustering Combined with TIM Evaluation

To preserve the wanted signal and cancel the interfering ones, we can apply TIM inside each cluster using any existing method in the literature, or any of our proposed rank minimization methods in Chapter 4. However, we prefer to adopt *eRM-TIM* method since previous results have shown that *eRM-TIM* outperforms the remaining ones in terms of rank reduction and complexity.

Table 5.3: Improvement of the total sum of symmetric DoF due to clustering

Topology	TDMA	TIM only (SVDAP)	TIM only (dirSVDAP)	TIM only (eRM-TIM)	Clustering with TIM (eRM-TIM)
5×5 (Fig. 2.1)	1	$\frac{5}{2} = 2.5$	$\frac{5}{2} = 2.5$	$\frac{5}{3} = 5.333$	$(\text{DoF}_{\text{sym}})_{\text{total}} = \frac{1}{3}(\frac{5}{1} + \frac{5}{1} + 0) = 1.667$
6×6 (Fig. 4.9(a))	1	$\frac{6}{3} = 2$	$\frac{6}{3} = 2$	$\frac{6}{5} = 2$	$(\text{DoF}_{\text{sym}})_{\text{total}} = \frac{1}{3}(\frac{6}{2} + \frac{6}{1} + \frac{6}{3}) = 1.5$
12×12 (Fig. 4.1)	1	$\frac{12}{11} = 1.09$	$\frac{12}{11} = 1.09$	$\frac{12}{7} = 1.7143$	$(\text{DoF}_{\text{sym}})_{\text{total}} = \frac{1}{3}(\frac{12}{2} + \frac{12}{2} + \frac{12}{2}) = 2.33$
15×15 (Fig. 5.1)	1	$\frac{15}{11} = 1.1538$	$\frac{15}{14} = 1.0714$	$\frac{15}{9} = 1.6667$	$(\text{DoF}_{\text{sym}})_{\text{total}} = \frac{1}{3}(\frac{15}{1} + \frac{15}{2} + \frac{15}{1}) = 4$
30×30 (Fig. 4.3(a))	1	$\frac{30}{29} = 1.0345$	$\frac{30}{29} = 1.0345$	$\frac{30}{15} = 2$	$(\text{DoF}_{\text{sym}})_{\text{total}} = \frac{1}{6}(\frac{6}{2} + \frac{6}{3} + \frac{6}{1} + \frac{6}{2} + \frac{6}{2} + \frac{6}{1}) = 3.33$

5.6.1 DoF Achieved

In Table 5.3, we show the improvement of the total sum of symmetric DoF due to clustering compared to TDMA and TIM only scenarios for different topologies. On a hand, in the TDMA case, where the whole frequency band is utilized, each user should wait T slots to be capable to re-transmit. For instance, for the 30×30 topology, the symmetric DoF_{sym} per user becomes equal to $\text{DoF}_{\text{sym}} = \frac{1}{T} = \frac{1}{30} = 0.03$, i.e., each user can use $1/30$ of the resources, and so, the total sum of symmetric DoF becomes equal to 1. On the other hand, although applying TIM on this network improves the total sum of symmetric DoF, especially while using our proposed TIM rank minimization method (*eRM-TIM*) which performs much better than the other existing methods, i.e., SVDAP and dirSVDAP (as discussed in Section 4.2.3.2 of Chapter 4), however, combining it with the clustering technique stays more beneficial, especially at higher network dimensions (as will be shown later). For example, for the 30×30 network, applying TIM *without clustering* using either SVDAP and dirSVDAP, increases the total sum of symmetric DoF per user to $(\text{DoF}_{\text{sym}})_{\text{total}}^{\text{woc}}|_{\text{SVDAP}} = (\text{DoF}_{\text{sym}})_{\text{total}}^{\text{woc}}|_{\text{dirSVDAP}} = \frac{30}{29}$ only, which is less than the one achieved using *eRM-TIM* only, $(\text{DoF}_{\text{sym}})_{\text{total}}^{\text{woc}}|_{\text{eRM-TIM}} = \frac{30}{15}$. Nevertheless, combining *eRM-TIM* with clustering increases the total sum of symmetric DoF $(\text{DoF}_{\text{sym}})_{\text{total}}^{\text{wc}}$ (as shown in the last column of Table 5.3), especially for large networks, such as the 30×30 network.

Numerically, the total sum of symmetric DoF attains $(\text{DoF}_{\text{sym}})_{\text{total}}^{\text{wc}} = 3.33$, while dividing the original TIM matrix of Fig. 4.3(a) into $k = 6$ sub-matrices, as shown in Fig. 5.6 (where their rows refer to the receivers, and the columns indicate the transmitters), and then applying rank minimization on each of these sub-matrices. Note that \mathbf{X}_{P_3} , \mathbf{X}_{P_5} , and \mathbf{X}_{P_6} are reduced to rank-1 matrices. However, \mathbf{X}_{P_1} and \mathbf{X}_{P_4} , which have one zero entry each, are reduced to rank-2 matrices only, while \mathbf{X}_{P_2} which has 3 zero entries, its rank is reduced to 3. Note that the clustering technique does not offer any gain when the number of devices is small, e.g., 5×5 topology of Table 5.3, and hence having multiple frequencies in this scenario is not necessary.

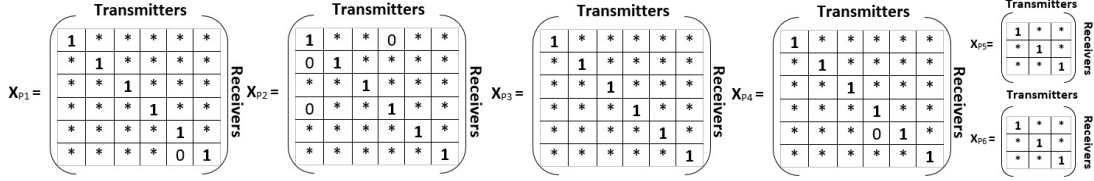


Figure 5.6: Resulting sub-matrices for the 30×30 network



Figure 5.7: Effect of the number of clusters on DoF

5.6.2 Effect of the Number of Clusters on the DoF

In Fig. 5.7, we show the impact of varying the number of clusters (with $L_{\max} = 6$ each) on the DoF achieved in the $n = 30$ network of Fig. 4.3(a). We observe that when k increases from 6 to 10, DoF continues to grow. This is because when the number of clusters increases, the matrix is divided into more sub-matrices, and thus the probability that the zeros are eliminated increases, reducing their ranks to 1.

5.6.3 Complexity and Computation Time

Our proposed algorithm for TIM clustering requires $\Theta(qn^3 + q^2n^2 + q^3 + n^3) + \Theta(k^2) + \Theta(L_{\max}^6)$ operations, where q is the number of constraints, while n , k and L_{\max} were already defined. The first two terms refer to the clustering algorithm and the third one corresponds to the TIM rank minimization method, namely *eRM-TIM*. In Algorithm 2, Step 1 necessitates $\Theta(qn^3 + q^2n^2 + q^3 + n^3)$ operations to be solved, since it is based on the primal dual barrier method (a built-in solver in CVX [159]). As for $\Theta(k^2)$, it derives from the inner and outer loops in (Steps 14-28), and $\Theta(L_{\max}^6)$ follows from solving the TIM algorithm. Note that complexity of our previous TIM method in [28] (also based on SDP) was in the order of $\mathcal{O}(n^6)$, and it becomes equal to $\Theta(L_{\max}^6)$ in this work. This outcome shows the importance of the clustering algorithm for reducing the complexity since TIM is now applied on L_{\max} instead of n , and $L_{\max} \ll n$.

From CPU time perspective, the efficiency of combining TIM with clustering appears better in larger networks, as shown in Fig. 5.8: the gain is negligible for a small network (i.e., below $n = 15$), but becomes significant, around 88% for $n = 45$ (noting that the processing time increases with n). This gain in the computation time is because the LRMC-based TIM approach is executed, in a parallel way, at each sub-matrix (corresponding to a cluster) of reduced size.

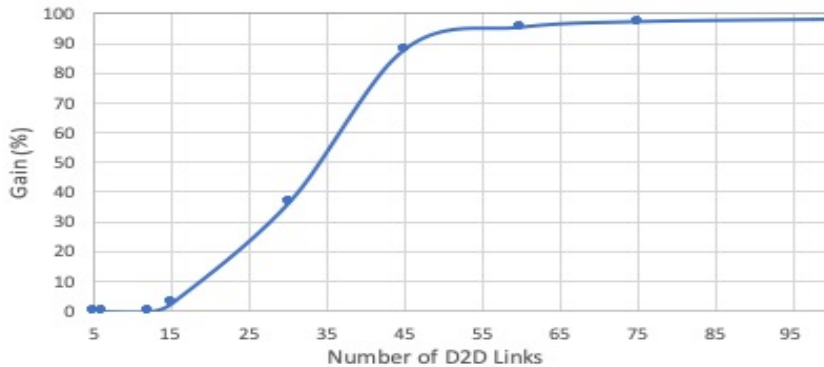


Figure 5.8: The gain in CPU time, after combining LRMC-based TIM with clustering

5.7 Summary

In this chapter, we propose a new joint clustering-topological interference management (TIM) framework, in a network with multiple available frequencies, where the objective is to cluster the D2D pairs into different groups (each with a different frequency) and to apply the low-rank matrix completion (LRMC) approach of TIM to manage the interference within each group. The challenge here is to choose the appropriate groups that work in the LRMC's favor, in order to enhance the network performance. To this end, we propose a clustering algorithm, based on max-k-cut, that can successfully group D2D devices with mutual interference in separate clusters, with bounded capacity. As for intra-cluster interference, which may still be present after the cut, it is suppressed by TIM (using any of the proposed methods in Chapter 4). It is good to mention here that by means of clustering, not only the interference gets reduced, but also the network will be characterized by a high SINR. This implicitly indicates that the DoF metric is useful in this case. Simulation results show that the combination of clustering with the LRMC approach for solving TIM reduces the computation time, by allowing parallel processing of LRMC on the resultant clusters, and also significantly improves the system DoF as compared to only using TIM.

As a summary, combining the LRMC approach of TIM with clustering:

- helps in overcoming the LRMC scalability problem (which is only suitable for up to a certain number of users [111]) and in reducing its complexity and computation time, since the whole resource allocation problem is now divided into several sub-problems with smaller dimensions, on which LRMC-based TIM is applied, in a parallel way.
- leads to an increase in the total symmetric degrees-of-freedom (DoF) of a system, with multiple set of frequencies. This is because we have developed a proper clustering algorithm for the LRMC approach of TIM that cuts the original adjacency matrix into several sub-matrices in a way that increases this metric (the symmetric DoF): our technique eliminates the "double" 0s in the matrix and replaces them by "*" (don't care values) to enhance the rank flexibility, based on the observation that two 0s in symmetric positions designate a mutual interference. It is clear that this formulation is different from the classical clustering techniques. From communication perspective, users with mutual interference will be divided into different groups.
- provides DoF and processing time gains especially for high number of devices, even if the network has only one frequency band. This is because this frequency band can be divided into multiple sub-bands, such that each sub-band is assigned to a cluster and LRMC is applied inside each cluster.

This work about the clustering approach has been published in IEEE Transactions on Communications [29].

Chapter 6

Conclusion

In this thesis, we applied the so-called Topological Interference Management problem (TIM) to manage interference in a Device-to-Device (D2D) network, where the instantaneous channel state information (CSI) is not known to the devices, but only the topology information. We found then solutions to the challenges that may arise in such application, such as developing ways to learn about the network topology. After recasting the problem as a low-rank matrix completion (LRMC) one, the objective was to minimize the TIM adjacency matrix rank in order to increase the system degrees-of-freedom (DoF). To accomplish this, we proposed three different rank minimization methods. In the first one, we approximated the matrix rank by a continuous generic approximation function that forces the SDP approximation to return a non-diagonal matrix, and hence allowing to decrease the TIM matrix rank. Although this method had a polynomial complexity, but it remained high due to the presence of five linear matrix inequalities (LMIs) in the constraints. To this end, we developed (also using SDP) an improved TIM rank minimization method, which represented a simpler optimization problem than the previous one, with much lower complexity, while achieving similar rank minimization performance. More specifically, this method was modeled as a “tweaked” nuclear norm heuristic that also was successful in overcoming the hard constraint of all ones on the main diagonal of the adjacency matrix. As for the third method, we exploited the characteristic polynomial function of the matrix and formulated an optimization problem, while relying on the existing relation between the coefficients of this function and the matrix rank. Within the same framework of LRMC, we also integrated the successive interference cancellation (SIC) capability of 5G handsets and combined it with TIM in such a way to decrease the rank even further. Simulations results related to the different methods proved their efficiency in minimizing the rank better than the existing works, with a polynomial complexity, while abiding by the special structure of the TIM matrix. When this matrix is carefully filled, the precoding and decoding matrices that the transmitters and the receivers should use to cancel the interference can be designed accordingly. Hence, the transmitters that can transmit simultane-

ously without interference can be deduced, and hence the system DoF increases.

To make TIM more realistic, we also studied its performance on more practical scenarios, like taking the path loss and mobility effects into account or considering its application on large D2D networks. To tackle the first point, we studied the path loss and mobility's effect on the achieved DoF and the conditions that should trigger the re-launching of TIM. Simulation results showed that taking the path losses into account reduced the achieved DoF values. However, defining the conditions under which TIM should re-run saved a lot of processing time. Now, concerning the second practical scenario (talking about TIM scalability), we proposed to combine TIM with a clustering framework, knowing that the adopted LRMC approach has some limitations in terms of the scalability and the structure itself, which prevents matrix rank reduction. In a network with multiple available frequencies, the objective was then to cluster the D2D pairs into different groups (each with a different frequency) and to apply the LRMC-based TIM approach (in a parallel way) to each of these sub-groups to manage the intra-cluster interference that may still be present after the cut. Mathematically speaking, this was translated as developing a clustering algorithm specific to the LRMC-based TIM approach that cuts the original adjacency matrix into sub-matrices in a way that increases the system DoF. Then, any of the developed rank minimization methods can be applied to each of these sub-matrices to reduce their ranks. To formulate the clustering problem, we used the semi-definite programming, while building on graph theory concepts. To solve the problem, we developed a heuristic algorithm based on max-k-cut algorithm, that can successfully group D2D devices with mutual interference in separate clusters, with bounded capacity. We also conducted an extensive analysis of the clustering model, by deriving a novel relatively tight upper bound for its SDP relaxation using Laplacian Algebra and matrix diagonal perturbation method. This allowed to determine the performance guarantee of our proposed heuristic algorithm as well as the randomized clustering method relative to the optimal method. Simulation results showed that the combination of clustering with the LRMC-based TIM approach reduced the computation time, by allowing parallel processing of LRMC on reduced number of devices per cluster, and also significantly improved the system DoF as compared to only using TIM, especially in large D2D networks.

6.1 Open Research Directions and Future Work

There are several open research problems that can be addressed after building on our framework, as follows:

- In this work, we recast the TIM problem as a matrix completion one. However, once can formulate it differently and solve it using another method, (other than semi-definite programming (SDP)) in order to reduce the com-

plexity.

- To solve the SDP optimization problems, we utilized CVX, a general-purpose toolbox. However, to reduce the complexity which was in the order of $\mathcal{O}(n^6)$, one can develop his/her own toolbox.
- In the TIM framework, we considered the acceptable noise floor as a threshold that the interference's strength is compared against in order to decide whether this interference is a weak or strong one. However, the optimal choice of the effective noise floor threshold by the receiver is an interesting issue to be tackled. This is because it affects on the TIM adjacency matrix content by making it sparser or more filled with "*" values. Perhaps, this threshold can be function of the fading and the average mobility.
- In the joint TIM-SIC framework, two interference categories were considered. However, the classification can include more categories (very weak, weak, medium, strong, very strong interference) and their effect on TIM can be explored.
- In the joint TIM-SIC framework, we considered an ideal SIC that makes perfect decision, and hence leads to a perfect decoding. However, SIC is not always ideal in practical scenarios, which may generate an error propagation and thus a degradation in users' performance. This necessitates then a successive error correction to suppress this error propagation.
- In the joint clustering-TIM approach, we assumed that the number of clusters is a-priori known (while relating it to the number of available frequencies). However, this metric can be learnt using machine learning techniques (instead of providing it as input) by considering different D2D network topologies, and more specifically by changing the density of these D2D pairs in the considered area.
- To study an asymmetric multiple-input multiple-output (MIMO) formulation of the topological interference management problem in a D2D scenario, knowing that this setting is more involved than the index coding problem because of the varieties of antenna configurations a device can have. This will definitely lead to a different DoF over the different D2D links, making the problem more challenging and complicated. Moreover, another interesting topic to be tackled is to check how this setting will affect the proposed clustering algorithm in this report, while dividing the D2D pairs into different clusters.

Appendix A

Proofs for Chapter 5

A.1 Proof of the Nuclear Norm Providing a Diagonal Matrix

For completion, we reproduce here the proof of [36] to show that the nuclear norm minimization of a matrix \mathbf{X} under the TIM constraint of $X_{i,j} = M_{i,j}$ (with predefined 1s in the main diagonal) leads to the trivial diagonal matrix solution (which is full rank), as an optimal one.

$$\|\mathbf{X}\|_* = \max\{\text{Tr}(\mathbf{X}^T \mathbf{B}); \mathbf{B} \in \mathbb{R}^{n \times n}, \|\mathbf{B}\| \leq 1\}$$

If we pick \mathbf{B} to be the identity matrix, then $\|\mathbf{X}\|_* \geq \text{Tr}(\mathbf{X}) = n$, where n is the matrix dimension, i.e., its maximum rank, where $\text{Tr}(\mathbf{X}) = n$ is due to the fact that all diagonal elements of \mathbf{X} are equal to 1.

A.2 Proof of Getting \mathbf{K} and \mathbf{E} Matrices as Diagonal Ones

We start by building on the Lemma of [101] and represented in (4.9). This Lemma means that, if one wants to minimize the rank of \mathbf{X} , then he/she has to find two PSD matrices such that the summation of their ranks is below or equal to $2r$, and that these matrices satisfy the constraints. Additionally, we know from [101] that $\text{rank}(\mathbf{K}) \geq \text{rank}(\mathbf{X})$ and $\text{rank}(\mathbf{E}) \geq \text{rank}(\mathbf{X})$ (for more details, the reader can refer to the end of this subsection). Based on the above, if \mathbf{X} is full rank, then \mathbf{K} and \mathbf{E} are also full rank, i.e., $\text{rank}(\mathbf{K}) \geq \text{rank}(\mathbf{X}) = n$ and $\text{rank}(\mathbf{E}) \geq \text{rank}(\mathbf{X}) = n$.

In fact, when the original rank minimization problem in (4.9) is relaxed, it has been also proven [101] that there is an equivalence between the trace formulation of (4.10) in function of \mathbf{K} and \mathbf{E} and the nuclear norm of \mathbf{X} in (4.11), which

leads to the same output. On the other hand, we know that minimizing the nuclear norm of \mathbf{X} gives the trivial solution of $\mathbf{X} = \mathbf{I}$ (a full rank diagonal matrix), which will make also then \mathbf{K} and \mathbf{E} as full rank diagonal matrices. Note that the output of (4.11) is an identity matrix, because the nuclear norm minimization of a matrix \mathbf{X} under the TIM constraint of $X_{i,j} = M_{i,j}$ (with predefined 1s in the main diagonal) leads to the trivial diagonal matrix solution (which is full rank), as an optimal one (proof in Appendix A.1).

Additionally, the three Schur complement conditions for positive semidefiniteness in (4.9) are simultaneously satisfied for a trivial solution when $\mathbf{X} = \mathbf{I}$, $\mathbf{K} = \mathbf{I}$, and $\mathbf{E} = \mathbf{I}$.

From all the above, minimizing $(\text{Trace}(\mathbf{K}) + \text{Trace}(\mathbf{E}))$ will give a trivial solution such that \mathbf{E} and \mathbf{K} are full rank diagonal matrices. This has been also observed in numerical solutions.

Note: Proof of $\text{rank}(\mathbf{K}) \geq \text{rank}(\mathbf{X})$ and $\text{rank}(\mathbf{E}) \geq \text{rank}(\mathbf{X})$ detailed in [101]:

The rank-nullity theorem [169] states that for any $m \times n$ matrix \mathbf{X} :

$$\text{rank}(\mathbf{X}) + \text{nullity}(\mathbf{X}) = n$$

where the nullity of \mathbf{X} is the dimension of its nullspace, such that:

$$\mathcal{N}(\mathbf{X}) = \text{nullspace}(\mathbf{X}) = \{\mathbf{b} \in \mathbb{R}^n : \mathbf{X}\mathbf{b} = 0\}$$

By this, the relation between the rank and the nullity of \mathbf{X} can be written as:

$$\text{rank}(\mathbf{X}) = n - \dim \mathcal{N}(\mathbf{X}) = m - \dim \mathcal{N}(\mathbf{X}^T)$$

In our case, having a square matrix $\mathbf{X} \in \mathbb{R}^{n \times n}$ makes the previous equation equal to:

$$\text{rank}(\mathbf{X}) = n - \dim \mathcal{N}(\mathbf{X}) = n - \dim \mathcal{N}(\mathbf{X}^T) \quad (\text{A.1})$$

Back to the Lemma in (4.9), authors in [101] showed that the conditions (i), (ii) and (iii) imply that $\text{rank}(\mathbf{K}) \geq \text{rank}(\mathbf{X})$ and $\text{rank}(\mathbf{E}) \geq \text{rank}(\mathbf{X})$: from condition (ii), since $\mathbf{I} - \mathbf{E}\mathbf{E}^+$ is a projector operator for $\mathcal{N}(\mathbf{E})$, it follows that

$$\mathcal{N}(\mathbf{X}^T) \supseteq \mathcal{N}(\mathbf{E}) \rightarrow \dim \mathcal{N}(\mathbf{X}^T) \geq \dim \mathcal{N}(\mathbf{E}) \quad (\text{A.2})$$

Using (A.1) and (A.2), we can write:

$$\begin{aligned} n - \text{rank}(\mathbf{X}) &= \dim \mathcal{N}(\mathbf{X}^T) \geq \dim \mathcal{N}(\mathbf{E}), \text{ and} \\ \dim \mathcal{N}(\mathbf{E}) &= n - \text{rank}(\mathbf{E}), \text{ then} \\ \text{rank}(\mathbf{E}) &\geq \text{rank}(\mathbf{X}^T) \end{aligned}$$

We can conclude that $\text{rank}(\mathbf{E}) \geq \text{rank}(\mathbf{X}^T) = \text{rank}(\mathbf{X})$. Since it is assumed here, without loss of generality, that $\text{rank}(\mathbf{K}) \geq \text{rank}(\mathbf{E})$, then also $\text{rank}(\mathbf{K}) \geq \text{rank}(\mathbf{X})$.

A.3 Proof of the Smooth Rank Function in terms of Trace

Let $\mathbf{K} = \mathbf{Y}\mathbf{S}\mathbf{Z}^T$ be the full singular value decomposition, where \mathbf{Y} , \mathbf{Z} are orthogonal matrices with n dimensions for each, and the matrix \mathbf{S} is such that:

$$\mathbf{S} = \begin{pmatrix} \mathbf{Diag}(\boldsymbol{\sigma}(\mathbf{K})) & \mathbf{0}_{r \times (n-r)} \\ \mathbf{0}_{(n-r) \times r} & \mathbf{0}_{(n-r) \times (n-r)} \end{pmatrix} \quad (\text{A.3})$$

where r is the target rank and $\mathbf{0}_{p \times q}$ denotes the $p \times q$ zero matrix. For instance, if $n = 5$ and $r = 3$, then:

$$\mathbf{S} = \begin{pmatrix} \mathbf{Diag}(\boldsymbol{\sigma}(\mathbf{K})) & \mathbf{0}_{3 \times 2} \\ \mathbf{0}_{2 \times 3} & \mathbf{0}_{2 \times 2} \end{pmatrix} = \begin{pmatrix} \sigma_1(\mathbf{K}) & 0 & 0 & 0 & 0 \\ 0 & \sigma_2(\mathbf{K}) & 0 & 0 & 0 \\ 0 & 0 & \sigma_3(\mathbf{K}) & 0 & 0 \\ 0 & 0 & 0 & 0 & 0 \\ 0 & 0 & 0 & 0 & 0 \end{pmatrix}$$

where "Diag" operator here stands for diagonal matrix having $\sigma_i(\mathbf{K})$ in its main diagonal entries and 0s on the off diagonal. Let $\boldsymbol{\sigma}^2(\mathbf{K}) = [\sigma_1^2(\mathbf{K}), \dots, \sigma_r^2(\mathbf{K})]$. Note that:

$$\mathbf{K}^T \mathbf{K} + \epsilon \mathbf{I} = \mathbf{Z}(\mathbf{S}^T \mathbf{S})\mathbf{Z}^T + \epsilon \mathbf{I} = \mathbf{Z} \begin{pmatrix} \mathbf{Diag}(\boldsymbol{\sigma}^2(\mathbf{K})) + \epsilon \mathbf{I}_r & 0 \\ 0 & \epsilon \mathbf{I}_{(n-r)} \end{pmatrix} \mathbf{Z}^T$$

where \mathbf{I} is partitioned into two small identity matrices \mathbf{I}_r and \mathbf{I}_{n-r} . Hence,

$$\begin{aligned} \Phi_\epsilon(\mathbf{K}) &= \text{Tr}(\mathbf{K}(\mathbf{K}^T \mathbf{K} + \epsilon \mathbf{I})^{-1} \mathbf{K}^T) \\ &= \left(\text{Tr} \left(\mathbf{Y} \mathbf{S} \begin{pmatrix} \mathbf{Diag}(\boldsymbol{\sigma}^2(\mathbf{K})) + \epsilon \mathbf{I}_r & 0 \\ 0 & \epsilon \mathbf{I}_{(n-r)} \end{pmatrix}^{-1} \mathbf{S}^T \mathbf{Y}^T \right) \right) \\ &= \text{Tr} \left(\begin{pmatrix} \mathbf{Diag}(\boldsymbol{\sigma}^2(\mathbf{K})) + \epsilon \mathbf{I}_r & 0 \\ 0 & \epsilon \mathbf{I}_{(n-r)} \end{pmatrix}^{-1} \mathbf{S}^T \mathbf{S} \right) \\ &= \text{Tr} \left(\begin{pmatrix} \mathbf{Diag}(\boldsymbol{\sigma}^2(\mathbf{K})) + \epsilon \mathbf{I}_r & 0 \\ 0 & \epsilon \mathbf{I}_{(n-r)} \end{pmatrix}^{-1} \begin{pmatrix} \mathbf{Diag}(\boldsymbol{\sigma}^2(\mathbf{K})) & 0 \\ 0 & 0 \end{pmatrix} \right) \\ &= \sum_{i=1}^r \frac{(\sigma_i(\mathbf{K}))^2}{(\sigma_i(\mathbf{K}))^2 + \epsilon} \end{aligned}$$

Appendix B

Proofs for Chapter 6

B.1 Proof of the Randomized Policy Bound

Based on the concept of the randomized policy explained in Section 5.4.1 of Chapter 5, we can express the expected value $\mathbb{E}(\cdot)$ of the summation of the weights of the edges connecting the different partitions in function of the total sum of weights $\sum_{1 \leq r \neq s \leq k} \sum_{i \in P_r, j \in P_s} w_{i,j}$, as follows:

$$\begin{aligned} \mathbb{E}(w) &= \text{average} \left(\frac{1}{2} \sum_{1 \leq r \neq s \leq k} \sum_{i \in P_r, j \in P_s} w_{i,j} \right) \\ &= \frac{1}{2} \sum_{1 \leq r \neq s \leq k} \sum_{i \in P_r, j \in P_s} w_{i,j} P(i, j \text{ in } \# \text{ clusters}) \end{aligned} \quad (\text{B.1})$$

where $P(i, j \text{ in } \# \text{ clusters})$ denotes the probability that two nodes i and j are in different clusters:

$$\begin{aligned} P(i, j \text{ in } \# \text{ clusters}) &= \\ & m \times P(i \in (\text{1st full cluster}), j \in \forall \text{ of the remaining full clusters}) \\ & + 2 \times P(i \in (\text{one of the full clusters}), j \notin (\text{one of the full clusters})) + (k - m) \times \\ & P(i \in (\text{1st partially full cluster}), j \in (\forall \text{ remaining partially full clusters})) \end{aligned} \quad (\text{B.2})$$

$$P(i \in \text{a full cluster}) = \frac{L_{\max}}{n} \quad (\text{B.3})$$

$$P(i \in \text{one of the full clusters}) = m \times \frac{L_{\max}}{n} \quad (\text{B.4})$$

$$P(j \notin \text{one of the full clusters}) = 1 - m \times \frac{L_{\max}}{n} \quad (\text{B.5})$$

$$P(j \in \text{one of the partially full clusters}) = \left(\frac{1}{k - m} \right) \left(1 - m \times \frac{L_{\max}}{n} \right) \quad (\text{B.6})$$

The probabilities in (B.3)-(B.6) are independent of any i and j since the users are randomly assigned in each cluster, regardless of their edges' weights. Hence, any two users can join a group with the same probability. Thus, replacing (B.3)-(B.6) in (B.2) leads to the bound in (5.20).

B.2 Proof of the Eigenvalue Bound

The proof of the conversion of the objective function and the first two constraints in (5.21) into \mathcal{L} domain can be found in [60] and [61], where $\frac{1}{2}\text{Tr}(\mathbf{L}\mathbf{Y}_{RS})$ becomes equivalent to $\frac{1}{2}\sum_{i=0}^d \lambda_i y_i f_i$, and $k\mathbf{Y}_{RS} - \mathbf{J}$ is transformed into $y_i \geq 0$ (knowing that \mathcal{L} contains \mathbf{L} , \mathbf{I} , and \mathbf{J} , then there exists an optimal solution \mathbf{Y}_{RS} to (5.21) in \mathcal{L} , and we may assume $\mathbf{Y}_{RS} = \sum_{i=0}^d y_i \mathbf{F}_i$ where $y_i \in \mathbb{R}$ ($i = 0, \dots, d$)). Our contribution appears in the proof of the conversion of the last constraint (related to each cluster's capacity) into the \mathcal{L} domain.

Following \mathcal{L} characteristics, we can write:

$$\text{Tr}(\mathbf{Y}_{RS}) = n \Leftrightarrow \text{Tr}\left(\sum_{i=0}^d y_i \mathbf{F}_i\right) = n \Leftrightarrow \sum_{i=0}^d y_i f_i = n \quad (\text{B.7})$$

$$\begin{aligned} \text{Tr}(\mathbf{J}\mathbf{Y}_{RS}) &= n\text{Tr}\left(\sum_{i=0}^d y_i \mathbf{F}_i \mathbf{F}_0\right) = n\text{Tr}\left(\sum_{i=0}^d y_i \delta_{i0} \mathbf{F}_i\right) \\ &= n\text{Tr}(y_0 \mathbf{F}_0) = n y_0 f_0 = n y_0 \end{aligned} \quad (\text{B.8})$$

since $f_0 = 1$ is the multiplicity of the eigenvalues of the all-ones matrix \mathbf{J} , while the dirac delta function $\delta_{i0} = 0$ if $i \neq 0$ and $\delta_{i0} = 1$ if $i = j = 0$. On the other hand,

$$\begin{aligned} \text{Tr}(\mathbf{J}\mathbf{Y}_{RS}) &\geq n^2 - k(k-1)L_{\max}^2, \text{ then} \\ \text{substituting } \text{Tr}(\mathbf{J}\mathbf{Y}_{RS}) \text{ in (B.8) gives } y_0 &\geq \frac{n^2 - k(k-1)L_{\max}^2}{n} \end{aligned} \quad (\text{B.9})$$

We can prove that:

$$\begin{aligned} \sum_{i=0}^d y_i f_i &= f_0 y_0 + \sum_{i=1}^d y_i f_i = n \\ \rightarrow \sum_{i=1}^d y_i f_i &= n - f_0 y_0 = n - y_0 \end{aligned} \quad (\text{B.10})$$

Replacing y_0 in (B.9) in Eq. (B.10) leads to

$$\sum_{i=1}^d y_i f_i \leq \frac{k(k-1)L_{\max}^2}{n} \quad (\text{B.11})$$

Combining the equivalent terms of the objective function and the first two constraints of (5.21) in the \mathcal{L} domain (as previously mentioned) along with (B.11) leads to the following linear program:

$$\begin{aligned} \max \quad & \frac{1}{2} \sum_{i=1}^d \lambda_i y_i f_i \\ \text{s.t.} \quad & \sum_{i=1}^d y_i f_i \leq \frac{k(k-1)L_{\max}^2}{n} \\ & y_i \geq 0 \end{aligned} \tag{B.12}$$

It is not difficult to conclude that the upper bound of the optimal value of (B.12) is $\frac{k(k-1)L_{\max}^2}{2n} \times \lambda_d$.

B.3 Proof of the Strengthened Bound

To get a strengthened upper bound for our clustering problem, we use the Laplacian algebra \mathcal{L} specifications, as in the proof of Proposition 1. However, the analysis here is more involved and requires proving a new Lemma and adding extra derivations, as will be shown later.

The scenario of having some clusters that are of full capacity and others that are partially filled motivated us to derive an interesting Lemma in (B.13) related to the summation of the product of the clusters' sizes. To maintain the flow, we defer its detailed derivation to Appendix B.4.

Lemma 5. *When at least one of the clusters is of full capacity, $\sum_{\ell \neq q} m_\ell m_q$ can be refined from $k(k-1)L_{\max}^2$ to the following bound:*

$$\sum_{\ell \neq q} m_\ell m_q \leq (n - L_{\max})(n + L_{\max} - \frac{n - L_{\max}}{k-1}) \tag{B.13}$$

By plugging (B.13) into (5.15), we can get a new relation for $\text{Tr}(\mathbf{J}\mathbf{Y}_{\text{RS}})$, as follows:

$$\text{Tr}(\mathbf{J}\mathbf{Y}_{\text{RS}}) = \sum_{\ell=1}^k m_\ell^2 \geq \frac{kL_{\max}^2 - 2nL_{\max} + n^2}{k-1} \tag{B.14}$$

Replacing (B.14) in the original formulation of (5.13.a) leads to a new tightened version, for which we show its trace formulation in (B.15.b) using a simple change of variables:

Tightened Matrix Lifting

$$\begin{aligned}
& \max_{\mathbf{Y}_{\text{RS}}} \frac{1}{2} \text{Tr}(\mathbf{L}\mathbf{Y}_{\text{RS}}) \\
& \text{s.t. } \text{diag}(\mathbf{Y}_{\text{RS}}) = \mathbf{u}_n \\
& \quad k\mathbf{Y}_{\text{RS}} - \mathbf{J} \succeq 0, \\
& \quad \mathbf{Y}_{\text{RS}} \succeq 0 \\
& \text{Tr}(\mathbf{J}\mathbf{Y}_{\text{RS}}) \geq \frac{kL_{\text{max}}^2 - 2nL_{\text{max}} + n^2}{k-1}
\end{aligned} \tag{B.15a}$$

Tightened Trace Formulation

$$\begin{aligned}
& \max_{\mathbf{Y}_{\text{FJ}}} \frac{k-1}{2k} \text{Tr}(\mathbf{L}\mathbf{Y}_{\text{FJ}}) \\
& \text{s.t. } \text{diag}(\mathbf{Y}_{\text{FJ}}) = \mathbf{u}_n \\
& \quad \mathbf{Y}_{\text{FJ}} \succeq 0 \\
& \quad (Y_{i,j})_{\text{FJ}} \geq \frac{-1}{k-1}, i \neq j \\
& \text{Tr}(\mathbf{J}\mathbf{Y}_{\text{FJ}}) \geq \frac{k^2L_{\text{max}}^2 - 2knL_{\text{max}} + n^2}{(k-1)^2}
\end{aligned} \tag{B.15b}$$

To apply the \mathcal{L} domain characteristics, we use the matrix lifting formulation in (B.15.a) for the same reason we mentioned in Section 5.4.2 of Chapter 5. Then, we relax (B.15.a) into (B.16.b) by adjusting the constraints similar to the method we followed in (5.21):

Tightened Matrix Lifting

$$\begin{aligned}
& \max_{\mathbf{Y}_{\text{RS}}} \frac{1}{2} \text{Tr}(\mathbf{L}\mathbf{Y}_{\text{RS}}) \\
& \text{s.t. } \text{diag}(\mathbf{Y}_{\text{RS}}) = \mathbf{u}_n \\
& \quad k\mathbf{Y}_{\text{RS}} - \mathbf{J} \succeq 0 \\
& \text{Tr}(\mathbf{J}\mathbf{Y}_{\text{RS}}) \geq \frac{kL_{\text{max}}^2 - 2nL_{\text{max}} + n^2}{k-1} \\
& \quad \mathbf{Y}_{\text{RS}} \succeq 0
\end{aligned} \tag{B.16a}$$

Tightened & Relaxed Matrix Lifting

$$\begin{aligned}
& \max_{\mathbf{Y}_{\text{RS}}} \frac{1}{2} \text{Tr}(\mathbf{L}\mathbf{Y}_{\text{RS}}) \\
& \text{s.t. } \text{Tr}(\mathbf{Y}_{\text{RS}}) = n \\
& \quad k\mathbf{Y}_{\text{RS}} - \mathbf{J} \succeq 0 \\
& \text{Tr}(\mathbf{J}\mathbf{Y}_{\text{RS}}) \geq \frac{kL_{\text{max}}^2 - 2nL_{\text{max}} + n^2}{k-1}
\end{aligned} \tag{B.16b}$$

Abiding by \mathcal{L} rules, we transform the objective function and the first two constraints of (B.16.b) in a similar way as we did in Proposition 1. As for the conversion of the last constraint, we follow the same methodology as in Appendix B.2, but we substitute $\text{Tr}(\mathbf{J}\mathbf{Y}_{\text{RS}})$ by its new bound (B.14) in Eq. (B.8) which generates $y_0 \geq \frac{kL_{\text{max}}^2 - 2nL_{\text{max}} + n^2}{n(k-1)}$ (i.e., a positive value and hence $y_i > 0$ constraint is satisfied). Replacing the value of y_0 in (B.10) leads to $\sum_{i=1}^d y_i f_i \leq \frac{k(n^2 - L_{\text{max}}^2) + 2n(L_{\text{max}} - n)}{n(k-1)}$. All of this allows us to write the corresponding linear program of (B.16.b) in the \mathcal{L} domain:

$$\begin{aligned}
& \max \quad \frac{1}{2} \sum_{i=1}^d \lambda_i y_i f_i \\
& \text{s.t.} \quad \sum_{i=1}^d y_i f_i \leq \frac{k(n^2 - L_{\text{max}}^2) + 2n(L_{\text{max}} - n)}{n(k-1)} \\
& \quad \quad y_i \geq 0
\end{aligned} \tag{B.17}$$

By this, we can derive the upper bound which is equal to $\text{MC}_{k,\text{cap}} \leq \frac{k(n^2 - L_{\text{max}}^2) + 2n(L_{\text{max}} - n)}{2n(k-1)} \times \lambda_d$.

B.4 Tightening the Clusters' Sizes Constraint

We prove that the summation of the product of the sizes m_ℓ of two different clusters $\sum_{\ell \neq q} m_\ell m_q$ can be tightened from $k(k-1)L_{\text{max}}^2$ to $(n - L_{\text{max}})(n + L_{\text{max}} - \frac{n - L_{\text{max}}}{k-1})$, when some clusters are of full capacity (k , and n are the total number of clusters and nodes respectively, and L_{max} is the cluster's capacity). Recall that the objective is to find an upper bound for the following problem:

$$\begin{aligned}
& \max_m \quad \sum_{\ell=1}^k \sum_{\ell \neq q} m_\ell m_q \\
& \text{s.t.} \quad \sum_{\ell=1}^k m_\ell = n, \\
& \quad \quad m_\ell \leq L_{\text{max}}
\end{aligned} \tag{B.18}$$

Now, let us consider the case when there exist one $m_\ell = L_{\text{max}}$. When more than one cluster is full, the achieved objective function will be less than (B.18), since the number of constraints is higher, i.e., $\exists q \neq \ell \mid m_q = L_{\text{max}}$. Back to the problem, the objective function F can be written as $F = \sum_{\ell} \sum_{q \neq \ell} m_\ell m_q =$

$\sum_{\ell=2}^k \sum_{q \neq \ell, q \neq 1} m_\ell m_q + 2L_{\max} \sum_{q \neq 1} m_q$. Then, (B.18) becomes:

$$\begin{aligned} \max_m \quad & \sum_{\ell=2}^k \sum_{q \neq \ell, 1} m_\ell m_q + 2L_{\max} \sum_{q \neq 1} m_q \\ \text{s.t.} \quad & \sum_{\ell=2}^k m_\ell = n - L_{\max}, \\ & m_\ell \leq L_{\max}, \quad \ell \neq q \end{aligned} \tag{B.19}$$

By removing the constraint $m_q \leq L_{\max}$, we get an upper bound for the optimization problem. Formally, we write the Karush–Kuhn–Tucker (KKT) conditions that are necessary for the optimality as follows:

$$\begin{aligned} L &= \sum_{\ell=2}^k \sum_{\ell \neq q, 1} m_\ell m_q + 2L_{\max} \sum_{q \neq 1} m_q - \lambda \left(\sum_{\ell=2}^k m_\ell - n + L_{\max} \right) \\ \frac{\partial L}{\partial m_\ell} &= 2 \sum_{q \neq \ell, 1} m_q + 2L_{\max} - \lambda \\ &= 2(n - L_{\max} - m_\ell) + 2L_{\max} - \lambda = 0 \\ &\Rightarrow 2(n - m_\ell) - \lambda = 0, \quad \forall \ell \end{aligned} \tag{B.20}$$

$$\begin{aligned} \sum_{\ell=2}^k 2(n - m_\ell) - (k-1)\lambda &= 0 \\ \rightarrow 2(k-1)n - 2(n - L_{\max}) &= (k-1)\lambda \\ \Rightarrow \lambda = 2n - \frac{2(n - L_{\max})}{k-1} \end{aligned} \tag{B.21}$$

Then, the objective function (optimal) becomes:

$$\begin{aligned} F' &= \sum_{\ell=2}^k \sum_{q \neq \ell, 1} m_\ell^* m_q^* + 2L_{\max} \sum_{q \neq 1} m_q^* \\ &= \sum_{i=2}^k m_i^* (n - L_{\max} - m_i^*) + 2L_{\max} (n - L_{\max}) \\ &\stackrel{(a)}{=} \sum_{\ell=2}^k m_\ell^* \left(\frac{\lambda}{2} - L_{\max} \right) + 2L_{\max} (n - L_{\max}) \quad (\text{due to (B.20)}) \\ &= \left(\frac{\lambda}{2} - L_{\max} \right) (n - L_{\max}) + 2L_{\max} (n - L_{\max}) \\ &= (n - L_{\max}) \left(\frac{\lambda}{2} + L_{\max} \right) \\ &\stackrel{(b)}{=} (n - L_{\max}) \left(n + L_{\max} - \frac{(n - L_{\max})}{k-1} \right) \quad (\text{due to (B.21)}) \end{aligned} \tag{B.22}$$

This implies that $F \leq (n - L_{\max})(n + L_{\max} - \frac{(n - L_{\max})}{k-1})$.

Nomenclature

\approx Approximation

Abbreviations

DoF_{sym} Symmetric DoF

AP Alternating Projection

BS Base Station

CDMA Code-Division Multiple Access

CG Conjugate Gradient

CSI Channel State Information

D2D Device-to-Device Communication

dirAP Directional Alternating Projection

dirSVDAP Directional Alternating Projection via Singular Value Decomposition

DoF Degrees-of-Freedom

FDMA Frequency-Division Multiple Access

IA Interference Alignment

IoT Internet of Things

KKT Karush–Kuhn–Tucker (KKT) conditions

LMI Linear Matrix Inequality

LRMC Low-rank matrix completion problem

LTE Long Term Evolution

MIMO Multiple-input Multiple output

NOMA Non-Orthogonal Multiple Access

OFDMA Orthogonal Frequency Division Multiple Access

RB Resource Block

RP Riemannian Pursuit

SDP Semi-definite Programming

SIC Successive Interference Cancellation
 SINR Signal-to-Interference-plus-Noise Ratio
 SIR Signal-to-Interference Ratio
 SNR Signal-to-noise ratio
 SOCP Second-Order Cone Program
 SVD Singular Value Decomposition
 SVDAP Alternating Projection via Singular Value Decomposition
 TDMA Time-division Multiple Access
 UE User Equipment

Notations

$(T-R)_i$ i^{th} D2D Transmitter-Receiver pair
 \mathbf{E}^\dagger Moore-Penrose pseudo-inverse of matrix \mathbf{E}
 \mathbf{I} Identity matrix
 \mathbf{J} All ones matrix
 \mathbf{K}^T Transpose of matrix \mathbf{K}
 \mathbf{L} Laplacian Matrix
 \mathbf{N} Index Coding Matrix
 \mathbf{u}_n All ones n vector
 $\mathbb{E}(\cdot)$ Expected value
 \mathbb{R} Real space
 \mathbb{S}^n Set of real symmetric matrices
 \mathcal{DOF} DoF region
 \mathcal{E} Set of edges
 \mathcal{G} Undirected graph
 \mathcal{L} Laplacian Algebra
 $\mathcal{N}(\mathbf{X})$ nullspace of \mathbf{X}
 \mathcal{V} Set of vertices
 $\succeq 0$ Positive Semidefinite
 $\mathbf{Diag}(\cdot)$ Semidefinite, block diagonal matrix
 $K_{i,i}$ Diagonal entry of the matrix \mathbf{K}
 sup Supremum
 $\text{Tr}(\cdot)$ Trace of a matrix

Bibliography

- [1] “Cisco visual networking index: Forecast and trends, 2017–2022.” <https://www.cisco.com/c/en/us/solutions/collateral/service-provider/visual-networking-index-vni/white-paper-c11-741490.pdf>.
- [2] Y. Birk and T. Kol, “Informed-source coding-on-demand (iscod) over broadcast channels,” in *INFOCOM’98. Seventeenth Annual Joint Conference of the IEEE Computer and Communications Societies. Proceedings. IEEE*, vol. 3, pp. 1257–1264, IEEE, 1998.
- [3] S. Doumiati and H. Artail, “Analytical study of a service discovery system based on an lte-a d2d implementation,” *Physical Communication*, vol. 19, pp. 145–162, 2016.
- [4] K. Doppler, M. Rinne, C. Wijting, C. B. Ribeiro, and K. Hugl, “Device-to-device communication as an underlay to lte-advanced networks,” *IEEE Communications Magazine*, vol. 47, no. 12, 2009.
- [5] G. Fodor, E. Dahlman, G. Mildh, S. Parkvall, N. Reider, G. Miklós, and Z. Turányi, “Design aspects of network assisted device-to-device communications,” *IEEE Communications Magazine*, vol. 50, no. 3, 2012.
- [6] M. S. Corson, R. Laroia, J. Li, V. Park, T. Richardson, and G. Tsirtsis, “Toward proximity-aware internetworking,” *IEEE Wireless Communications*, vol. 17, no. 6, 2010.
- [7] S. Doumiati, H. Artail, and K. Kabalan, “A framework for clustering lte devices for implementing group d2d communication and multicast capability,” in *Information and Communication Systems (ICICS), 2017 8th International Conference on*, pp. 216–221, IEEE, 2017.
- [8] K. Mahmood, G. K. Kurt, and I. Ali, “Mode selection rules for device-to-device communication: Design criteria and performance metrics,” in *IEEE International Symposium on Signal Processing and Information Technology*, pp. 000315–000320, IEEE, 2013.
- [9] Y. Li, D. Jin, J. Yuan, and Z. Han, “Coalitional games for resource allocation in the device-to-device uplink underlaying cellular networks,” *IEEE Transactions on wireless communications*, vol. 13, no. 7, pp. 3965–3977, 2014.

- [10] C.-H. Yu, K. Doppler, C. B. Ribeiro, and O. Tirkkonen, “Resource sharing optimization for device-to-device communication underlying cellular networks,” *IEEE Transactions on Wireless communications*, vol. 10, no. 8, pp. 2752–2763, 2011.
- [11] X.-Y. Li, J. Li, W. Liu, Y. Zhang, and H.-S. Shan, “Group-sparse-based joint power and resource block allocation design of hybrid device-to-device and lte-advanced networks,” *IEEE Journal on Selected Areas in Communications*, vol. 34, no. 1, pp. 41–57, 2015.
- [12] J. G. Andrews, S. Buzzi, W. Choi, S. V. Hanly, A. Lozano, A. C. Soong, and J. C. Zhang, “What will 5g be?,” *IEEE Journal on selected areas in communications*, vol. 32, no. 6, pp. 1065–1082, 2014.
- [13] S.-L. Chiu, K. C.-J. Lin, G.-X. Lin, and H.-Y. Wei, “Empowering device-to-device networks with cross-link interference management,” *IEEE Transactions on Mobile Computing*, vol. 16, no. 4, pp. 950–963, 2016.
- [14] C. Wang, C. Qin, Y. Yao, Y. Li, and W. Wang, “Low complexity interference alignment for mmwave mimo channels in three-cell mobile network,” *IEEE Journal on Selected Areas in Communications*, vol. 35, no. 7, pp. 1513–1523, 2017.
- [15] V. R. Cadambe and S. A. Jafar, “Interference alignment and degrees of freedom of the k -user interference channel,” *IEEE Transactions on Information Theory*, vol. 54, no. 8, pp. 3425–3441, 2008.
- [16] B. Nazer, M. Gastpar, S. A. Jafar, and S. Vishwanath, “Ergodic interference alignment,” *IEEE Transactions on Information Theory*, vol. 58, no. 10, pp. 6355–6371, 2012.
- [17] C.-Y. Wang, G.-Y. Lin, C.-C. Chou, C.-W. Yeh, and H.-Y. Wei, “Device-to-device communication in lte-advanced system: A strategy-proof resource exchange framework,” *IEEE Transactions on Vehicular Technology*, vol. 65, no. 12, pp. 10022–10036, 2016.
- [18] C. Geng, H. Sun, and S. A. Jafar, “Multilevel topological interference management,” in *2013 IEEE Information Theory Workshop (ITW)*, pp. 1–5, IEEE, 2013.
- [19] S. A. Jafar, “Topological interference management through index coding,” *IEEE Transactions on Information Theory*, vol. 60, no. 1, pp. 529–568, 2014.
- [20] N. Naderializadeh and A. S. Avestimehr, “Interference networks with no csit: Impact of topology,” *IEEE Transactions on Information Theory*, vol. 61, no. 2, pp. 917–938, 2015.
- [21] X. Yi and D. Gesbert, “Topological interference management with transmitter cooperation,” *IEEE Transactions on Information Theory*, vol. 61, no. 11, pp. 6107–6130, 2015.

- [22] H. Maleki, V. R. Cadambe, and S. A. Jafar, “Index coding—an interference alignment perspective,” *IEEE Transactions on Information Theory*, vol. 60, no. 9, pp. 5402–5432, 2014.
- [23] V. V. Veeravalli and A. El Gamal, *Interference Management in Wireless Networks: Fundamental Bounds and the Role of Cooperation*. Cambridge University Press, 2018.
- [24] E. J. Candès and B. Recht, “Exact matrix completion via convex optimization,” *Foundations of Computational mathematics*, vol. 9, no. 6, p. 717, 2009.
- [25] H. Esfahanizadeh, F. Lahouti, and B. Hassibi, “A matrix completion approach to linear index coding problem,” in *Information Theory Workshop (ITW), 2014 IEEE*, pp. 531–535, IEEE, 2014.
- [26] B. Hassibi, “Topological interference alignment in wireless networks,” in *Smart Antennas Workshop*, 2014.
- [27] Y. Shi, J. Zhang, and K. B. Letaief, “Low-rank matrix completion for topological interference management by riemannian pursuit,” *IEEE Transactions on Wireless Communications*, vol. 15, no. 7, pp. 4703–4717, 2016.
- [28] S. Doumiati, M. Assaad, and H. A. Artail, “Topological interference management framework for device-to-device communication,” *IEEE Wireless Communications Letters*, 2018.
- [29] S. Doumiati, M. Assaad, and H. A. Artail, “A framework of topological interference management and clustering for d2d networks,” *IEEE Transactions on Communications*, DOI: 10.1109/TCOMM.2019.2931319, July 2019.
- [30] S. Doumiati, H. A. Artail, and M. Assaad, “Toward optimal dof maximization with interference categorization using tim and sic,” in *IEEE Transactions on Communications*, submitted.
- [31] S. Doumiati, H. A. Artail, and M. Assaad, “Managing interference in d2d networks via clustering and topological awareness,” in *2019 IEEE 15th International Conference on Wireless and Mobile Computing, Networking and Communications (WiMOB 2019)*, accepted.
- [32] S. Doumiati, H. A. Artail, and M. Assaad, “Managing interference in d2d networks via clustering and topological awareness,” in *2018 IEEE 23rd International Workshop on Computer Aided Modeling and Design of Communication Links and Networks (CAMAD)*, pp. 1–7, IEEE, 2018.
- [33] H. Sung, S.-H. Park, K.-J. Lee, and I. Lee, “Linear precoder designs for k-user interference channels,” *IEEE Transactions on Wireless Communications*, vol. 9, no. 1, 2010.
- [34] J. Bennett, S. Lanning, *et al.*, “The netflix prize,” in *Proceedings of KDD cup and workshop*, vol. 2007, p. 35, New York, NY, USA., 2007.

- [35] X. Zhou, C. Yang, H. Zhao, and W. Yu, “Low-rank modeling and its applications in image analysis,” *ACM Computing Surveys (CSUR)*, vol. 47, no. 2, p. 36, 2015.
- [36] X. Huang and S. El Rouayheb, “Index coding and network coding via rank minimization,” in *Information Theory Workshop-Fall (ITW), 2015 IEEE*, pp. 14–18, IEEE, 2015.
- [37] M. Laurent and F. Vallentin, “Semidefinite optimization,” *Lecture Notes, available at <http://page.mi.fu-berlin.de/fmario/sdp/laurentv.pdf>*, 2012.
- [38] V. Mehrmann, “On classes of matrices containing m-matrices and hermitian positive semidefinite matrices,” *Linear algebra and its applications*, vol. 58, pp. 217–234, 1984.
- [39] J. E. Gentle, *Numerical linear algebra for applications in statistics*. Springer Science & Business Media, 2012.
- [40] S. L. Campbell and C. D. Meyer, *Generalized inverses of linear transformations*. SIAM, 2009.
- [41] Y.-B. Zhao, “An approximation theory of matrix rank minimization and its application to quadratic equations,” *Linear Algebra and its Applications*, vol. 437, no. 1, pp. 77–93, 2012.
- [42] A. N. Tikhonov and V. I. Arsenin, *Solutions of ill-posed problems*, vol. 14. Vh Winston, 1977.
- [43] P. C. Hansen, *The L-curve and its use in the numerical treatment of inverse problems*. IMM, Department of Mathematical Modelling, Technical University of Denmark, 1999.
- [44] D. Kundur and D. Hatzinakos, “Blind image deconvolution,” *IEEE signal processing magazine*, vol. 13, no. 3, pp. 43–64, 1996.
- [45] C. Eckart and G. Young, “The approximation of one matrix by another of lower rank,” *Psychometrika*, vol. 1, no. 3, pp. 211–218, 1936.
- [46] A. S. Householder, “The numerical treatment of a single nonlinear equation,” 1970.
- [47] L. N. Trefethen and D. Bau III, *Numerical linear algebra*, vol. 50. Siam, 1997.
- [48] “Gram-schmidt process.” <http://web.mit.edu/18.06/www/Essays/gramschmidtmat.pdf>.
- [49] F. Alizadeh, “Interior point methods in semidefinite programming with applications to combinatorial optimization,” *SIAM journal on Optimization*, vol. 5, no. 1, pp. 13–51, 1995.
- [50] L. Vandenberghe and S. Boyd, “Semidefinite programming,” *SIAM review*, vol. 38, no. 1, pp. 49–95, 1996.
- [51] F. Zhang, *The Schur complement and its applications*, vol. 4. Springer Science & Business Media, 2006.

- [52] E. V. Haynsworth, “On the schur complement.,” tech. rep., BASEL UNIV (SWITZERLAND) MATHEMATICS INST, 1968.
- [53] S. Boyd and L. Vandenberghe, *Convex optimization*. Cambridge university press, 2004.
- [54] S. Boyd, L. El Ghaoui, E. Feron, and V. Balakrishnan, *Linear matrix inequalities in system and control theory*, vol. 15. Siam, 1994.
- [55] M. S. Lobo, L. Vandenberghe, S. Boyd, and H. Lebert, “Applications of second-order cone programming,” *Linear algebra and its applications*, vol. 284, no. 1-3, pp. 193–228, 1998.
- [56] B. P. Brooks, “The coefficients of the characteristic polynomial in terms of the eigenvalues and the elements of an $n \times n$ matrix,” *Applied mathematics letters*, vol. 19, no. 6, pp. 511–515, 2006.
- [57] A. Frieze and M. Jerrum, “Improved approximation algorithms for max-cut and max bisection,” *Algorithmica*, vol. 18, no. 1, pp. 67–81, 1997.
- [58] M. X. Goemans and D. P. Williamson, “. 879-approximation algorithms for max cut and max 2sat,” in *Proceedings of the twenty-sixth annual ACM symposium on Theory of computing*, pp. 422–431, ACM, 1994.
- [59] A. Eisenblätter *et al.*, *Frequency assignment in GSM networks: Models, heuristics, and lower bounds*. Cuvillier, 2001.
- [60] E. R. van Dam and R. Sotirov, “New bounds for the max-k-cut and chromatic number of a graph,” *Linear Algebra and its Applications*, vol. 488, pp. 216–234, 2016.
- [61] E. R. van Dam and R. Sotirov, “Semidefinite programming and eigenvalue bounds for the graph partition problem,” *Mathematical Programming*, vol. 151, no. 2, pp. 379–404, 2015.
- [62] J. Zhao, Y. Liu, K. K. Chai, Y. Chen, M. ElKashlan, and J. Alonso-Zarate, “Noma-based d2d communications: Towards 5g,” in *Global Communications Conference (GLOBECOM), 2016 IEEE*, pp. 1–6, IEEE, 2016.
- [63] S. A. Kazmi, N. H. Tran, T. M. Ho, A. Manzoor, D. Niyato, and C. S. Hong, “Coordinated device-to-device communication with non-orthogonal multiple access in future wireless cellular networks,” *IEEE Access*, vol. 6, pp. 39860–39875, 2018.
- [64] B. Kim, W. Chung, S. Lim, S. Suh, J. Kwun, S. Choi, and D. Hong, “Uplink noma with multi-antenna,” in *2015 IEEE 81st Vehicular Technology Conference (VTC Spring)*, pp. 1–5, IEEE, 2015.
- [65] J. Zhao, Y. Liu, K. K. Chai, Y. Chen, and M. ElKashlan, “Joint subchannel and power allocation for noma enhanced d2d communications,” *IEEE Transactions on Communications*, vol. 65, no. 11, pp. 5081–5094, 2017.
- [66] L. Dai, B. Wang, Y. Yuan, S. Han, I. Chih-Lin, and Z. Wang, “Non-orthogonal multiple access for 5g: solutions, challenges, opportunities, and

- future research trends,” *IEEE Communications Magazine*, vol. 53, no. 9, pp. 74–81, 2015.
- [67] C. Ma, W. Wu, Y. Cui, and X. Wang, “On the performance of successive interference cancellation in d2d-enabled cellular networks,” in *Computer Communications (INFOCOM), 2015 IEEE Conference on*, pp. 37–45, IEEE, 2015.
- [68] B. Cho, K. Koufos, and R. Jantti, “Spectrum allocation and mode selection for overlay d2d using carrier sensing threshold,” in *Cognitive Radio Oriented Wireless Networks and Communications (CROWNCOM), 2014 9th International Conference on*, pp. 26–31, IEEE, 2014.
- [69] N. Lee, X. Lin, J. G. Andrews, and R. W. Heath, “Power control for d2d underlaid cellular networks: Modeling, algorithms, and analysis,” *IEEE Journal on Selected Areas in Communications*, vol. 33, no. 1, pp. 1–13, 2015.
- [70] S. Shalmashi, G. Miao, and S. B. Slimane, “Interference management for multiple device-to-device communications underlying cellular networks,” in *Personal Indoor and Mobile Radio Communications (PIMRC), 2013 IEEE 24th International Symposium on*, pp. 223–227, IEEE, 2013.
- [71] D. Della Penda, L. Fu, and M. Johansson, “Energy efficient d2d communications in dynamic tdd systems,” *IEEE Transactions on Communications*, vol. 65, no. 3, pp. 1260–1273, 2017.
- [72] H. ElSawy, E. Hossain, and M.-S. Alouini, “Analytical modeling of mode selection and power control for underlay d2d communication in cellular networks,” *IEEE Transactions on Communications*, vol. 62, no. 11, pp. 4147–4161, 2014.
- [73] S. Mumtaz, K. M. S. Huq, A. Radwan, J. Rodriguez, and R. L. Aguiar, “Energy efficient interference-aware resource allocation in lte-d2d communication,” in *Communications (ICC), 2014 IEEE International Conference on*, pp. 282–287, IEEE, 2014.
- [74] Q. Ye, M. Al-Shalash, C. Caramanis, and J. G. Andrews, “Resource optimization in device-to-device cellular systems using time-frequency hopping,” *IEEE Transactions on Wireless Communications*, vol. 13, no. 10, pp. 5467–5480, 2014.
- [75] Y. Li, C. Song, D. Jin, and S. Chen, “A dynamic graph optimization framework for multihop device-to-device communication underlying cellular networks,” *IEEE Wireless Communications*, vol. 21, no. 5, pp. 52–61, 2014.
- [76] A. H. Sakr, H. Tabassum, E. Hossain, and D. I. Kim, “Cognitive spectrum access in device-to-device-enabled cellular networks,” *IEEE Communications Magazine*, vol. 53, no. 7, pp. 126–133, 2015.
- [77] W. Zhibo, T. Hui, C. Nannan, and H. Yao, “Device-to-device resource allocation for qos support using a graphic theory,” in *Consumer Communica-*

- tions and Networking Conference (CCNC), 2014 IEEE 11th, pp. 525–530, IEEE, 2014.
- [78] C. Xu, L. Song, Z. Han, Q. Zhao, X. Wang, X. Cheng, and B. Jiao, “Efficiency resource allocation for device-to-device underlay communication systems: A reverse iterative combinatorial auction based approach,” *IEEE Journal on Selected Areas in Communications*, vol. 31, no. 9, pp. 348–358, 2013.
- [79] G. Yu, L. Xu, D. Feng, R. Yin, G. Y. Li, and Y. Jiang, “Joint mode selection and resource allocation for device-to-device communications,” *IEEE Transactions on Communications*, vol. 62, no. 11, pp. 3814–3824, 2014.
- [80] L. S. Jayasinghe, P. Jayasinghe, N. Rajatheva, and M. Latva-aho, “Mimo physical layer network coding based underlay device-to-device communication,” in *Personal Indoor and Mobile Radio Communications (PIMRC), 2013 IEEE 24th International Symposium on*, pp. 89–94, IEEE, 2013.
- [81] K. Jayasinghe, P. Jayasinghe, N. Rajatheva, and M. Latva-Aho, “Linear precoder-decoder design of mimo device-to-device communication underlying cellular communication,” *IEEE Transactions on Communications*, vol. 62, no. 12, pp. 4304–4319, 2014.
- [82] W. Fu, R. Yao, F. Gao, J. C. Li, and M. Lei, “Robust null-space based interference avoiding scheme for d2d communication underlying cellular networks,” in *Wireless Communications and Networking Conference (WCNC), 2013 IEEE*, pp. 4158–4162, IEEE, 2013.
- [83] C. Ma, G. Sun, X. Tian, K. Ying, Y. Hui, and X. Wang, “Cooperative relaying schemes for device-to-device communication underlying cellular networks,” in *Global Communications Conference (GLOBECOM), 2013 IEEE*, pp. 3890–3895, IEEE, 2013.
- [84] C.-H. Yu and O. Tirkkonen, “Device-to-device underlay cellular network based on rate splitting,” in *Wireless Communications and Networking Conference (WCNC), 2012 IEEE*, pp. 262–266, IEEE, 2012.
- [85] S. Mumtaz, K. M. S. Huq, and J. Rodriguez, “Coordinated paradigm for d2d communications,” in *Computer Communications Workshops (INFOCOM WKSHPS), 2014 IEEE Conference on*, pp. 718–723, IEEE, 2014.
- [86] J. Han, Q. Cui, C. Yang, and X. Tao, “Bipartite matching approach to optimal resource allocation in device to device underlying cellular network,” *Electronics letters*, vol. 50, no. 3, pp. 212–214, 2014.
- [87] H. E. Elkotby, K. M. Elsayed, and M. H. Ismail, “Exploiting interference alignment for sum rate enhancement in d2d-enabled cellular networks,” in *Wireless Communications and Networking Conference (WCNC), 2012 IEEE*, pp. 1624–1629, IEEE, 2012.
- [88] H. Min, W. Seo, J. Lee, S. Park, and D. Hong, “Reliability improvement using receive mode selection in the device-to-device uplink period under-

- laying cellular networks,” *IEEE Transactions on Wireless Communications*, vol. 10, no. 2, pp. 413–418, 2010.
- [89] B. Kaufman, J. Lilleberg, and B. Aazhang, “Spectrum sharing scheme between cellular users and ad-hoc device-to-device users,” *IEEE Transactions on Wireless Communications*, vol. 12, no. 3, pp. 1038–1049, 2013.
- [90] Y. Pei and Y.-C. Liang, “Resource allocation for device-to-device communications overlaying two-way cellular networks,” *IEEE Transactions on Wireless Communications*, vol. 12, no. 7, pp. 3611–3621, 2013.
- [91] X. Yi and G. Caire, “Topological interference management with decoded message passing,” *IEEE Transactions on Information Theory*, vol. 64, no. 5, pp. 3842–3864, 2018.
- [92] H. Sun and S. A. Jafar, “Topological interference management with multiple antennas,” in *2014 IEEE International Symposium on Information Theory*, pp. 1767–1771, IEEE, 2014.
- [93] H. Yang, N. Naderializadeh, A. S. Avestimehr, and J. Lee, “Topological interference management with reconfigurable antennas,” *IEEE Transactions on Communications*, vol. 65, no. 11, pp. 4926–4939, 2017.
- [94] Y. Gao, G. Wang, and S. A. Jafar, “Topological interference management for hexagonal cellular networks,” *IEEE Transactions on Wireless Communications*, vol. 14, no. 5, pp. 2368–2376, 2015.
- [95] H. Sun, C. Geng, and S. A. Jafar, “Topological interference management with alternating connectivity,” in *2013 IEEE International Symposium on Information Theory*, pp. 399–403, IEEE, 2013.
- [96] B. Recht, M. Fazel, and P. A. Parrilo, “Guaranteed minimum-rank solutions of linear matrix equations via nuclear norm minimization,” *SIAM review*, vol. 52, no. 3, pp. 471–501, 2010.
- [97] L. El Ghaoui and S.-I. Niculescu, *Advances in linear matrix inequality methods in control*. SIAM, 2000.
- [98] M. Hardt, “Understanding alternating minimization for matrix completion,” in *Foundations of Computer Science (FOCS), 2014 IEEE 55th Annual Symposium on*, pp. 651–660, IEEE, 2014.
- [99] Y. Birk and T. Kol, “Coding on demand by an informed source (iscod) for efficient broadcast of different supplemental data to caching clients,” *IEEE/ACM Transactions on Networking (TON)*, vol. 14, no. SI, pp. 2825–2830, 2006.
- [100] E. J. Candès and T. Tao, “The power of convex relaxation: Near-optimal matrix completion,” *IEEE Transactions on Information Theory*, vol. 56, no. 5, pp. 2053–2080, 2010.
- [101] M. Fazel, *Matrix rank minimization with applications*. PhD thesis, PhD thesis, Stanford University, 2002.

- [102] M. Fazel, H. Hindi, and S. P. Boyd, “Log-det heuristic for matrix rank minimization with applications to hankel and euclidean distance matrices,” in *American Control Conference, 2003. Proceedings of the 2003*, vol. 3, pp. 2156–2162, IEEE, 2003.
- [103] B. Vandereycken, “Low-rank matrix completion by riemannian optimization,” *SIAM Journal on Optimization*, vol. 23, no. 2, pp. 1214–1236, 2013.
- [104] N. Boumal and P.-a. Absil, “Rtrmc: A riemannian trust-region method for low-rank matrix completion,” in *Advances in neural information processing systems*, pp. 406–414, 2011.
- [105] M. Tan, I. W. Tsang, L. Wang, B. Vandereycken, and S. J. Pan, “Riemannian pursuit for big matrix recovery,” in *International Conference on Machine Learning*, pp. 1539–1547, 2014.
- [106] J. Zhang, Y. Shi, *et al.*, “Low-rank matrix completion for topological interference management by riemannian pursuit,” in *IEEE International Symposium on Information Theory-Proceedings*, p. 1831, 2015.
- [107] L. Wang, G. Araniti, C. Cao, W. Wang, and Y. Liu, “Device-to-device users clustering based on physical and social characteristics,” *International Journal of Distributed Sensor Networks*, vol. 11, no. 8, p. 165608, 2015.
- [108] S. Chen and R. S. Cheng, “Clustering for interference alignment in a multiuser interference channel,” in *Vehicular Technology Conference (VTC Spring), 2012 IEEE 75th*, pp. 1–5, IEEE, 2012.
- [109] Z. Wu, L. Jiang, G. Ren, N. Zhao, and Y. Zhao, “A novel joint spatial-code clustered interference alignment scheme for large-scale wireless sensor networks,” *Sensors*, vol. 15, no. 1, pp. 1964–1997, 2015.
- [110] S. W. Peters and R. W. Heath, “User partitioning for less overhead in mimo interference channels,” *IEEE Transactions on Wireless Communications*, vol. 11, no. 2, pp. 592–603, 2012.
- [111] S. Chen and R. S. Cheng, “Clustering for interference alignment in multiuser interference network,” *IEEE Transactions on Vehicular Technology*, vol. 63, no. 6, pp. 2613–2624, 2014.
- [112] H. E. Elkotby, K. M. Elsayed, and M. H. Ismail, “Shrinking the reuse distance: Spectrally-efficient radio resource management in d2d-enabled cellular networks with interference alignment,” in *Wireless Days (WD), 2012 IFIP*, pp. 1–6, IEEE, 2012.
- [113] G. Andersson, “An approximation algorithm for max p-section,” in *Annual Symposium on Theoretical Aspects of Computer Science*, pp. 237–247, Springer, 1999.
- [114] N. I. Miridakis and D. D. Vergados, “A survey on the successive interference cancellation performance for single-antenna and multiple-antenna ofdm systems,” *IEEE Communications Surveys & Tutorials*, vol. 15, no. 1, pp. 312–335, 2012.

- [115] I. Chih-Lin, S. Han, Z. Xu, S. Wang, Q. Sun, and Y. Chen, “New paradigm of 5g wireless internet,” *IEEE Journal on Selected Areas in Communications*, vol. 34, no. 3, pp. 474–482, 2016.
- [116] H. Song, J. Y. Ryu, W. Choi, and R. Schober, “Joint power and rate control for device-to-device communications in cellular systems,” *IEEE Transactions on Wireless Communications*, vol. 14, no. 10, pp. 5750–5762, 2015.
- [117] H. Sun, Y. Xu, and R. Q. Hu, “A noma and mu-mimo supported cellular network with underlaid d2d communications,” in *Vehicular Technology Conference (VTC Spring), 2016 IEEE 83rd*, pp. 1–5, IEEE, 2016.
- [118] K. S. Ali, H. Elsayy, A. Chaaban, and M.-S. Alouini, “Non-orthogonal multiple access for large-scale 5g networks: Interference aware design,” *IEEE Access*, vol. 5, pp. 21204–21216, 2017.
- [119] V. Kalokidou, O. Johnson, and R. Piechocki, “A hybrid tim-noma scheme for the siso broadcast channel,” in *Communication Workshop (ICCW), 2015 IEEE International Conference on*, pp. 387–392, IEEE, 2015.
- [120] V. Kalokidou, O. Johnson, and R. Piechocki, “A hybrid tim-noma scheme for the broadcast channel,” *arXiv preprint arXiv:1508.03658*, 2015.
- [121] R. Yin, C. Zhong, G. Yu, Z. Zhang, K. K. Wong, and X. Chen, “Joint spectrum and power allocation for d2d communications underlying cellular networks,” *IEEE Transactions on Vehicular Technology*, vol. 65, no. 4, pp. 2182–2195, 2016.
- [122] Q. Ye, M. Al-Shalash, C. Caramanis, and J. G. Andrews, “Distributed resource allocation in device-to-device enhanced cellular networks,” *IEEE Transactions on Communications*, vol. 63, no. 2, pp. 441–454, 2015.
- [123] H. Tang and Z. Ding, “Monotonic optimization for power control of d2d underlay with partial csi,” in *2016 IEEE International Conference on Communications (ICC)*, pp. 1–6, IEEE, 2016.
- [124] D. Feng, L. Lu, Y.-W. Yi, G. Y. Li, G. Feng, and S. Li, “Qos-aware resource allocation for device-to-device communications with channel uncertainty,” *IEEE Transactions on Vehicular Technology*, vol. 65, no. 8, pp. 6051–6062, 2016.
- [125] C. Vitale, V. Mancuso, and G. Rizzo, “Modelling d2d communications in cellular access networks via coupled processors,” in *2015 7th International Conference on Communication Systems and Networks (COMSNETS)*, pp. 1–8, IEEE, 2015.
- [126] L. Su, Y. Ji, P. Wang, and F. Liu, “Resource allocation using particle swarm optimization for d2d communication underlay of cellular networks,” in *2013 IEEE wireless communications and networking conference (WCNC)*, pp. 129–133, IEEE, 2013.
- [127] A. Aijaz, M. Tshangini, M. R. Nakhai, X. Chu, and A.-H. Aghvami, “Energy-efficient uplink resource allocation in lte networks with m2m/h2h

- co-existence under statistical qos guarantees,” *IEEE Transactions on Communications*, vol. 62, no. 7, pp. 2353–2365, 2014.
- [128] T. Han, R. Yin, Y. Xu, and G. Yu, “Uplink channel reusing selection optimization for device-to-device communication underlaying cellular networks,” in *2012 IEEE 23rd International Symposium on Personal, Indoor and Mobile Radio Communications-(PIMRC)*, pp. 559–564, IEEE, 2012.
- [129] M. Zulhasnine, C. Huang, and A. Srinivasan, “Efficient resource allocation for device-to-device communication underlaying lte network,” in *2010 IEEE 6th International conference on wireless and mobile computing, networking and communications*, pp. 368–375, IEEE, 2010.
- [130] R. Zhang, X. Cheng, L. Yang, and B. Jiao, “Interference-aware graph based resource sharing for device-to-device communications underlaying cellular networks,” in *2013 IEEE wireless communications and networking conference (WCNC)*, pp. 140–145, IEEE, 2013.
- [131] S. Maghsudi and S. Stańczak, “Hybrid centralized–distributed resource allocation for device-to-device communication underlaying cellular networks,” *IEEE Transactions on Vehicular Technology*, vol. 65, no. 4, pp. 2481–2495, 2016.
- [132] A. Liu, V. Lau, F. Zhuang, and J. Chen, “Mixed timescale cross-layer optimization for multi-antenna d2d networks,” in *2015 IEEE Global Communications Conference (GLOBECOM)*, pp. 1–6, IEEE, 2015.
- [133] 3GPP, “Technical Specification Group Radio Access Network; Study on LTE Device to Device Proximity Services; Radio Aspects,” Technical Report (TR) 36.843, 3rd Generation Partnership Project (3GPP), 03 2014. Version 12.0.1.
- [134] G. A. Safdar, M. Ur-Rehman, M. Muhammad, M. A. Imran, and R. Tafazolli, “Interference mitigation in d2d communication underlaying lte-a network,” *IEEE Access*, vol. 4, pp. 7967–7987, 2016.
- [135] F. Baccelli, N. Khude, R. Laroia, J. Li, T. Richardson, S. Shakkottai, S. Tavildar, and X. Wu, “On the design of device-to-device autonomous discovery,” in *2012 Fourth international conference on communication systems and networks (COMSNETS 2012)*, pp. 1–9, IEEE, 2012.
- [136] A. Vigato, L. Vangelista, C. Measson, and X. Wu, “Joint discovery in synchronous wireless networks,” *IEEE Transactions on Communications*, vol. 59, no. 8, pp. 2296–2305, 2011.
- [137] D. Tsolkas, N. Passas, and L. Merakos, “Device discovery in lte networks: A radio access perspective,” *Computer Networks*, vol. 106, pp. 245–259, 2016.
- [138] Alcatel-Lucent, “Discussion of d2d discovery methods,” in *3GPP doc. R1-132068, RAN1, meeting 73, Fukuoka, Japan. 3GPP*, May 2013.

- [139] J. Hong, S. Park, H. Kim, S. Choi, and K. B. Lee, “Analysis of device-to-device discovery and link setup in lte networks,” in *2013 IEEE 24th Annual International Symposium on Personal, Indoor, and Mobile Radio Communications (PIMRC)*, pp. 2856–2860, IEEE, 2013.
- [140] Qualcomm-whitepaper, “Lte direct always-on device-to-device proximal discovery,” tech. rep., August 2014.
- [141] K. Doppler, C. B. Ribeiro, and J. Knecht, “Advances in d2d communications: Energy efficient service and device discovery radio,” in *2011 2nd international conference on wireless communication, vehicular technology, information theory and aerospace & electronic systems technology (Wireless VITAE)*, pp. 1–6, IEEE, 2011.
- [142] F. Jameel, Z. Hamid, F. Jabeen, S. Zeadally, and M. A. Javed, “A survey of device-to-device communications: Research issues and challenges,” *IEEE Communications Surveys & Tutorials*, vol. 20, no. 3, pp. 2133–2168, 2018.
- [143] 3GPP, “Technical Specification Group Radio Access Network; Evolved Universal Terrestrial Radio Access (E-UTRA); Physical channels and modulation (Release 15) ,” Technical Specification (TS) 36.211, 3rd Generation Partnership Project (3GPP), 06 2019. V15.6.0.
- [144] 3GPP, “Technical Specification Group Radio Access Network; LTE Device to Device (D2D) Proximity Services (ProSe); User Equipment (UE) radio transmission and reception (Release 12) ,” Technical Report (TR) 36.877, 3rd Generation Partnership Project (3GPP), 03 2015. Version 12.0.0.
- [145] 3GPP, “Technical Specification Group Services and System Aspects; Study on architecture enhancements to support Proximity-based Services (ProSe) (Release 12) ,” Technical Report (TR) 23.703, 3rd Generation Partnership Project (3GPP), 02 2014. Version 12.0.0.
- [146] M. Grant, S. Boyd, and Y. Ye, “Cvx: Matlab software for disciplined convex programming,” 2008.
- [147] G. Yuan and B. Ghanem, “A proximal alternating direction method for semi-definite rank minimization.,” in *AAAI*, pp. 2300–2308, 2016.
- [148] D. Henrion, “Optimization on linear matrix inequalities for polynomial systems control,” 2014.
- [149] X.-Y. Li, C. He, H.-S. Shan, J. Li, and Z. J. Wang, “Feasibility-aware partial interference alignment for hybrid d2d and cellular communication networks,” *IEEE Access*, vol. 6, pp. 71069–71083, 2018.
- [150] T. Cover, “Broadcast channels,” *IEEE Transactions on Information Theory*, vol. 18, no. 1, pp. 2–14, 1972.
- [151] S. Sen, N. Santhapuri, R. R. Choudhury, and S. Nelakuditi, “Successive interference cancellation: Carving out mac layer opportunities,” *IEEE Transactions on Mobile Computing*, vol. 12, no. 2, pp. 346–357, 2012.

- [152] R. C. Kizilirmak, “Non-orthogonal multiple access (noma) for 5g networks,” in *Towards 5G Wireless Networks-A Physical Layer Perspective*, InTech, 2016.
- [153] F. Fang, H. Zhang, J. Cheng, and V. C. Leung, “Energy-efficient resource allocation for downlink non-orthogonal multiple access network,” *IEEE Transactions on Communications*, vol. 64, no. 9, pp. 3722–3732, 2016.
- [154] A. Benjebbour, Y. Saito, Y. Kishiyama, A. Li, A. Harada, and T. Nakamura, “Concept and practical considerations of non-orthogonal multiple access (noma) for future radio access,” in *Intelligent Signal Processing and Communications Systems (ISPACS), 2013 International Symposium on*, pp. 770–774, IEEE, 2013.
- [155] S. R. Islam, N. Avazov, O. A. Dobre, and K.-S. Kwak, “Power-domain non-orthogonal multiple access (noma) in 5g systems: Potentials and challenges,” *IEEE Communications Surveys & Tutorials*, vol. 19, no. 2, pp. 721–742, 2016.
- [156] M. Soltys, “Berkowitz’s algorithm and clow sequences,” *Electronic Journal of Linear Algebra*, vol. 9, no. 1, p. 5, 2002.
- [157] S. Lo, M. Monagan, and A. Wittkopf, “A modular algorithm for computing the characteristic polynomial of an integer matrix in maple,” in *Maple Summer Workshop*, 2005.
- [158] “Minimum of constrained nonlinear multi-variable function.” <https://www.mathworks.com/help/optim/ug/fmincon-interior-point-algorithm-with-analytic-hessian.html>.
- [159] W.-K. Ma, C.-C. Su, J. Jaldén, and C.-Y. Chi, “Some results on 16-qam mimo detection using semidefinite relaxation,” in *IEEE International Conference on Acoustics, Speech and Signal Processing*, pp. 2673–2676, IEEE, 2008.
- [160] “Matlab documentation.” <https://www.mathworks.com/help/optim/ug/constrained-nonlinear-optimization-algorithms.html#brnpd5f>.
- [161] G. H. Golub and C. F. Van Loan, “Matrix computations the john hopkins university press,” *Baltimore and London*, 1996.
- [162] R. A. Horn and C. R. Johnson, *Matrix analysis*. Cambridge university press, 2012.
- [163] J. Stoer and R. Bulirsch, *Introduction to numerical analysis*, vol. 12. Springer Science & Business Media, 2013.
- [164] “Matlab optimization toolbox,” Version 8.2. The MathWorks, Natick, MA, USA.
- [165] S. Shalmashi, E. Björnson, M. Kountouris, K. W. Sung, and M. Debbah, “Energy efficiency and sum rate when massive mimo meets device-to-device communication,” in *2015 IEEE Int. Conf. on Commun. Workshop (ICCW)*, pp. 627–632, 2015.

- [166] Q. Duong, Y. Shin, and O.-S. Shin, “Distance-based resource allocation scheme for device-to-device communications underlying cellular networks,” *AEU-International Journal of Electronics and Communications*, vol. 69, no. 10, pp. 1437–1444, 2015.
- [167] S. Shalmashi, G. Miao, Z. Han, and S. B. Slimane, “Interference constrained device-to-device communications,” in *2014 IEEE Int. Conf. on Commun. (ICC)*, pp. 5245–5250, IEEE, 2014.
- [168] R. Sotirov, “An efficient semidefinite programming relaxation for the graph partition problem,” *INFORMS Journal on Computing*, vol. 26, no. 1, pp. 16–30, 2013.
- [169] A. Roy and S. Banerjee, *Linear algebra and matrix analysis for statistics*. Chapman and Hall/CRC, 2014.